

# **Investigation of host specificity mechanisms of *Sporisorium reilianum* in maize and sorghum**

Von der Fakultät für Mathematik, Informatik und Naturwissenschaften der RWTH  
Aachen University zur Erlangung des akademischen Grades  
einer Doktorin der Naturwissenschaften  
genehmigte Dissertation

vorgelegt von  
M. Sc. Alana Poloni  
aus Caxias do Sul, Brazil

Berichter: Prof. Dr. Jan Schirawski  
Prof. Dr. Alan Slusarenko

Tag der mündlichen Prüfung: 19.02.2015

Diese Dissertation ist auf den Internetseiten der Hochschulbibliothek online  
verfügbar.

“...nonconformity is a great asset to a scientist. We must be curious to see if what we see is what we seem to see. We must analyse it, open it up, turn it over, look underneath it, and look behind.”

**James G. Horsfall, 1975**

# Content

|  |    |
|--|----|
| <b>Summary</b> .....   | 1  |
| <b>Zusammenfassung</b> .....   | 2  |
| <b>1. Introduction</b> .....   | 3  |
| 1.1 Host specificity in plant pathogens .....  | 3  |
| 1.2 Host resistance and plant immunity .....   | 4  |
| 1.3 Downstream responses in plant defense .....  | 7  |
| 1.3.1 Reactive oxygen species .....  | 7  |
| 1.3.2 Reinforcement of the cell wall .....   | 8  |
| 1.3.3 Phytohormones .....  | 8  |
| 1.3.4 Antimicrobial compounds .....  | 9  |
| 1.3.5 Pathogenesis related proteins (PRs) .....  | 9  |
| 1.4 The smut fungi .....   | 11 |
| 1.4.1 Head smut of maize and sorghum is caused by <i>Sporisorium reilianum</i> .....                             | 12 |
| Aims of this study .....   | 14 |
| <b>2. Materials and Methods</b> .....  | 15 |
| 2.1 Materials .....  | 15 |
| 2.1.1 Plant material .....   | 15 |
| 2.1.2 Fungal strains .....   | 15 |
| 2.2 Methods .....  | 17 |
| 2.2.1 Plant inoculation .....  | 17 |
| 2.2.2 Microscopic characterization of plant infection .....  | 18 |
| 2.2.3 Genomic DNA extraction from <i>S. reilianum</i> .....  | 18 |
| 2.2.4 Genomic DNA extraction from infected maize and sorghum .....   | 18 |
| 2.2.5 RNA extraction from infected maize and sorghum .....   | 19 |
| 2.2.6 RNA quantification and cDNA synthesis .....  | 20 |
| 2.2.7 Polymerase Chain Reaction (PCR) .....  | 20 |
| 2.2.8 Gel electrophoresis .....  | 21 |
| 2.2.9 Quantitative RT-PCR .....  | 21 |
| 2.2.10 Staining of plant material for H <sub>2</sub> O <sub>2</sub> , callose, lignin and plant cell death ..... | 22 |
| 2.2.11 Sample preparation and transmission electron microscopy (TEM) .....                                       | 23 |
| 2.2.12 Sample preparation for scanning electron microscopy (SEM) .....   | 25 |
| 2.2.13 Laser microdissection (LMD) .....   | 25 |
| 2.2.14 Cell separation by mechanical methods .....   | 26 |
| 2.2.15 Transcriptome analysis .....  | 26 |
| <b>3. Results</b> .....  | 28 |
| 3.1 The fungal side of the interaction: colonization of maize and sorghum by <i>S. reilianum</i> .....           | 28 |

|   |     |
|---|-----|
| 3.1.1 <i>S. reilianum f. sp. reilianum</i> successfully infects sorghum, while <i>S. reilianum f. sp. zea</i> does not trigger symptoms in sorghum inflorescences ..... | 28  |
| 3.1.2 SRZ causes head smut in maize cobs and tassels, while SRS only induces phyllody in cobs as the strongest symptom .....  | 31  |
| 3.1.3 Sorghum stems are colonized only by SRS .....   | 32  |
| 3.1.4 Both SRS and SRZ can reach maize stems .....  | 35  |
| 3.1.5 Quantification of fungal genomic DNA reveals contrasting proliferation behavior of SRS and SRZ in maize and sorghum .....   | 36  |
| 3.1.6 Transmission electron microscopy shows differences in SRS and SRZ cell wall thickness in maize .....  | 38  |
| 3.1.7 No differences in apressorium morphology were observed between SRS and SRZ on maize, but differences appear on sorghum .....                                      | 42  |
| 3.1.8 SRS seems to form a more tight physical interaction with sorghum than SRZ.....  | 44  |
| 3.2 The plant side: defense responses in maize and sorghum .....  | 45  |
| 3.2.1 H <sub>2</sub> O <sub>2</sub> accumulates at penetrating hyphae of SRZ in sorghum .....   | 45  |
| 3.2.2 Sorghum cells are reinforced against SRS colonization .....   | 46  |
| 3.2.3 No plant cell death is observed when plants are inoculated with <i>S. reilianum</i> .....   | 50  |
| 3.2.4 Phytoalexin deposition is a late response during the interaction of sorghum with SRZ .....  | 51  |
| 3.2.5 Expression analysis of marker genes reveals differential plant responses for SRS and SRZ in maize and sorghum .....   | 52  |
| 3.2.6 Maize transcriptome shows mild differences in gene regulation between SRZ and SRS-infected plants.....  | 55  |
| 3.2.7 Transcriptome analysis in sorghum shows strong differences in gene regulation between SRZ- and SRS-infected plants .....  | 62  |
| 3.3 Cell separation in sorghum: establishment of methods to isolate .....   | 72  |
| mesophyll and vascular bundle cells in sorghum leaves .....   | 72  |
| 3.3.1 Isolation of vascular bundles and mesophyll cells by laser microdissection (LMD) .....  | 72  |
| 3.3.2 Vascular bundles and mesophyll cells isolation by mechanical and enzymatic methods...   | 74  |
| <b>4. Discussion</b> .....  | 77  |
| 4.1 The <i>Sporisorium reilianum</i> -maize pathosystem .....   | 77  |
| 4.2 The <i>Sporisorium reilianum</i> -sorghum pathosystem.....  | 82  |
| <b>5. References</b> .....  | 90  |
| <b>6. Appendix</b> .....  | 105 |
| 6.1 List of Abbreviations .....   | 105 |
| 6.2 Supplemental tables .....   | 107 |
| 6.3 Acknowledgements .....  | 122 |

## List of figures

|  |    |
|--|----|
| <b>Figure 1.</b> The phases of immune response in plants when attacked by a pathogen .....   | 6  |
| <b>Figure 2.</b> Life cycle of <i>Sporisorium reilianum</i> .....  | 13 |
| <b>Figure 3.</b> Inoculation of sorghum seedlings with a <i>S. reilianum</i> suspension .....  | 17 |
| <b>Figure 4.</b> Macroscopic symptoms on sorghum after inoculation with the different <i>ff.ssp.</i> of <i>S. reilianum</i> .....  | 29 |
| <b>Figure 5.</b> Different sorghum varieties infected with <i>S.reilianum</i> .....  | 30 |
| <b>Figure 6.</b> Macroscopic symptoms on maize after inoculation with <i>S. reilianum</i> .....  | 32 |
| <b>Figure 7.</b> Microscopic characterization of sorghum infection by SRS and SRZ.....   | 34 |
| <b>Figure 8.</b> Fluorescence microscopy of vascular bundles infected with SRS or SRZ at 9 dpi .....   | 35 |
| <b>Figure 9.</b> Microscopic characterization of maize colonization by SRS and SRZ.....  | 36 |
| <b>Figure 10.</b> Quantification of fungal genomic DNA in sorghum and maize by quantitative PCR.....   | 37 |
| <b>Figure 11.</b> Electron micrographs of sections obtained from sorghum infected with SRS .....   | 39 |
| <b>Figure 12.</b> Electron micrographs of sections obtained from sorghum infected with SRZ.....  | 40 |
| <b>Figure 13.</b> Electron micrographs of sections obtained from maize infected with <i>S. reilianum</i> .....   | 41 |
| <b>Figure 14.</b> Scanning microscopy of sorghum and maize inoculated leaves collected at 1 dai. ....  | 43 |
| <b>Figure 15.</b> Scanning microscopy of infected sorghum leaves at 3 dpi .....  | 44 |
| <b>Figure 16.</b> Accumulation of H <sub>2</sub> O <sub>2</sub> in sorghum infected with SRS or SRZ showing the percentage of appressoria presenting H <sub>2</sub> O <sub>2</sub> ..... | 45 |
| <b>Figure 17.</b> H <sub>2</sub> O <sub>2</sub> accumulation at <i>S. reilianum</i> infection sites .....  | 47 |
| <b>Figure 18.</b> Black and white pictures showing callose deposition in infected plants .....   | 48 |
| <b>Figure 19.</b> Lignin deposition in stems of sorghum and maize .....  | 49 |
| <b>Figure 20.</b> Trypan blue staining of infected leaves at at 9 dai .....  | 50 |
| <b>Figure 21.</b> Deposition of 3-deoxyanthocyanidins in sorghum.....  | 51 |
| <b>Figure 22.</b> qRT-PCR of marker genes for plant defense responses in sorghum .....   | 53 |
| <b>Figure 23.</b> qRT-PCR of marker genes for plant defense responses in maize.....  | 54 |
| <b>Figure 24.</b> Venn diagram showing distribution of genes in the p-value-ranked expression list with a calculated p-value of ≤0.05 in maize .....                                     | 56 |
| <b>Figure 25.</b> Pathway mapping of the significantly enriched GO terms among the SRZ-specifically upregulated maize genes .....  | 58 |
| <b>Figure 26.</b> Pathway mapping of the significantly enriched GO terms among the SRS-specifically upregulated maize genes .....  | 59 |
| <b>Figure 27.</b> Distribution and annotation of the genes differentially regulated between SRS- and SRZ- infected samples.....  | 60 |
| <b>Figure 28.</b> Venn diagram showing distribution of genes in the p-value-ranked expression list with a calculated p-value of ≤0.05 in sorghum.....                                    | 63 |
| <b>Figure 29.</b> Pathway mapping of the significantly enriched GO terms among the SRZ-specifically upregulated maize sorghum within the category "Biological process" .....             | 66 |
| <b>Figure 30.</b> Pathway mapping of the significantly enriched GO terms among the SRZ-specifically upregulated sorghum genes within the "Molecular function" category.....              | 67 |

|   |    |
|---|----|
| <b>Figure 31.</b> Pathway mapping of the significantly enriched GO terms among the SRZ-specifically upregulated sorghum genes within the category "Cellular component" .....          | 68 |
| <b>Figure 32.</b> Pathway mapping of the significantly enriched GO terms among the SRS-specifically upregulated sorghum genes within the category "Biological process" .....          | 69 |
| <b>Figure 33.</b> Pathway mapping of the significantly enriched GO terms among the SRS-specifically upregulated sorghum genes within the category "Molecular function" category ..... | 70 |
| <b>Figure 34.</b> Pathway mapping of the significantly enriched GO terms among the SRS-specifically upregulated sorghum genes within the "Cellular component" category .....          | 71 |
| <b>Figure 35.</b> Cross sections (20 $\mu$ m) of sorghum leaves showing different cell types .....  | 72 |
| <b>Figure 36.</b> Samples before and after LMD .....  | 74 |
| <b>Figure 37.</b> Vascular bundles isolated by a mechanical method .....  | 75 |
| <b>Figure 38.</b> Separation of mesophyll cells in sorghum.....   | 76 |

## List of tables

|   |     |
|---|-----|
| <b>Table 1.</b> Oligonucleotides used in this study.....  | 16  |
| <b>Table 2.</b> Steps for dehydration and embedding of samples prior to TEM.....  | 24  |
| <b>Supplemental Table S1.</b> Genes significantly upregulated for SRZ in the comparison SRZ versus SRS infected plants..... | 107 |
| <b>Supplemental Table S2.</b> Genes significantly upregulated for SRS in the comparison SRZ versus SRS infected plants..... | 111 |
| <b>Supplemental Table S3.</b> Sorghum and maize genes used for qRT-PCR .....  | 116 |
| <b>Supplemental Table S4.</b> GO terms upregulated for SRZ in the comparison SRS-SRZ infected sorghum.....                  | 117 |
| <b>Supplemental Table S5.</b> GO terms upregulated for SRS in the comparison SRS-SRZ infected sorghum.....                  | 120 |

## Summary

*Sporisorium reilianum* is a smut fungus that causes head smut of maize and sorghum. The fungus exists in two host-adapted *formae speciales*: *S. reilianum* f. sp. *reilianum* (SRS) produces spores on sorghum, while *S. reilianum* f. sp. *zetae* (SRZ) generates spores on maize. To elucidate the factors leading to host specificity in *S. reilianum*, a detailed characterization of SRS and SRZ colonizing maize and sorghum was performed. To this end, fungal proliferation, plant defense responses and transcriptome changes in both host plants were examined. In sorghum, SRS entered the vascular bundles and reached the apical meristems, while SRZ stopped in the inoculated leaves. In maize, both SRS and SRZ were able to grow from inoculated leaves to the nodes, but SRS was not able to produce spores, only inducing the formation of phyllody. Additionally, EM microscopy revealed differences in cell wall thickness between hyphae of SRS and SRZ in maize. To understand the differences in colonization behavior, different plant defense responses were investigated. Maize reacted similarly to both SRS and SRZ with a very weak production of H<sub>2</sub>O<sub>2</sub> and callose for both strains. Expression analysis of marker genes involved in plant defense and transcriptome analysis showed small differences between SRS and SRZ. Mainly, different sets of genes involved in similar processes were upregulated by SRS and SRZ, suggesting that the plant reacts similarly when infected with SRS or SRZ. In sorghum, very early stages of the infection process already showed differences between SRS and SRZ regarding the morphology and abundance of appressoria. Hyphae of SRZ induced strong deposition of H<sub>2</sub>O<sub>2</sub>, callose, and phytoalexins, while SRS triggered only a weak deposition of H<sub>2</sub>O<sub>2</sub> and callose. Expression and transcriptome analysis revealed a dramatic upregulation of several genes involved in defense responses in sorghum infected with SRZ, while SRS-induced genes were mainly involved in plant cell multiplication. These results indicate that host specificity in *S. reilianum* is governed by distinct factors in maize and sorghum and it is determined at a much earlier stage in sorghum than in maize.

## Zusammenfassung

*Sporisorium reilianum* ist ein Brandpilz und verursacht Kopfbrand bei Mais und Hirse. Es existieren zwei *formae speciales* der Pilze: *S. reilianum f. sp. reilianum* (SRS) ist sehr virulent auf Hirse, kann jedoch auf Maispflanzen keine Sporen bilden, während *S. reilianum f. sp. zae* (SRZ) Kopfbrand auf Mais verursacht, aber unfähig ist diese Symptome in Hirse zu erzeugen. Um Wirtsspezifität in *S. reilianum* zu verstehen, wurde eine detaillierte Charakterisierung der Kolonisierung von Hirse und Mais mit SRS und SRZ durchgeführt. Dazu wurden verschiedene Techniken verwendet: Fluoreszenz- und Elektronenmikroskopie, Quantifizierung der Pilz-DNA, RT-PCR und Transkriptomanalyse. SRS erreichte die Apikalmeristeme von Hirse, während SRZ in den beimpften Blättern verblieb. In Mais können sowohl SRS als auch SRZ von inokulierten Blättern zu den Knoten wachsen, wogegen SRS keine Sporen produzierte und Phyllopie induzierte. Desweiteren wurden Unterschiede in den Zellwanddicken in Mais für SRS und SRZ beobachtet. Um die Unterschiede in der Pflanzenbesiedlung zu verstehen, untersuchte ich die Abwehrreaktionen der Pflanzen. Mais reagierte ähnlich für SRS und SRZ mit einer sehr schwachen Bildung von Wasserstoffperoxid und Callose. Genexpression und Transkriptom-Analysen zeigten geringe Unterschiede zwischen SRS und SRZ. Von SRS und SRZ wurden unterschiedliche Gruppen an Genen hochreguliert, die jedoch an ähnlichen Prozessen beteiligt waren. Das deutet darauf hin, dass Mais auf die Infektion mit SRS oder SRZ ähnlich reagiert. In Hirse induzierten SRZ-Hyphen Wasserstoffperoxid, Callose, Phytoalexine und die Expression von mehreren Genen, die an Abwehrreaktionen beteiligt sind, während SRS nur leichte Abwehrreaktionen verursachte. In mit SRZ infizierter Hirse Pflanzen zeigten Genexpression und Transkriptom-Analysen eine dramatische Hochregulation von mehreren Genen, die an Abwehrreaktionen beteiligt sind, während SRS induzierte Gene hauptsächlich an der pflanzlichen Zellvermehrung beteiligt waren. Diese Ergebnisse zeigen, dass Wirtsspezifität in *S. reilianum* bei Mais und Hirse durch verschiedene Faktoren geregelt wird.

## **1. Introduction**

The world population is increasing about 1% a year (Worldometers, 2014), so an increase in food production is necessary. The largest part of food supply is originated from cereal crops, such as maize and sorghum. Maize is the most cultivated cereal in the world, with a production that reached 875 million tons in 2012 (Food and Agriculture Organization of the United Nations - FAO) and a worldwide consumption of more than 116 million tons. Likewise, sorghum is the fifth most highly produced crop and the total yield came to 58 million tons in 2012 (FAO). Both plants are utilized for human and animal livestock feed, and also for non-food products and generation of bioenergy through agricultural biogas production (Schittenhelm, 2008). However, part of the harvest is lost either during cultivation or storage, especially due to the attack of several fungal pathogens that affect the amount and quality of the grains. In addition to known diseases, newly emerging fungal pathogens challenge the plants, making the control of plant pathologies even more difficult.

### **1.1 Host specificity in plant pathogens**

Host switches or host range extensions of existing phytopathogens contribute to the emergence of new fungal diseases (Giraud et al., 2010; Friesen et al., 2006). An example is *Pyrenophora tritici-repentis*, a fungus that only became an important pathogen of wheat during the last few decades (Oliver et al., 2008, Manning et al., 2013). Like *P. tritici-repentis*, most pathogenic fungi have a narrow host range, infecting only one or few plant species. However, some pathogen strains within a species, with no or very small morphological differences, are adapted to distinct plant hosts. These groups of pathogens are described as *formae speciales* (Schulze-Lefert and Panstruga, 2011), indicating that reproductive isolation on their respective hosts is a recent event that has not yet led to the evolution into distinct species.

For some fungi, the mechanism of host adaptation has been elucidated. In the necrotrophic fungus *Alternaria alternata*, host specificity is connected with toxins that are produced specifically to attack specific hosts. Strains able to produce the AAL

toxins are virulent on tomato (Morisseau et al., 1999) whereas strains producing AM toxins are virulent on apples (Miyashita et al., 2001). Host specific toxins are also produced in *Pyrenophora tritici-repentis*, where a single toxin, ToxA, is able to make a nonpathogenic strain become virulent on wheat (Ciuffetti et al., 1997). For the hemibiotroph fungus *Fusarium oxysporum f. sp. lycopersici*, a pathogen of tomato causing vascular wilt, host specificity has been associated to the presence of proteins known as “Six” that are secreted by the fungus into the plant xylem and work as disease effectors (Lievens et al., 2009; Takken and Rep, 2010, Schmidt et al., 2013).

In the powdery mildew *Blumeria graminis*, eight *formae speciales* have been identified that show different levels of specialization. The ones found on cereals are highly specific to their respective host, while the ones from wild grasses have a higher host range (Troch et al., 2014). The fungus *Puccinia graminis* exists in three *formae speciales*: *P. graminis f. sp. tritici* infects wheat and barley, *P. graminis f. sp. lolii* prefers perennial ryegrass and tall fescue, while *P. graminis f. sp. phlei-pratensis* is a pathogen of timothy grass. Those *formae speciales* are very important pathogens, causing stem rust in the respective hosts (Figuroa et al., 2013).

The presence of different avirulence genes (Avr) in *Magnaporthe oryzae* shape some strains as nonpathogenic to different hosts, such as rice and weeping lovegrass (Kang et al., 1995; Tosa et al., 2005; Sweigard et al., 1995). In the same manner, the tomato pathogen *Cladosporium fulvum* exhibits Avr proteins and also extracellular proteins (Ecps), some of them necessary for full virulence, such as Ecp1 and Ecp2 (van der Does and Rep, 2007).

## **1.2 Host resistance and plant immunity**

During the evolution of plants and pathogens, plants developed strategies to fight pathogens that, in turn, also evolved to deactivate or suppress these defenses. This suppression of defense forces the host to continue the evolution through the generation of new strategies, therefore establishing co-evolutionary arms race between host and pathogens (Anderson et al., 2010). When challenged with pathogens, plants react by the induction of a battery of responses, which are more intense in nonhost and incompatible interactions. Even prior to the activation of these

responses, the intruding pathogen has to face the constitutive resistance in the leaf surface formed by the cuticle, which includes cutin and soluble waxes embedded in a polyester matrix (Serrano et al., 2014). These features act as barriers that can inhibit pathogen penetration and impede the spread between cells (Reina-Pinto and Yephremov, 2009; Serrano et al., 2014). The invader may cross this barrier either by passing through natural openings, like stomata, or by using enzymes to destroy the cuticle. After winning against the constitutive defenses, the pathogen still has to deal with an inducible system that can be activated as soon as the organism is recognized, provoking several defense responses (Graham and Graham, 1991). This inducible immune system presents two layers of defense, one situated on the cell surface, known as PAMP-triggered immunity (PTI) and other within the plant cell, named effector-triggered immunity (ETI, Figure 1). In the PTI layer, highly conserved molecules within a class of microbes, known as pathogen associated molecular patterns (PAMPs), are recognized by plant cell surface pattern recognition receptors, the PRRs (Jones and Dangl, 2006; Zipfel, 2008). These PAMPs include, for example, flagellin, lipopolysaccharide, and peptidoglycan in bacteria, and chitin,  $\beta$ -1,3- glucan, oligosaccharides and ergosterol in fungi (Boller and Felix, 2009). Chitin is recognized by PRRs such as the LysM receptor AtCERK1 in Arabidopsis, which directly binds chitin *in vivo* (Miya et al., 2007, Shinya et al., 2012) or CEBiP and OsCERK1, which cooperatively form a chitin-induced heterodimeric receptor complex in rice (Shimizu et al., 2010). PTI is a relatively primitive and weak layer of defense, and is not specific to any particular organism, acting against all classes of pathogens that hold similar PAMPs.

However, adapted pathogens evolved the ability to inhibit or deactivate PTI through the secretion of proteins known as effectors, resulting in successful infection, so-called effector triggered susceptibility (ETS, Flor, 1942). For example, to inhibit the detection of chitin fragments, fungal pathogens can secrete LysM domain-containing effectors that can either sequester fragments of chitin, preventing them to reach the plant receptors (De Jonge et al., 2010), or bind to chitin in the fungal cell wall, protecting the fungus against degradation by chitinases (van den Burg et al., 2006). An alternative of phytopathogens to escape recognition of the host is to alter chitin into the acetylated form chitosan, which is a weaker elicitor of PTI (El Gueddari et al., 2002). The main component of the fungal cell wall,  $\beta$ -1,3-glucan, is also an important elicitor of PTI (Shetty et al., 2009). It is reported that treating wheat with  $\beta$ -1,3-glucan

from the fungus *Septoria tritici* results in complete protection against the disease caused by the fungus (Shetty et al., 2009). Recently, it was discovered that the hemibiotrophic fungus *Colletotrichum graminicola* downregulates the levels of  $\beta$ -1,3-glucan during the first hours after plant penetration, hence avoiding the recognition by the plant and consequently suppressing defense responses during its biotrophic growth phase (Oliveira-Garcia and Deising, 2013). The fungus *Magnaporthe grisea* is capable of producing  $\alpha$ -1,3-glucan to mask  $\beta$ -1,3-glucan in the cell wall, and therefore it can escape from plant glucanases and PTI (Fujikawa et al., 2009; Fujikawa et al., 2012).

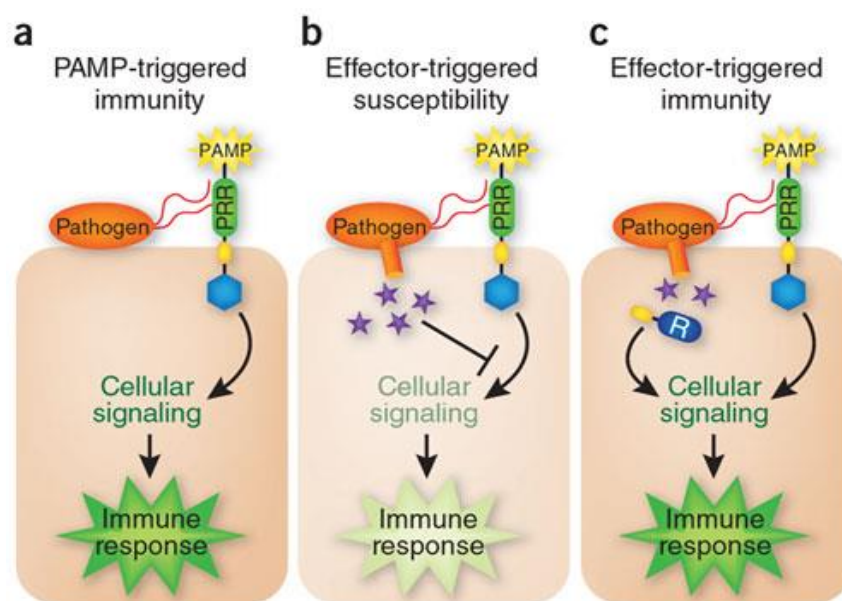


**Figure 1.** The phases of immune response in plants when attacked by a pathogen (a) During pathogen attack, PAMPs are recognized by PRRs in the host, generating PAMP-triggered immunity (PTI). (b) Pathogen effectors (purple stars) can inhibit PTI, resulting in effector-triggered susceptibility (ETS). (c) Hosts can recognize effectors through (R) proteins, causing effector-triggered immunity (ETI). Figure from Pieterse et al., 2009.

Due to constant challenges with pathogens, plants developed receptor proteins (R) that are mainly represented by nucleotide binding-leucine rich repeat proteins (NB-LRR). These NB-LRR proteins can recognize and directly or indirectly interact with pathogen effectors, leading to the second layer of defense, ETI (Jones and Dangl, 2006; Pieterse et al., 2009). Compared to PTI, ETI is a much stronger and specific defense layer that activates a cascade of events resulting in disease resistance. Generally, ETI is accompanied by a characteristic form of programmed cell death

known as hypersensitive response (HR). This cell death occurs at or close to the pathogen entry site and assists the plant in stopping colonization by the pathogen (Jones and Dangl, 2006). Interestingly, research indicates that many of the signaling components induced during PTI and ETI overlap, showing similarities between these two layers of immunity. The differences are manifested in the speed and amplitude of defense gene expression (Thomma et al., 2011).

### **1.3 Downstream responses in plant defense**

After pathogen recognition, several responses are induced in the plant, including changes in ion-fluxes across the plasma membrane, stomata closure, activation of mitogen-activated protein kinases (MAPKs), oxidative burst in the form of reactive-oxygen species (ROS), cell wall reinforcement, production of plant hormones, expression of defense response genes and production of antimicrobial substances (van Loon et al., 2006; Zipfel et al., 2004; Chinchilla et al., 2006; Miya et al., 2007, Monaghan and Zipfel, 2012; Underwood, 2012; Ahuja et al., 2012).

#### **1.3.1 Reactive oxygen species**

The accumulation of reactive oxygen species (ROS) is one of the first defense reactions observed. The generated ROS include superoxide ( $O_2^-$ ), hydroxyl radicals ( $OH\cdot$ ) and hydrogen peroxide ( $H_2O_2$ ). These molecules have important roles in the plant, not only acting in signal transduction and as substrates for enzymes, but also activating cell wall strengthening (Kuzniak and Urbanek, 2000; Hüchelhoven, 2007, Gilchrist, 1998). A massive accumulation of ROS can also trigger programmed cell death, which can effectively block spread of biotrophic pathogens (Levine et al., 1994).

$H_2O_2$  is a relatively stable molecule that is produced during the regular metabolism of the plant and also during stress, being able to reach areas located far from the generation site (Wojtaszek, 1997; Lamb and Dixon, 1997). Although helpful in plant defense, this molecule is also harmful for the plant, since it is toxic. Therefore, plants use scavenging systems composed of enzymes such as peroxidases, superoxide dismutases and catalases to control the level of  $H_2O_2$ . However, during oxidative

stress caused by pathogen infection, this system may not be completely effective (Sharma et al., 2012). In the course of plant defenses, two phases of oxidative burst have been reported, a very short one that appears quickly after pathogen detection and a second one that last longer and occurs later (Lamb and Dixon, 1997).

### **1.3.2 Reinforcement of the cell wall**

In addition to ROS generation, typical and early defense responses include the reinforcement of the plant cell wall through the deposition of papillae that may consist of callose, lignin and other polysaccharides, in addition to phenolic compounds, reactive oxygen intermediates, and proteins (Thordal-Christensen et al., 1997; Heath, 2002). Callose is a strong and insoluble polymer composed of  $\beta$ -1,3-glucan. During microbial attack, it is deposited between the plasma membrane and the cell wall, in the form of plugs, drops, or plates, making the cell stronger and therefore acting as a physical barrier against pathogens (Luna et al., 2010). This physical resistance can also slow down pathogen spread from cell to cell, helping the plant to gain time for the induction of other defense responses (Lamb and Dixon, 1997).

Lignin is one of the most important components of the plant cell wall and is derived from phenylpropanoid hydroxycinnamyl alcohols (Vanholme et al., 2010). Lignification occurs through the oxidative cross-linking of the monolignans into long-chain polymers of lignin. Similarly as callose, lignin makes the cell more resistant against pathogen penetration and protects the cell against microbial enzymes and toxins. Lignin is a complex molecule that can be made up of different monomers, having different levels of cross-linking and different chain lengths. Several compositions of lignin are found in the plant that vary according to the plant organ and age. The lignin deposited during defense against pathogens presents a particular composition that differs from the ones normally produced by the plant (Kawasaki et al., 2006).

### **1.3.3 Phytohormones**

Salicylic acid (SA), jasmonic acid (JA) and ethylene (ET) are the major plant hormones involved in stress against microbial attack. SA is mainly triggered in

defense against biotrophic and hemibiotrophic pathogens, while JA and ET are involved in responses to necrotrophic pathogens, wounding and insects. Pathways of SA and JA/ET are known to act antagonistically (Bari and Jones, 2008; Glazenbrook, 2005). The induction of SA coincides with the activation of genes encoding the pathogenesis-related (PR) proteins and to the accumulation of several compounds, such as H<sub>2</sub>O<sub>2</sub> and phenol, which may result in plant resistance.

### **1.3.4 Antimicrobial compounds**

The synthesis and transport of antimicrobial compounds is another very efficient method for plants to combat microbial intruders. Among these substances, a very important group is known as phytoalexins, compounds of low molecular weight that are induced by stress (Ahuja et al., 2012; Hammerschmidt, 1999; Mert-Türk, 2002).

Sorghum produces a unique class of flavonoid phytoalexins, the 3-deoxyanthocyanidins, divided in apigenidin and luteolinidin, in addition to several derivatives (Wharton and Nicholson, 2000; Lo et al., 2002, Du et al, 2010a). In maize, phytoalexins are represented by terpenoids, which include a group of acidic sesquiterpenoids known as zealexins and *ent*-kaurane related diterpenoids named kauralexins. A group of benzoxazinoid phytoalexins is also described, which include DIMBOA, HDMBOA and derivatives (Dafoe et al., 201, Song et al., 2011; Huffaker et al., 2011; Schmelz et al., 2011).

### **1.3.5 Pathogenesis related proteins (PRs)**

Pathogenesis related proteins (PRs) are proteins mostly undetectable in healthy tissues, but upregulated during pathogen attack or other stresses (Linthorst 1991, van Loon et al., 1994). During plant responses, these proteins cause some modifications in the plant cell or work to inhibit the dissemination of the pathogen by targeting specific cellular components of the organism. PRs are classified in 17 families, namely, PR-1 to PR-17 (van Loon et al., 2006). They were discovered in tobacco leaves (*Nicotiana tabacum* L.) responding to tobacco mosaic virus (TMV) (Van Loon and Van Kammen, 1968), and lately found in a large range of other plant species.

The family of PR1 proteins includes strongly conserved proteins found in many plants (van Loon et al., 2006). These proteins are utilized as markers of pathogen-induced systemic acquired resistance (SAR), but their role in defense is still unclear. Studies using transgenic tobacco expressing PR1 (Alexander et al., 1993) or testing *in vitro* activity against pathogens (Niderman et al., 1995) suggest an involvement of these proteins in plant resistance.

$\beta$ -(1,3) glucanases are PR-2 proteins that hydrolyze the  $\beta$ -1,3-glucosidic bonds of  $\beta$ -(1,3) glucans, the main components of the fungal cell wall. They also assist PTI by attacking fungal hyphal tips and generating fragments of oligosaccharides that can reach plant receptors. They are grouped in two main classes (I and II) and two minor classes (III and IV), according to the amino acid sequence, localization and function. Class I has basic proteins that localize in the plant vacuole, while classes II, III and IV include acidic extracellular proteins of about 36 kDa (Selitrennikoff, 2001). Members of different  $\beta$ -1,3-glucanase classes may co-exist in one plant species.

Chitinases are found in the families of PR-3, PR-4, PR-8 and PR-11 and are divided in seven classes (Class I–VII) based on their primary structure (Neuhaus 1996). Similar to  $\beta$ -(1,3) glucanases and often presenting an expression coordinated with them, chitinases hydrolyse the  $\beta$ -1,4-*N* acetylglucosamine linkages from chitin localized in the fungal cell wall, thereby blocking the fungal growth and liberating chitin fragments that can reach plant receptors and elicit additional defenses. These enzymes have no known function in plant growth and development, since plants do not contain chitin. Therefore, their exclusive function seems to be in plant defense which is supported by *in vitro* and *in vivo* studies where their induction is reported to be higher in resistant than in susceptible plants (Schlumbaum et al., 1986; Salzer et al., 2000; Park et al., 2004; Su et al., 2014).

The PR5 proteins are represented by thaumatin-like proteins (TLPs) that show homology to the thaumatin isolated from the plant *Thaumatococcus daniell* (Iyengar et al. 1979). In contrast to thaumatin, TLPs present an antifungal activity, apparently permeabilizing pathogen membranes (van der Wel and Loeve, 1972). In monocots, their presence has long been known in barley, wheat, oat, sorghum and maize (Hejgaard et al. 1991; Vigers, et al. 1991).

Peroxidases are PR-9 proteins that can be upregulated during both ETI and PTI, since they participate in the oxidation of a variety of substrates. These enzymes mainly use H<sub>2</sub>O<sub>2</sub> as a substrate and also participate in cell wall reinforcement by catalyzing polymerization of lignin, being regularly secreted into the apoplast during the plant defense responses (Almagro et al., 2009). Research indicates that overexpression of some peroxidases, especially members of class III peroxidases, increases resistance to pathogens (Johrde and Schweizer, 2008).

PR10 are represented by small acidic intracellular proteins of about 16 kDa. They are induced by pathogen attack, drought and salinity in several plant species (Liu et al. 2003, Park et al., 2004) and have homology to ribonucleases (Moiseyev et al. 1994). In sorghum, PR10 proteins are elicited by fungal infection (Lo and Nicholson, 1998).

Other proteins induced by pathogens include ribosome inactivating proteins, antifungal proteins (AFP), sormatin, and phenylalanine ammonia-lyase (PAL), an enzyme that catalyzes the first reaction in the biosynthesis from L-phenylalanine of lignin deposition (Whetten and Sederoff, 1995) and production of phytoalexins (Graham, 1995).

#### **1.4 The smut fungi**

Smut fungi form a group of basidiomycetes that belongs to the order Ustilaginales and comprises about 77 genera and more than 1450 species. They received this name because they typically produce a black mass of spores that resembles smut. Smuts are the second most important group of phytopathogens within the Basidiomycota, and infect more than 4000 species of flowering plants, mostly species of Poaceae and Cyperaceae (Vanky, 2002; Martinez-Espinoza et al., 2002). An interesting characteristic of smuts is the very limited host range, with most of them having between one and three different host plants (Bauer et al., 2000).

Smut fungi live in a very intimate balance with their host plants, staying mostly near the meristematic tissues until the flowering time. Different species can cause distinct symptoms, that vary from abnormal plant growth, modifications in individual organs known as galls, or even symptoms that appear only when the inflorescence emerges, transformed in masses of teliospores. These pathogens are biotrophic, since they do

not kill the host and need the plant alive to obtain nutrients and complete their life cycle.

The most important diseases are caused by species from the genera *Ustilago*, *Tilletia* and *Sporisorium*. The best studied smut fungus, *Ustilago maydis*, causes local infections and develops spores in the region where the hyphae colonize the plant. *Sporisorium* species are not able to do so, and cause systemic infections, generating spores exclusively in inflorescences (Martinez-Espinoza et al., 2002).

#### **1.4.1 Head smut of maize and sorghum is caused by *Sporisorium reilianum***

*Sporisorium reilianum* (Kühn) Langdon & Fullerton is a smut fungus that causes head smut of maize and sorghum, being also reported in Sudan grass and teosinte. The fungus presents a dimorphic cycle, with a saprophytic yeast phase and a parasitic filamentous phase (Fig. 2). In the field, the main sources of inoculum are soil-borne diploid teliospores that can survive in the soil for several years.

Under favorable conditions, which include low soil moisture content and temperatures of about 28°C, the spores germinate forming a basidium that undergoes meiosis, giving rise to haploid sporidia of different mating type (Hanna et al., 1929; Fig. 2). Compatible haploid sporidia have to recognize a partner with a different mating type through a pheromone/pheromone receptor system. Two mating type loci exist, named *a* and *b* (Schirawski et al., 2005). The *a* locus occurs in three alleles that each encode two active pheromone and one pheromone receptor involved in cell recognition, while the *b* locus presents at least five alleles and encodes two subunits of a heterodimeric homeodomain transcription factor, involved in the regulation of pathogenicity (Schirawski et al., 2005). When recognition happens, sporidia form conjugation hyphae that grow towards each other and fuse at their tips (Schirawski et al., 2005). From then on, the fungus grows as a dikaryotic filament, forming an appressorium that can penetrate the expanding leaf epidermis (Schirawski et al., 2010; Prom et al., 2011; Zuther et al., 2012). After penetration, the fungus colonizes the plant in the form of dikaryotic hyphae. Although the fungal hyphae spread through the plant and reach the apical meristem, the colonization does not cause obvious symptoms (Martinez et al., 1999). When the fungus invades the undifferentiated floral tissue, the emerging inflorescence is partially or completely replaced by the smut

sorus containing vascular strands from the plant and black masses of diploid teliospores (Wilson and Frederiksen, 1970; Ghareeb et al., 2011). Sometimes no sorus is present and instead, the tassels have a structure known as phyllody, showing a leafy-like morphology (Halisky, 1963, Ghareeb et al., 2011).

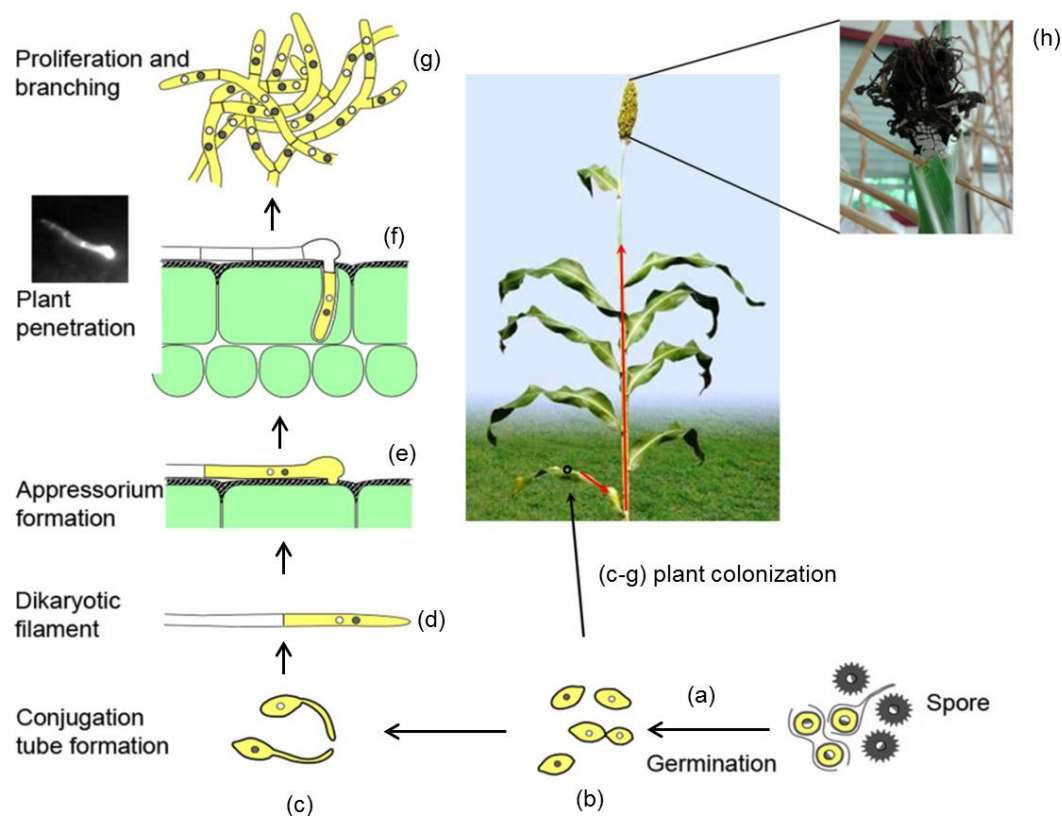


**Figure 2.** Life cycle of *Sporisorium reilianum*. Teliospores can remain in the soil for several years. Under favorable conditions, they germinate and undergo meiosis (a). Haploid sporidia are produced that have different mating types (represented by black and white nuclei, b). Cells of opposite mating type grow towards each other (c) and fuse at their tips forming a dikaryotic filament (d). This filament penetrates the plant surface through the formation of an appressorium (e,f). The fungus then grows intracellularly without causing symptoms (g). During flowering time, the fungus reprograms the plant meristem and when the inflorescence emerges, it is completely filled with spores (h).

The spores can be dispersed by several vectors, such as water and wind, and rest in the soil where they serve as inoculum for new plants. Reports say that more than 80% of plants in a field can present head smut (Frederiksen, 1977). Disease control is based on the utilization of fungicides, resistant cultivars or crop rotation, but still the spores can persist up to 10 years in the soil (Sarh, 1992).

*S. reilianum* exists in two *formae speciales* with different host preferences (Zuther et al., 2012; Halisky, 1963). One of them, *S. reilianum f. sp. reilianum*, was isolated from sorghum and is highly virulent in this plant, but does not produce spores on maize. *S. reilianum f. sp. zaeae*, was isolated from maize and does not cause disease on sorghum. The only symptom recognized in sorghum leaves inoculated with *S. reilianum f. sp. zaeae* is the appearance of red dots indicating phytoalexin production, which was shown to inhibit the fungus *in vitro* and therefore seems to be linked with host specificity in this interaction (Zuther et al., 2012). In maize, the factors involved in the differences between a successful and an unsuccessful strain are still completely unknown and remain to be investigated.

### **Aims of this study**

The objective of this study was to investigate the mechanisms involved in host specificity in the smut *Sporisorium reilianum* through comparison of two *formae speciales* (*ff. spp.*) with preferences for different hosts. The first aim was to determine the differences in colonization for both *ff. spp.* in maize and sorghum and to identify time points and plant tissues in which developmental differences become apparent. This was done using microscopy of the infection process, of hyphae morphology and of the growth behavior of the two strains. A second level of the comparison was performed on the plant defense responses that are induced upon plant inoculation with the two *ff. spp.* of *S. reilianum*. Through an analysis of plant gene expression patterns, the interaction of *S. reilianum* with the host was investigated on a molecular level.

## **2. Materials and Methods**

### **2.1 Materials**

The chemicals, media and kits used during this study were obtained from Carl Roth GmbH, Sigma Aldrich, Roche, Bio-Rad, Difco, Roth, Biotek, Fermentas, Qiagen, or otherwise described.

#### **2.1.1 Plant material**

Seeds of *Zea mays* cultivar Gaspé Flint were obtained from Prof. Regine Kahmann, Max Planck Institute for Terrestrial Microbiology, Marburg. *Sorghum bicolor* cultivar Tall Polish was obtained from Leibniz Institute of Plant Genetics and Crop Plant Research, Gatersleben. The sorghum varieties Super Dolce 15, Emese, Super Sile 20, Zerberus and Sudangrass Jumbo were received from Yvonne Schleusner, HU-Berlin. The varieties Sila, LuluD and Epuripur were received from Ingela Fridborg, Swedish University of Agricultural Sciences. Maize and sorghum seeds were grown, respectively, for 7 and 14 days, in a growth chamber (Johnson Controls) under conditions of 15 h day light at 28°C and 50% relative humidity, and 9 h night at 22°C and 60% relative humidity.

#### **2.1.2 Fungal strains**

The compatible wild-type *Sporisorium reilianum* strains SRZ1\_5-2 (*a1b1*) and SRZ2\_5-1 (*a2b2*), originally isolated from maize (Schirawski et al., 2010), and SRS1\_H2-8 (*a1b1*) and SRS2\_H2-7 (*a2b6*), isolated from sorghum (Zuther et al., 2012), were used in this study. The strains were maintained at -80°C in NSY Glycerin Medium (8 g/l Nutrient Broth, 10 g/l Yeast extract, 5 g/l Sucrose, 696 ml/l Glycerin) or on potato dextrose agar plates (Becton, Dickinson and Company- BD, Heidelberg, Germany; 24 g/l Potato Dextrose Broth, 20 g/l Agar) at 4°C for no longer than 1 week.

**Table 1.** Oligonucleotides used in this study

| Name   | Sequence                             | Use                                      |
|--------|--------------------------------------|--|
| oSP101 | GTGCATCAACTGCCAGAAGG                 | qPCR of <i>S. reilianum</i> gene Sr16559 |
| oSP102 | TCGTAGCCGTAGTACCAAGC                 | qPCR of <i>S. reilianum</i> gene Sr16559 |
| oJI08  | GCGACCTTACCGACTACCTC                 | qPCR of <i>Sb</i> actin                  |
| oJI09  | AATATCCACGTGCGACTTCA                 | qPCR of <i>Sb</i> actin                  |
| oBH73  | ACCTCACCGACCACCTAATG                 | qPCR of <i>Zm</i> actin                  |
| oBH74  | ACCTGACCATCAGGCATCTC                 | qPCR of <i>Zm</i> actin                  |
| oYZ96  | ACTACGTGGACCCGCACAAC                 | qRT-PCR of <i>Zm</i> PR1                 |
| oYZ97  | CGGAGTGGATCAGCTTGCAGTC               | qRT-PCR of <i>Zm</i> PR1                 |
| oYZ94  | TATCGGCCGGAATAGGCTCTG                | qRT-PCR of <i>Zm</i> PR5                 |
| oYZ95  | CGCGTACATACAAATGCGTGC                | qRT-PCR of <i>Zm</i> PR5                 |
| oYZ121 | CATTGGACTGGGATGAGCTT                 | qRT-PCR of <i>Zm</i> PR10                |
| oYZ122 | CCACACAGAAAACCATGACG                 | qRT-PCR of <i>Zm</i> PR10                |
| oHG218 | CTTGCGGTCGTTCAACTAGG                 | qRT-PCR of <i>Zm</i> An2                 |
| oHG219 | TTCTCACGATGGGCGTTAGG                 | qRT-PCR of <i>Zm</i> An2                 |
| JI001  | CGCAAGACCACCGTCTTCTT                 | qRT-PCR of <i>Sb</i> DFR3                |
| JI002  | GGTAGCTTTTCTGTTGCCG                  | qRT-PCR of <i>Sb</i> DFR3                |
| oJU28  | GACTGACGCAAAGTTGACCG                 | qRT-PCR of <i>Sb</i> glucan synthase     |
| oJU29  | ATATAGGCCACTCAGGCCGCTGAGCTGTGAACTCCT | qRT-PCR of <i>Sb</i> glucan synthase     |
| oAP31  | GCTATCAAGGGCGTTGGCAAG                | qRT-PCR of <i>Sb</i> chitinase           |
| oAP32  | ACCTGGGCGCTGTAGTTGTTT                | qRT-PCR of <i>Sb</i> chitinase           |
| oAP33  | CCGACGCCTACAATAAATCTG                | qRT-PCR of <i>Sb</i> PR10                |
| oAP34  | CATACACCACACACCGCATAGAG              | qRT-PCR of <i>Sb</i> PR10                |
| oAP37  | GTCCTCTCCCTTGTCAATTC                 | qRT-PCR of <i>Sb</i> LRR receptor        |
| oAP38  | GGATAATCGCAGTCACTCTC                 | qRT-PCR of <i>Sb</i> LRR receptor        |
| oAP39  | CGCATCAGGGCATTGTTG                   | qRT-PCR of <i>Sb</i> thaumatin           |
| oAP40  | CCGCAGGATTACTACGACATCTC              | qRT-PCR of <i>Sb</i> thaumatin           |
| oAP55  | CAGACGTGTCCGAGTTTC                   | qRT-PCR of <i>Sb</i> ubiquitin           |
| oAP56  | CTCTCCTGTTGGCAGATG                   | qRT-PCR of <i>Sb</i> ubiquitin           |
| oAP57  | GTTGTTCCGCCCTGGTGGTTC                | qRT-PCR of <i>Sb</i> GAPDH               |
| oAP58  | CTGCTGCACCACAGCTCAAG                 | qRT-PCR of <i>Sb</i> GAPDH               |
| oAP59  | GTCACCGGCTCCTTCTTCAAC                | qRT-PCR of <i>Zm</i> chitinase           |
| oAP60  | GCTCCGGGTGTAGAAGTTCTTG               | qRT-PCR of <i>Zm</i> chitinase           |
| oAP63  | TTCAGTCACGCCTCTTCC                   | qRT-PCR of <i>Zm</i> thaumatin           |
| oAP64  | TTCGTTAGCCGTAGCAG                    | qRT-PCR of <i>Zm</i> thaumatin           |
| oAP65  | GCAAGGAAAGGAATTCATCTCTGCTA           | qRT-PCR of <i>Zm</i> Glucan synthase     |
| oAP66  | GTGTCCCACCCTTGTCTCAACCATAG           | qRT-PCR of <i>Zm</i> glucan synthase     |
| oAP67  | CTTCGGCATTGTTGAGGGTTTG               | qRT-PCR of <i>Zm</i> GAPDH               |
| oAP68  | TCCTTGGCTGAGGGTCCGTC                 | qRT-PCR of <i>Zm</i> GAPDH               |
| oAP85  | ATGCAACGGGATTCAGAG                   | qRT-PCR of <i>Zm</i> tubulin             |
| oAP86  | CAGCAGCAACGGAATAC                    | qRT-PCR of <i>Zm</i> tubulin             |
| oAP87  | AGACCCTGACTGGAAAAACC                 | qRT-PCR of <i>Zm</i> ubiquitin           |
| oAP88  | CGACCCATGACTTACTGACC                 | qRT-PCR of <i>Zm</i> ubiquitin           |

## **2.2 Methods**

### **2.2.1 Plant inoculation**

Prior to use, fungal strains were streaked on potato dextrose agar (Becton, Dickinson and Company- BD, Heidelberg, Germany) and kept at 28°C for 3-4 days. The strains were inoculated in 2 ml of YEPS light medium (1% tryptone, 1% yeast extract, and 1% sucrose) and maintained at 28°C with 200 rpm shaking for about 8 h. Then, the cultures were used to inoculate 50 ml of potato dextrose (2.4%) broth (BD, Heidelberg, Germany) and were incubated at 28°C overnight, until they reached an optical density at 600 nm ( $OD_{600}$ ) of 0.6 to 0.8. The fungal cultures were pelleted by centrifugation (Heraeus Multifuge X3R, Thermo Scientific) at 3500 rpm for 5 min, and the cell pellets were suspended in water to reach an  $OD_{600}$  of 2.0. Suspension cultures of SRZ1\_5-2 and SRZ2\_5-1, or SRS1\_H2-8 and SRS2\_H2-7 were mixed in a ratio 1:1 and the mixture was syringe-inoculated into the leaf whorls of 7 day old maize and 14 day old sorghum seedlings as described in Gilissen et al., 1992 (Fig. 3).

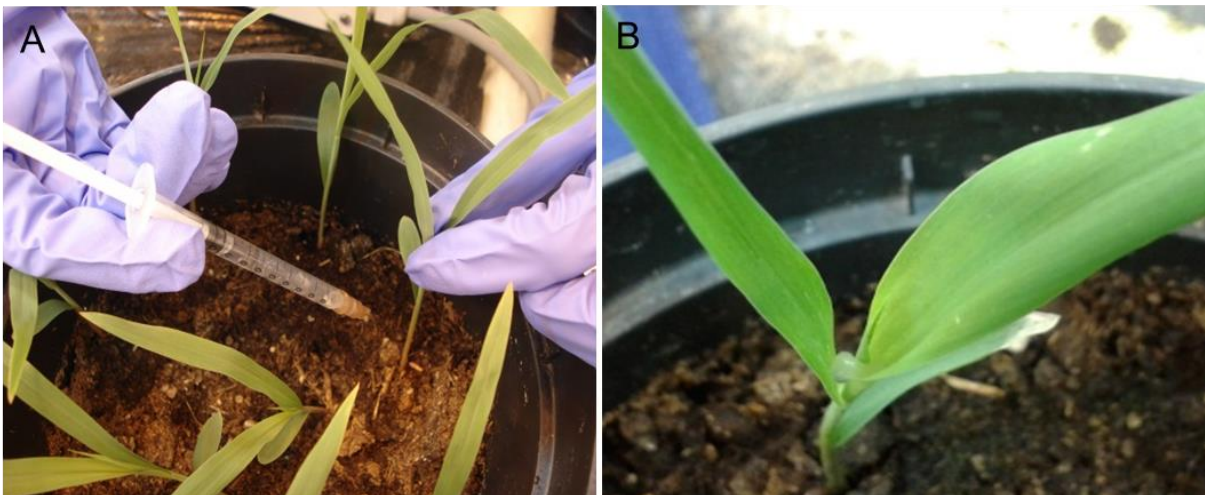


**Figure 3.** Inoculation of sorghum seedlings with a *S. reilianum* suspension. (A) The culture-mix is deposited on the inner leaf whole using a syringe. (B) A drop of culture that has emerged on top, indicating that the fungal suspension is in contact with the surface of the most inner leaf.

### **2.2.2 Microscopic characterization of plant infection**

Several parts of the sorghum and maize plants were collected for microscopic analysis, including inoculated leaf blades, ligules, leaves, and stems containing the nodes and floral meristems. The tissues were collected at different time points between 4 and 75 days after inoculation. The samples were either directly used for light microscopic analysis, or were stained with WGA-Alexa Fluor 488 (Doehlemann et al., 2008a) prior to analysis by fluorescence microscopy.

For staining, samples were soaked in ethanol overnight and then treated with 10% KOH at 90°C for at least 4 hours. The material was washed in phosphate-buffered saline (PBS; 137 mM NaCl, 2.7 mM KCl, 4.3 mM Na<sub>2</sub>HPO<sub>4</sub>, 1.47 mM KH<sub>2</sub>PO<sub>4</sub>, pH 7.4) and incubated in a staining solution containing WGA-Alexa Fluor 488 (Molecular Probes, Invitrogen, Karlsruhe, 10 mg/ml), propidium iodide (20 mg/ml), and Tween 20 (0.2 µl/ml) in PBS for about 30 minutes, being vacuum infiltrated three times for 2 minutes each during this time. The samples were analysed by microscopy using an Axio Observer Z1 microscope (Zeiss) equipped with filters FITC (EX BP 475/40, BS FT 500, EM BP 530/50) for detection of WGA-Alexa Fluor, and Cy3 (EX BP 545/25, BS FT 570, EM BP 605/70) for detection of propidium iodide.

### **2.2.3 Genomic DNA extraction from *S. reilianum***

The protocol used for DNA extraction was modified from Hoffman and Winston, 1987. Initially, single colonies of *S. reilianum* were inoculated in YEPS light medium and kept at 28°C with 200 rpm shaking for 36-40 h. The culture was centrifuged together with 200 µl glass beads at 13000 rpm for 5 min. The supernatant was removed and the pellet was frozen at -20°C for about 20 min. The pellet was suspended in 500 µl *Ustilago* lysis buffer and 600 µl phenol-chloroform mixture (1:1), vortexed for 15 min and centrifuged at 13000 rpm for 25 min. The upper phase was collected and the DNA was precipitated with 1 ml of ethanol 96%, followed by centrifugation at 13000 rpm for 15 min. The pellet was dried at room temperature and suspended in 50 µl TE with 20 mg/ml RNase A at 55°C for 15 min and then stored at -20°C.

### **2.2.4 Genomic DNA extraction from infected maize and sorghum**

For quantification of fungal DNA in plant material, maize and sorghum plants inoculated with SRS, SRZ or only water (mock inoculation) were harvested at 9 days after inoculation. For each experiment, 10 plants were harvested and pooled together for each condition, and the experiment was repeated 3 times, using a total of 30 plants per condition. Samples of 5 cm length were collected from different tissues (leaf blade, ligule, leaf sheath and stem). The plant material was frozen and ground in liquid nitrogen until a fine powder was obtained. From the powdery plant material, DNA was extracted using the DNeasy Plant Mini Kit (Qiagen, Hilden, Germany).

The quantification of fungal DNA in infected tissues was done by quantitative PCR, using an iCycler iQ system (Bio-Rad). Oligonucleotides oSP101 and oSP102 were used to amplify a 396-bp fragment of *S. reilianum* genomic DNA derived from the gene sr16559. This primer combination did not result in any PCR product if used on sorghum or maize genomic DNA. As reference genes, the sorghum actin gene *SbActin* was amplified using oligonucleotides oJI008 and oJI009 (Zuther et al, 2012), while in maize *ZmActin* gene was amplified with primers oBH73 and oBH74 (Reinecke et al., 2008). A 25- $\mu$ l reaction mixture was composed of 1X NH<sub>4</sub>-reaction buffer, 2 mM MgCl<sub>2</sub>, 0.25 U BIOTaq DNA polymerase, 100  $\mu$ M dNTPs (all from Biotline, Luckenwalde, Germany), and 0.2X SYBR Green solution (Invitrogen, Karlsruhe, Germany), as well as 0.25  $\mu$ M of each oligonucleotide (Sigma-Aldrich), and 1  $\mu$ l of template DNA. PCR amplification was carried out with an initial denaturation of 95°C for 6 min, followed by 40 cycles of 95°C for 30 s, 60°C for 1 min, plate read step at 72 °C, followed by product melting curve.

### **2.2.5 RNA extraction from infected maize and sorghum**

At 3 dai, leaf pieces of about 3 cm from inoculated and mock-inoculated maize and sorghum plants were collected. For each treatment, the tissue of eight plants was pooled, and the experiment was conducted three times. The samples were macerated in liquid nitrogen until a fine powder was obtained, and 100 mg of the powder was used for RNA extraction.

The RNA extraction was performed using the Trizol method. For that, 1 ml of Trizol (Sigma) was added to the sample, mixed and kept at room temperature for 15 minutes. Then, 300  $\mu$ l of chloroform was added, the mixture was centrifuged at 13000 rpm for 15 min, and the upper phase was collected and mixed with the same volume of phenol: chloroform: isoamyl alcohol (25:24:1), being again centrifuged at 13000 rpm for 15 min. In the next step, the upper phase was collected, mixed with isopropanol and centrifuged for 15 min. The isopropanol was removed and the pellet was washed with 80% ethanol by inverting the tubes several times. The pellet was centrifuged for 10 min to remove any remaining ethanol and air dried at room temperature, being finally dissolved in 80  $\mu$ l RNase free water. A cleanup step was performed using the Qiagen RNeasy Plus Mini Kit and RNA samples were stored at -80 °C.

### **2.2.6 RNA quantification and cDNA synthesis**

The final RNA concentration was determined using a NanoDrop Spectrophotometer (Peqlab, Germany), and RNA integrity was confirmed using agarose gel-electrophoresis. One microgram of total RNA was subjected to cDNA synthesis using oligo(dT)<sub>18</sub> oligonucleotides (First Strand cDNA Synthesis Kit, Fermentas, Germany) following the manufacturer's protocol.

### **2.2.7 Polymerase Chain Reaction (PCR)**

PCR was performed using Taq polymerase to amplify a DNA fragment and to test oligonucleotides used in quantitative PCR. The amplification was done using a TPersonal thermocycler (Biometra) and the cycling conditions were set as follows: initial denaturation at 94°C for 2 min, denaturation at 94°C for 20 s, annealing 60-63°C for 20 s, extension at 72°C, using 1 min/kb and a final extension at 72°C for 10 min, totalizing 35 cycles. The reaction was composed as described below:

| <b>PCR component</b>    | <b>Quantity</b> |
|-------------------------|-----------------|
| DNA template            | 10-100 ng       |
| PCR buffer              | 2.5 µl of 10X   |
| dNTPs                   | 0.2 µl of 25 mM |
| Forward primer          | 0.5 µl of 10 µM |
| Reverse primer          | 0.5 µl of 10 µM |
| Taq polymerase          | 1.25 U          |
| DMSO                    | 0.75 µl         |
| 1.5 M MgCl <sub>2</sub> | 1.5 µl          |
| Water                   | remaining       |
| <b>Total</b>            | <b>25 µl</b>    |

### **2.2.8 Gel electrophoresis**

Nucleic acids were visualized and quantified by gel electrophoresis on a 0.8-2% agarose gel, using TAE (40mM Tris-Acetate, 1mM Na<sub>2</sub>-EDTA) or TBE (50mM Tris-Borate, pH 7.9, 1 mM Na<sub>2</sub>-EDTA). Agarose was weighed and boiled in 1X TAE or 0.5X TBE buffers until agarose melted. Roti®-GelStain (Carl Roth) was added to the gel (0.05 µl/ ml). The gel was poured in a closed cassette, solidified, and placed in an electrophoresis tank filled with the corresponding buffer. A mix of DNA or RNA and loading buffer (0,25% bromphenol blue, 10 mM HCl, pH 7.9, 1 mM Na<sub>2</sub>-EDTA) was loaded in the gel as well as 5 µl GeneRuler 1kb DNA ladder (Thermo Scientific).

### **2.2.9 Quantitative RT-PCR**

Real-time PCR assays were performed in a CFX 96 Thermal Cycler (Bio-Rad Laboratories, Hercules, CA, USA) in a 25-µl reaction mixture composed of 1x NH<sub>4</sub>-reaction buffer (Bioline), 3 mM MgCl<sub>2</sub>, 100 µM deoxynucleotide triphosphate, 0.4 µM of each gene-specific primer, 0.25 units BIOTaq DNA polymerase (Bioline), and 10.000 times diluted SYBR Green I solution (Cambrex). Primers used for several marker genes for plant defenses in maize and sorghum are cited in the Table 1. As

reference genes in sorghum actin, ubiquitin and GAPDH genes were selected, while for maize ubiquitin, GAPDH and tubulin were used. PCR conditions consisted of an initial denaturation at 95°C for 6 min, followed by 40 cycles of 95°C for 30 s, 60°C for 1 min, plate read step at 72°, then product melting curve at 55–95°C. Quantitative analysis was performed using the CFX96 Real Time PCR Detection System (Bio-Rad Laboratories). The amplification specificity of primers was confirmed by identification of a single peak in the melting curve analysis. Primers were designed using Clone Manager Professional Suite version 8. Expression ratios in samples of inoculated plants compared with mock-inoculated plants were calculated using the CFX Manager 3.0 (Bio-Rad). Statistical calculations were performed using Graph Pad software.

#### **2.2.10 Staining of plant material for H<sub>2</sub>O<sub>2</sub>, callose, lignin and plant cell death**

##### **Calcofluor/diaminobenzidine staining**

The detection of hydrogen peroxide was performed according to Thordal-Christensen et al. (1997). For that, leaf samples were collected at 18, 42 and 66 hours after inoculation (to get the production peaks at 1, 2 and 3 days after inoculation), washed with sterile distilled water, vacuum-infiltrated for 3 min in 3,3'-diaminobenzidine (DAB) solution in water (1 mg/ml, Sigma D3939), and then allowed to stain for 6 hours in the dark. As a control, leaves infiltrated with H<sub>2</sub>O<sub>2</sub> were stained with DAB. Sections were kept in ethanol for 48 h, washed three times in sterile distilled water, and soaked for 30 seconds in a solution of calcofluor white (10 mg/ml, Sigma) before mounting on microscope slides in 50% glycerol. H<sub>2</sub>O<sub>2</sub> was visualized as a reddish-brown coloration, while fungal surface structures were fluorescent under UV-illumination using the 4',6-diamino-phenylindole filter set (DAPI, EX BP 365, BS FT 395, EM BP 445/50).

### **Aniline blue staining**

For detection of callose, infected leaves were collected at 1 and 2 days after inoculation and soaked overnight in ethanol. The samples were then incubated for 1 h in a staining solution containing aniline blue (0,005%) in 50 mM phosphate buffer pH 8,2. The material was analysed by epifluorescence microscopy using the DAPI filter set (EX BP 365, BS FT 395, EM BP 445/50). Callose was visualized in tissue sections through the formation of an intense blue, UV light–induced fluorescence with the aniline blue fluorochrome (Stone et al., 1985).

### **Phloroglucinol staining**

For visualization of lignin, the phloroglucinol/HCl (PGH) test was performed (Vallet et al., 1996). Leaf slices were incubated for 5 min in a solution of 2% (w/v) phloroglucinol in ethanol 20%. Samples were mounted in a few drops of 6N hydrochloric acid in microscopy slides. The stained sections were observed immediately by light microscopy. Lignified structures appeared red-orange color.

### **Trypan blue staining**

Plant cell death (PCD) was observed using lactophenol-trypan blue, according to Koch and Slusarenko (1990). For that, leaf slices were boiled for 3 min in lactophenol trypan blue stain (10 ml of water, 10 ml of lactic acid, 10 ml of glycerol, 10 ml of phenol, 10 mg of trypan blue) and stored in this solution overnight. The samples were destained with 2.5 g/ml<sup>-1</sup> chloral hydrate overnight, being observed by light microscopy.

### **2.2.11 Sample preparation and transmission electron microscopy (TEM)**

Infected leaves were collected at 3 dai, cut in small pieces of 0.5-1 cm, and kept in phosphate buffered saline (PBS). For the fixation, first the PBS was exchanged for a solution of glutaraldehyde 2.5% in water and kept on ice. During this step, samples were vacuum-infiltrated several times until the shiny appearance of the leaf surface

was gone, and then stored overnight at 4°C. The second step was performed exchanging the glutaraldehyde solution for 1 % aqueous osmium tetroxyd solution, where the samples were kept for 90 min at room temperature. Afterwards, samples were washed in water and subjected to several steps of ethanol dehydration (Table 2). The last step was the embedding, first performed in a mixture of ethanol and LR White resin (1:2) and then a second step used pure LR White resin.

**Table 2.** Steps for dehydration and embedding of samples prior to TEM.

| <b>Step</b>                                   | <b>Incubation time</b> | <b>Temperature</b> |
|---|------------------------|--------------------|
| <b>Dehydration</b>                            |                        |                    |
| 15 % (w/v) ethanol in H <sub>2</sub> O bidest | 15 min                 | 4 °C               |
| 30 % ethanol                                  | 30 min                 | 4 °C               |
| 50 % ethanol                                  | 30 min                 | - 20 °C            |
| 70 % ethanol                                  | 30 min                 | - 20 °C            |
| 95 % ethanol                                  | 30 min                 | - 20 °C            |
| 100 % ethanol                                 | two times 30 min       | - 20 °C            |
| <b>Embedding</b>                              |                        |                    |
| 33,3 % ethanol/66,6 % LR white resin          | 2 h                    | 4 °C               |
| 100 % LR white resin                          | overnight              | 4 °C               |

After embedding, samples were transferred to capsules filled with fresh LR White resin and arranged in parallel inside the capsule, in order to perform transverse cuts. The polymerization of embedded samples was performed at 50 °C for 24 h. Then, polymerized samples were trimmed with a diamond milling cutter until a pyramid-like form was obtained, and the tip was also removed. The trimmed samples were then brought to an ultramicrotome equipped with glass knives, where ultra-thin cuts were obtained. First, 2 µm cuts were performed, collected with an eyelash, deposited in microscope slides and stained with a 0.1 % solution of toluidine blue O. These samples were checked by light microscopy to verify the presence of fungal structures and the quality of the samples. Then, ultra-thin cuts of 90 nm were produced and deposited on support metal grids with 3.05 mm of diameter and coated with a Formvar film. The cuts were stained with a solution of 4% uranyl acetate (UO<sub>2</sub>(CH<sub>3</sub>COO)<sub>2</sub>), a negative staining that was used to contrast the sections. For

that, droplets of the solution were deposited on a piece of Parafilm and the grids were placed with the cut-supporting side down on the solution for 5 min. The grids were then dried and stored in petri dishes until use.

### **2.2.12 Sample preparation for scanning electron microscopy (SEM)**

For SEM, infected leaf samples were collected at 1 dai for visualization of appressoria and at 3 dai for analysis of fungal cell wall. Infected leaves were cut in small pieces and mounted on aluminum stubs using O.C.T. compound (BDH Laboratory Supplies). Samples were then immersed in liquid nitrogen at  $-210^{\circ}\text{C}$  to preserve the material, and then put in a cryostage of a cryotransfer system attached to a Field Emission Scanning electron microscope SIGMA VP (Zeiss). Samples were sublimated for 10-12 min at  $-95^{\circ}\text{C}$  and then a sputtering with platinum was performed for 60 seconds. Samples were moved to the cryostage in the main chamber of the microscope and imaged.

### **2.2.13 Laser microdissection (LMD)**

Infected sorghum leaves were collected at 4 days after infection, cut in small fragments of about 0.5 cm and fixed (Kerk et al., 2003). First, samples were infiltrated in a mixture of 3:1 ethanol: acetic acid for 20 minutes. The samples were stored in the solution overnight and the procedure was repeated. Then, a cryoprotection step was carried out, where the samples were infiltrated in a solution of sucrose 10% for 15 minutes and stored for 1 hour at  $4^{\circ}\text{C}$  and the step was repeated using sucrose 15%.

The fixed samples were mounted in a cryomold to allow transverse cuts, embedded in tissue freezing medium (TFM) and kept at  $-80^{\circ}\text{C}$ . Samples were sectioned in a cryostat (HM525 NX Cryostat, Zeiss) at  $-21^{\circ}\text{C}$  and collected on UV-treated poly-L-lysine slides (Sigma). The slides were placed in a jar containing EtOH 70% for 5 minutes, quickly washed in Diethylpyrocarbonate (DEPC) water, then placed in EtOH 100% for 2 minutes. Samples were dried at room temperature for 15 minutes and stored at  $-80^{\circ}\text{C}$ .

Laser microdissection was performed in order to collect mesophyll cells and vascular bundles using a laser microbeam system (PALM Microbeam, Zeiss). For cutting, the 40-fold magnification was selected, with the following parameters: auto-LPC focus 60, with energy of 50 and a speed of 59. Groups of about 6000 cells were collected on the lid of a 0.5 ml reaction tube and immediately subjected to lytic digestion and posterior RNA extraction using RNeasy plant micro kit (Qiagen).

#### **2.2.14 Cell separation by mechanical methods**

In addition to LMD, mechanical methods were used to separate vascular bundles and mesophyll cells from infected sorghum leaves. For vascular bundle isolation, a protocol developed by Chang et al. (2012) was adapted. Infected leaves were sliced in small fragments and added to 50 ml of isolation medium (0.6 M sorbitol, 50 mM Tris-HCl pH 8.0, 5 mM EDTA, 0.5% polyvinylpyrrolidone-10, 10 mM DTT, and 100 mM  $\beta$ -mercaptoethanol) on ice and homogenized twice in a Waring blender. The mixture was then filtered through a 500- $\mu$ m mesh and the tissue retained was added to new isolation medium, where the previous step was repeated. The liquid that passed through the mesh was filtered through an 80- $\mu$ m nylon net, where the vascular bundles were saved, collected and frozen in liquid nitrogen.

For mesophyll separation, the protocol described by Covshoof et al. (2012) was used with some modifications. For this method, 5 cm leaf slices were placed on top of glass plates kept on ice, and a wallpaper seam roller was used to press the leaf. The fluid that emerged was collected by pipetting and deposited in 2 ml tubes containing RNA free water, and was immediately frozen at -80 °C.

#### **2.2.15 Transcriptome analysis**

The sequencing of mRNA was performed with maize and sorghum leaves infected with SRS, SRZ or water treated (mock). The RNA was extracted as described before (2.2.5) from 3 biological replicates containing 10 plants each and pooled prior to sequencing. Illumina sequencing was performed by external companies (GATC for sorghum and Beckman Coulter for maize) using the paired-end sequencing protocol.

Read files were imported into CLC genomics workbench version 6 and trimmed with the software tool by ambiguous bases, quality, and Illumina adapter sequences. Reads shorter than 11 bp were discarded. The resulting reads were mapped to three genome references in sorghum: *S. reilianum* 5-1, *S. reilianum* H2-8 (unpublished) and *Sorghum bicolor* (Sbicolor\_79, Paterson et al., 2009). In maize, the reads were mapped to the reference genome of *Zea mays* (maize B73, Schnable et al., 2009) and either *S. reilianum* 5-1 or *S. reilianum* H2-8.

In sorghum, unmapped reads were de-novo assembled into new contigs, whose function was searched by blast using ncbi database and a new annotation file was created. A new mapping with the same settings was performed against the three genomes and the newly assembled contigs. RPKM were also calculated using CLC Genomics Workbench. The extension package edgeR 1.6.5 was used to calculate the log fold change (logarithm 2 of the fold-change of a tag count between two samples), p and FDR (false discovery rate) values. Comparisons were made between grouped samples (SRS-infected plants, SRZ-infected plants, control). Genes with p-value  $\leq 0.05$  were considered significantly regulated. Gene annotation was obtained from maize GDB (<http://www.maizegdb.org/>), Plant GDB (<http://www.plantgdb.org/ZmGDB/>), or Phytosome (<http://www.phytozome.net>) when available. Genes that did not present annotation were subjected to blast search on NCBI (<http://blast.ncbi.nlm.nih.gov/Blast.cgi>). Gene ontology enrichment (GO) was performed for genes that showed significant expression change using the AGRIGO tool kit (<http://bioinfo.cau.edu.cn/agriGO/>). The GO terms that were overrepresented (FDR  $\leq 0,5$ ) were used for the construction of pathway maps.

### **3. Results**

#### **3.1 The fungal side of the interaction: colonization of maize and sorghum by *S. reilianum***

##### **3.1.1 *S. reilianum* f. sp. *reilianum* successfully infects sorghum, while *S. reilianum* f. sp. *zeae* does not trigger symptoms in sorghum inflorescences**

To investigate the interaction of sorghum and maize with the two *ff. ssp.* of *S. reilianum*, I started conducting a macroscopic analysis of symptoms and fungal spread in the host. To this end, seedlings of sorghum and maize were inoculated with a mixture of the compatible haploid *S. reilianum* f. sp. *reilianum* strains SRS1\_H2-7 and SRS2\_H2-8 (hereafter referred to as SRS) or a mixture of compatible haploid *S. reilianum* f. sp. *zeae* strains SRZ1\_5-2 and SRZ2\_5-1 (hereafter referred to as SRZ).

Sorghum leaves inoculated with SRS did not show visual signs of plant defense at 4 days after inoculation (dai) and only a weak chlorosis could be observed near the inoculation point (Fig. 4A), although fungal hyphae were colonizing the leaf tissues (Fig. 4A, inset). However, at 35 dai, the apical growing point that normally forms the developing inflorescence was replaced by a small sorus surrounded by a white peridium (Fig. 4B) in more than 90% of the plants evaluated (n=20). When the inflorescence emerged at 75 dai, the sorus had grown in size and released the dark brown teliospores of SRS (Fig. 4C). On the other hand, sorghum seedlings inoculated with SRZ at 4 dai showed leaf blades covered with red spots that intensified in color and spread over larger parts of the leaf at later time points (Fig. 4D). The appearance of red spots indicated the production of phytoalexins luteolinidin and apigenidin (Zuther et al., 2012). Fungal hyphae in leaf blades were stained in red and had an uneven morphology, showing varied thickness and bulbous or forked tips (Fig. 4D, inset).

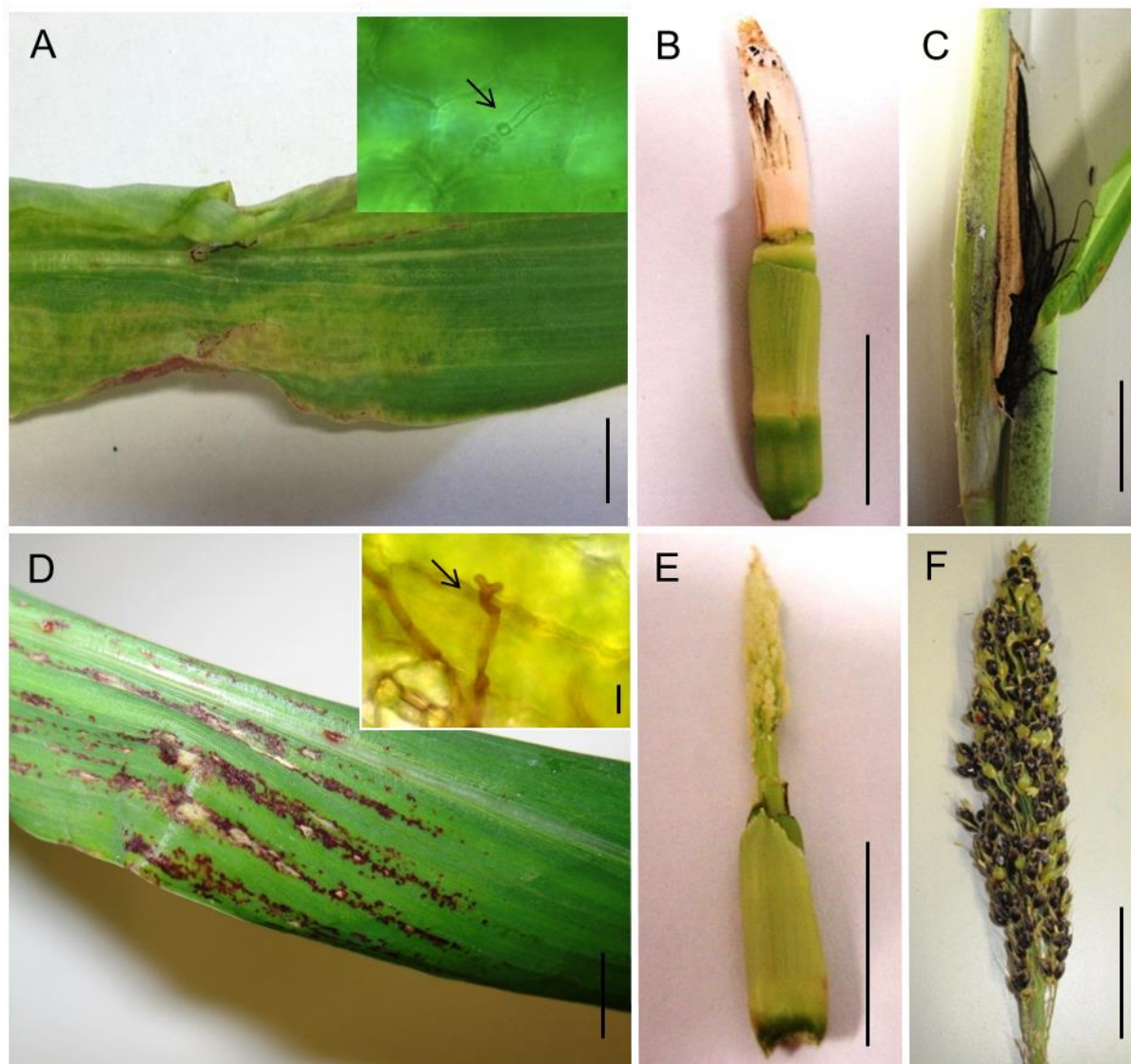


**Figure 4.** Macroscopic symptoms on sorghum after inoculation with the different *ff.ssp.* of *S. reilianum*. Seedling plants were syringe inoculated with SRS (A, B, C) or SRZ (D, E, F). Shown are inoculated leaves at 4 dai (A, D) with examples of fungal hyphae (insets), apical growing points at 35 dai (B, E), and inflorescences at 75 dai (C, F). SRS-inoculated plants showed only chlorosis on leaves (A) but resulted in infected meristems (B) and spore formation in the apical inflorescence (panicle, C), while SRZ-inoculated plants displayed phytoalexin accumulation in leaves (D) and produced healthy meristems (E) and inflorescences containing normal seeds (F). Bars: 1 cm in A - F, and 20  $\mu$ m in the insets in A and D. Arrows show fungal hyphae.

At 35 dai, growing points of SRZ-inoculated plants showed the presence of a healthy developing inflorescence (Fig. 4E) in all samples analysed (n=20). At 75 dai, all plants (n=20) harbored viable seeds after inflorescence emergence (Fig. 4F) and no fungal spores were observed. This confirms that SRZ is not able to cause head smut

disease on the tested sorghum variety. Instead, its presence induces the generation of phytoalexins, a plant defense reaction that is not induced by SRS.

To investigate if this behavior, where SRS is able to infect sorghum and SRZ is not, was only observed in the tested sorghum variety (Tall Polish), I assayed different varieties of sorghum and Sudan grass. The varieties tested were Super Dolce 15 (Sorghum x Sudangrass), *S. bicolor* Emese, *S. saccharum* Super Sile 20, *S. bicolor* Zerberus, Sudangrass Jumbo (hybrid of *S. bicolor* x *S. sudanense*), and three African varieties of white sorghum: Sila, LuluD and Epuripur.



**Figure 5.** Different sorghum varieties infected with *S. reilianum*. SRS (A-D) or SRZ (E-H). Sorghum varieties shown are Super Dolce 15 (A, E), Körner hirse Emese (B, F), Super Sile 20 (C, G), Sudangrass Jumbo (D, H). Infections are observed for sorghum varieties inoculated with SRS, while plants inoculated with SRZ produced healthy flowers. Sudangrass Jumbo presented healthy flowers when infected with SRS and SRZ.

Although described as early flowering varieties (predicted to flower at 3,5 months after sowing), Sila, LuluD and Epuripur did not produce flowers even after more than seven months of cultivation under the conditions tested in the greenhouse, so it was

not possible to score the virulence of *S. reilianum* in these plants. The varieties Super Dolce 15, Emese and Super Sile 20 showed infections very similar to the ones observed in Tall Polish, where flowers of SRS-infected plants showed spores, and SRZ-infected plants presented always healthy flowers (Fig. 5). Only one plant of the variety *S. bicolor* Zerberus produced a panicle after more than 9 months of cultivation. This plant had been inoculated with SRS and the panicle contained spores of SRS. The Sudan grass Jumbo yielded healthy flowers when infected with either SRS or SRZ. In summary, SRS was virulent in the sorghum varieties Tall Polish (the variety used in the previous experiment), Super Dolce 15, Emese, Super Sile 20, and Zerberus, while SRZ was not virulent in any of the tested varieties, indicating that the results obtained for SRS and SRZ on Tall Polish might be generally valid for the interaction of SRS and SRZ with sorghum.

### **3.1.2 SRZ causes head smut in maize cobs and tassels, while SRS only induces phyllody in cobs as the strongest symptom**

In the same manner as in sorghum, maize seedlings were inoculated with SRS or SRZ. Maize inoculated with SRS presented a weak and diffuse discoloration on the inoculated leaves at 4 dai (Fig. 6A). At 21 dai, the young cobs did not present spores, but instead of flowers showed phyllody, that is a morphological modification in the form of leafy-like structures (Fig. 6B) in about 70% of the evaluated plants (n=20). The tassels that appeared showed a healthy morphology in all plants evaluated (Fig. 6C). In contrast, maize seedlings inoculated with SRZ presented a very strong chlorosis near the inoculation point (Fig. 6D). At 21 dai, about 60% of the young cobs already exhibited characteristic black spores, whose distribution and quantity varied between the samples (Fig. 6E). At the same time point, some tassels showed phyllody and spores (Fig. 6F), but the quantity of infected tassels was much smaller than the cobs. The macroscopic observation confirmed that SRZ causes head smut in maize, while SRS does not, being only able to induce developmental modifications in maize cobs.

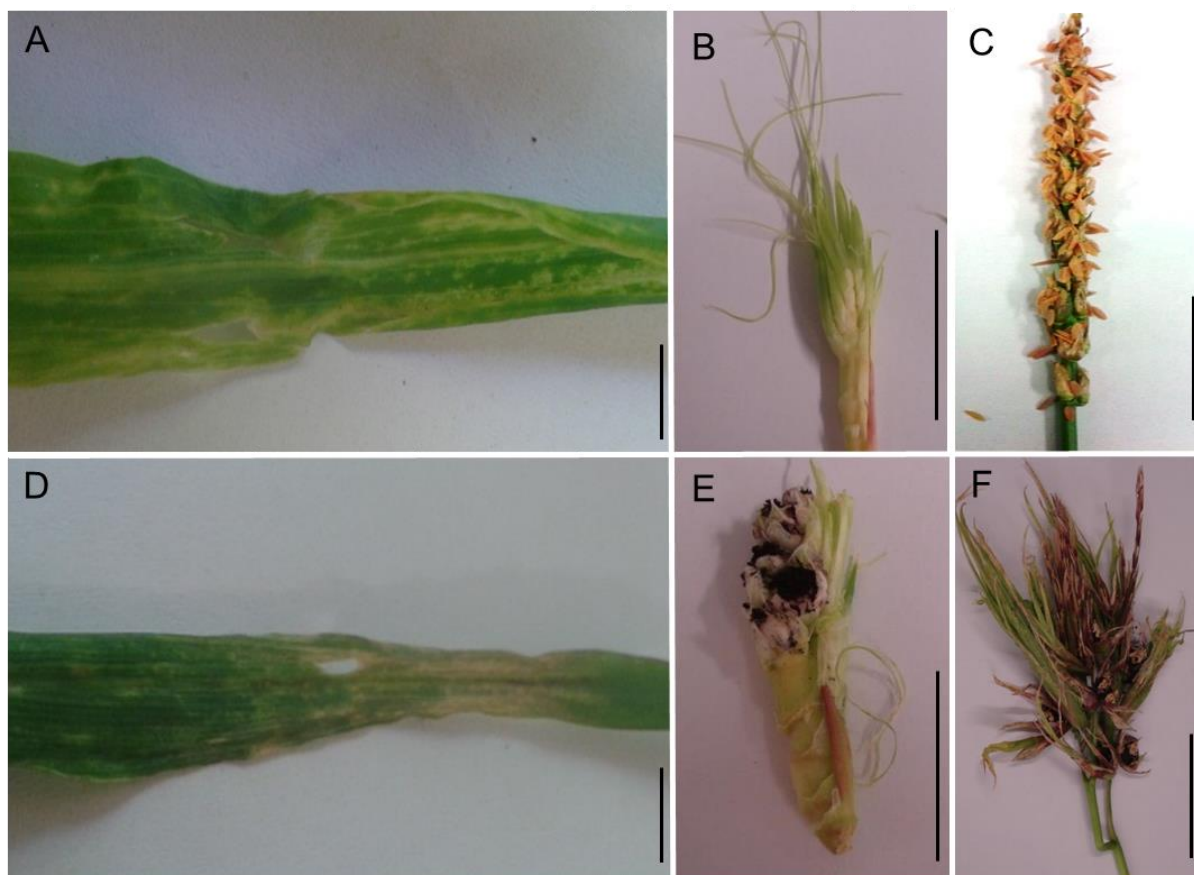


**Figure 6.** Macroscopic symptoms on maize after inoculation with *S. reilianum*. Seedling plants were syringe-inoculated with SRS (A, B, C) or SRZ (D, E, F). Shown are inoculated leaves at 4 dai (A, D), young cobs at 21 dai (B, E) and tassels at 21 dai (C, F). SRS-inoculated plants showed weak chlorosis on leaves and leafy structures in cobs, while SRZ-inoculated plants presented strong chlorosis on leaves and produced infected cobs and tassels. Bars: 1 cm

### **3.1.3 Sorghum stems are colonized only by SRS**

To further investigate the behavior of *S. reilianum* during plant colonization, a comparison of both strains in maize and sorghum was performed by fluorescence microscopy of stained samples taken from different tissues and collected at different time points. For staining, a combination of WGA-Alexa Fluor 488 and propidium iodide was used. WGA-Alexa Fluor stains fungal structures in green, while propidium iodide stains plant cells and dead fungal hyphae in red.

At 4 dai, both strains had efficiently spread into sorghum leaves and hyphae were found colonizing mesophyll and vascular bundles (Fig. 7A, B). However, while SRS seemed to have a preference for vascular bundles, hyphae of SRZ did not show such

a pronounced inclination and were more prominent in the mesophyll areas in between neighboring vascular bundles (Fig. 7A, B). At 9 dai, hyphae of SRS colonized bundle sheath cells and vascular bundles in leaf sheaths of inoculated leaves, while hyphae of SRZ were found in mesophyll and bundle sheath, but rarely in vascular cells (Fig. 7C, D). When the stem tissue was investigated at 15 dai, hyphae of SRS were readily visible colonizing bundle sheaths and vascular bundles near the growing point of the plant (Fig. 7E, G). However, in stem tissue of plants inoculated with SRZ no hyphae could be observed (Fig. 7F, H). These results suggest that SRS penetrates sorghum leaves, reaches nodes and apical meristems, and produces spores in inflorescences. SRZ, on the other hand, penetrates the plant, grows on the leaves but stops inside the leaf sheaths of inoculated leaves, being not able to reach nodes and apical meristems, what results in healthy panicles.

Moreover, microscopy of vascular bundles localized in lower parts of the infected leaves showed differences in distribution and morphology of hyphae. SRS-infected leaves displayed heavy colonization in bundle sheath cells and vascular bundles (Fig. 8A, C, E). In SRZ-infected leaves, several events showed vascular bundles presenting only few or even a single hypha that often exhibited deformities (Fig. 8B, D, F). This indicates that SRS efficiently colonize vascular bundles, while SRZ may have difficulty to grow into this tissue.

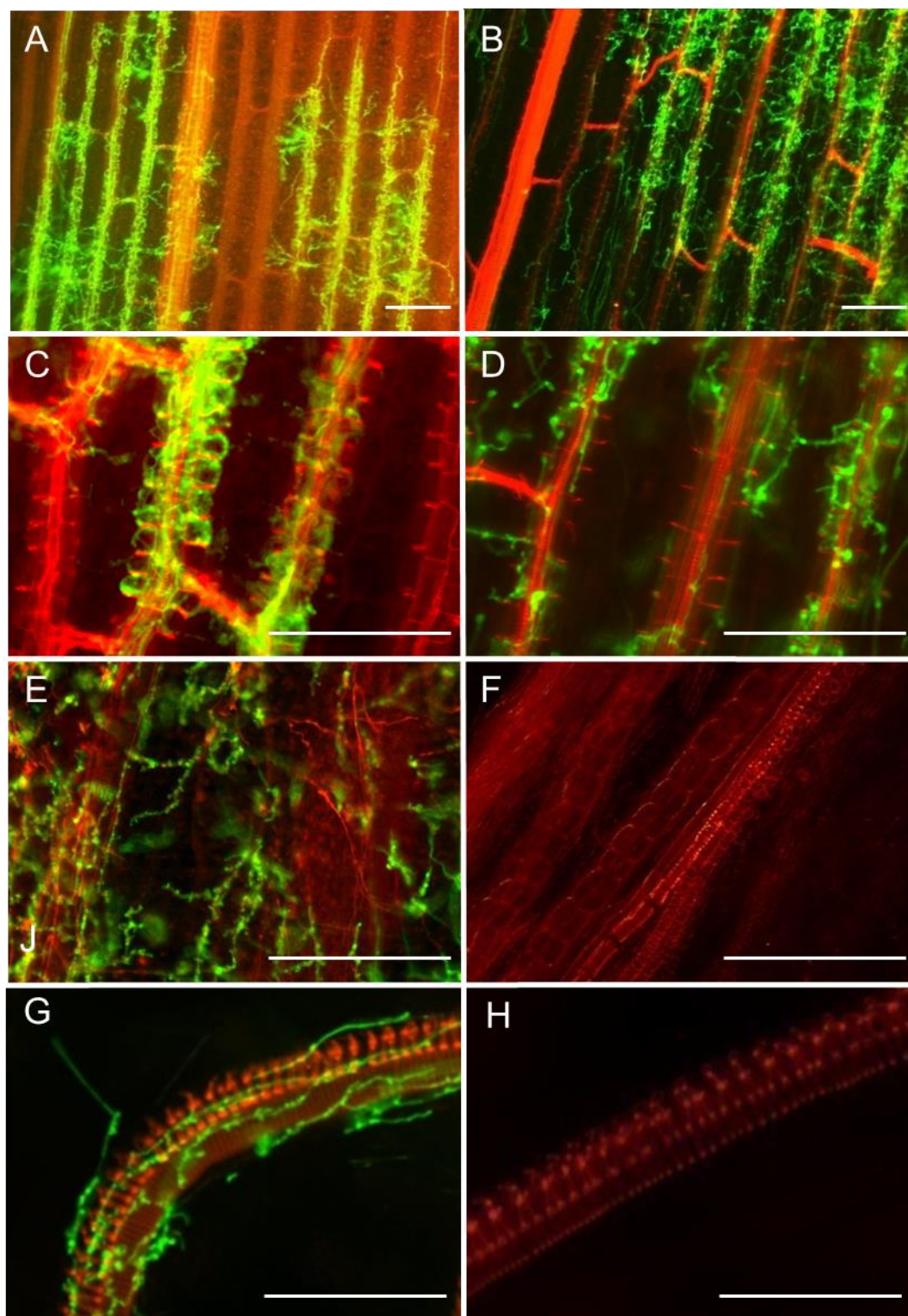


**Figure 7.** Microscopic characterization of sorghum infection by SRS and SRZ. Seedling plants were syringe-inoculated with SRS (A, C, E, G) or SRZ (B, D, F, H). Samples were collected from inoculated leaves at 4 dai (A, B), leaf sheath at 9 dai (C, D) and stems at 15 dai (E, F, G, H). Plant cells and dead hyphae are stained with propidium iodide and appear red, fungal structures are stained with WGA-Alexa Fluor-488 and appear green. Samples inoculated with SRS show hyphae colonizing leaves and reaching the nodes and apical meristem, while SRZ infects leaves and leaf sheaths, but does not reach the nodes and apical meristems. Bars: 100  $\mu$ m

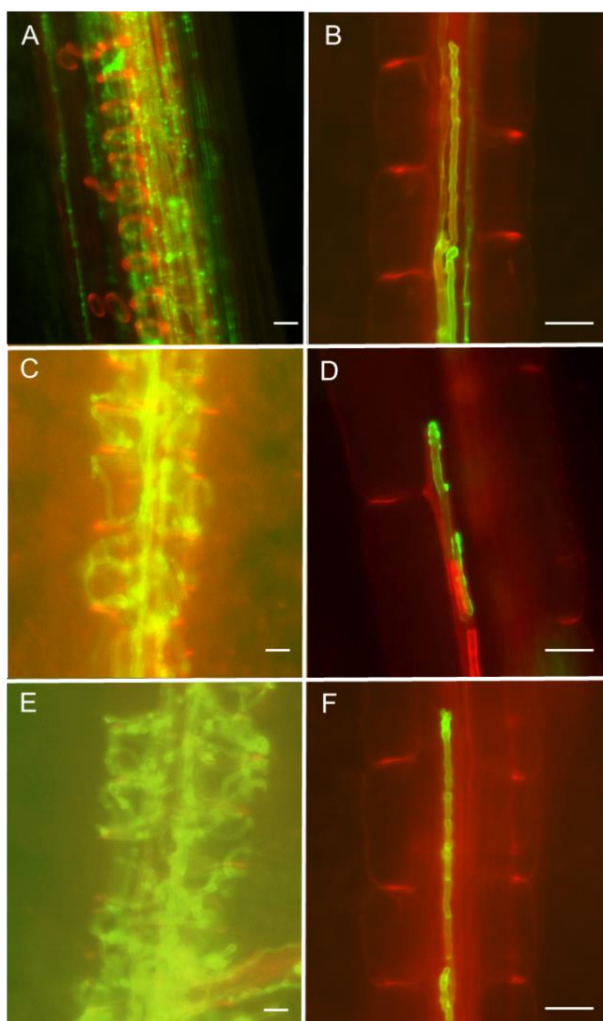


**Figure 8.** Fluorescence microscopy of vascular bundles infected with SRS or SRZ at 9 dpi. Samples infected with SRS (A, C, E) show heavily colonized vascular bundles, while SRZ hyphae (B, D, F) are found in lower amounts and present deformities. Bars: 10  $\mu$ m.

### **3.1.4 Both SRS and SRZ can reach maize stems**

In maize, SRS penetrated the plant and grew inside the leaves (Fig. 9A), although the quantity of hyphae observed was not very high. Nevertheless, the fungus colonized the entire leaf and reached the plant stem, despite the presence of many dead hyphae (Fig. 9C). SRZ colonized leaves and showed a good spreading capacity (Fig. 9B), which was also observed inside plant stems (Fig. 9D). This way, a different scenario was observed in this host, since both SRS and SRZ were able to penetrate, proliferate and reach maize stems.

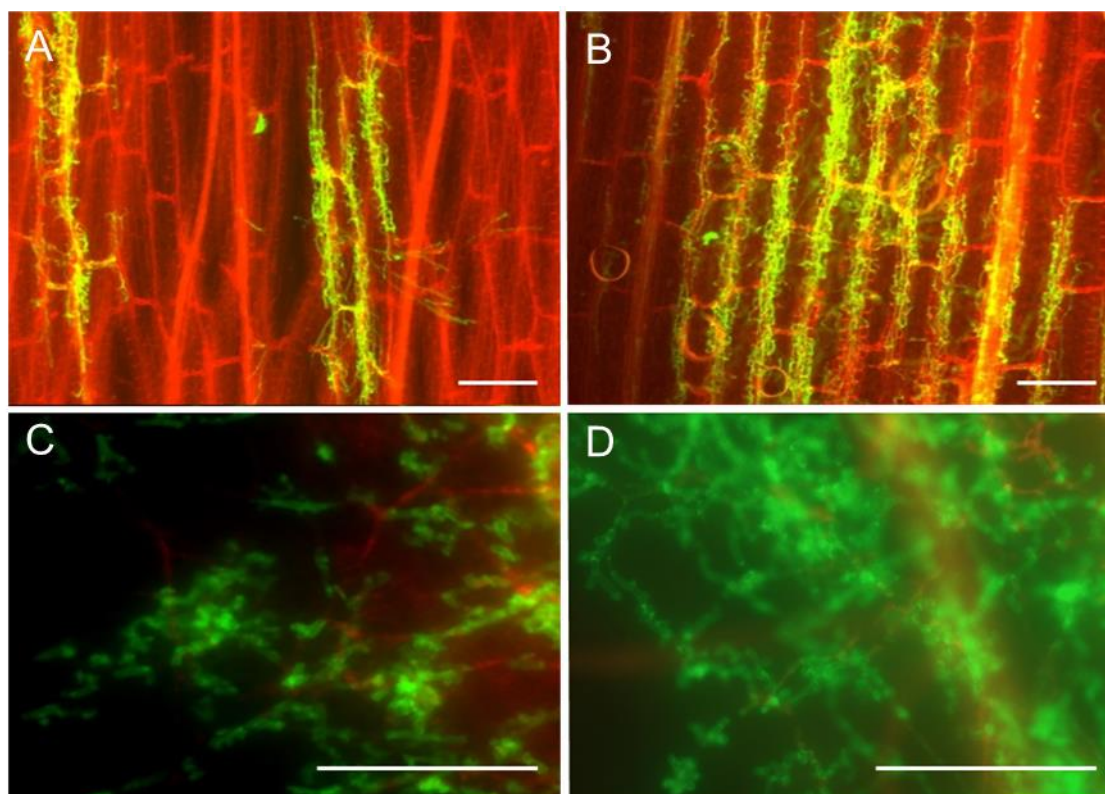


**Figure 9.** Microscopic characterization of maize colonization by SRS and SRZ. Seedling plants were inoculated with SRS (A, C) or SRZ (B, D), and samples were collected at 4 dai from infected leaves (A, B) and stems at 15 dai (C, D). Plants inoculated with SRS show hyphae (visible in green) colonizing leaf tissues (A) and reaching the nodes and apical meristem (C), where some dead hyphae are also observed. Leaves inoculated with SRZ show abundant fungal growth (B) and the pathogen reaches the nodes and apical meristems (D). Bars: 100  $\mu$ m

### **3.1.5 Quantification of fungal genomic DNA reveals contrasting proliferation behavior of SRS and SRZ in maize and sorghum**

To confirm the previous macroscopic and microscopic observations and investigate whether quantitative differences in fungal proliferation on maize and sorghum existed, fungal DNA was quantified by qPCR. Plants were collected at 9 dai from H<sub>2</sub>O-inoculated control plants and plants inoculated with SRS or SRZ. Samples were taken from the leaf blade near the inoculation site, the ligule and the sheath of the inoculated leaf, and the stem tissue containing the nodes and apical meristems. Genomic DNA was extracted and a 396-bp fragment of the gene *sr16559* from *S. reilianum* was amplified, which did not produce any product in non-inoculated maize and sorghum. Actin genes from sorghum and maize were used as references.

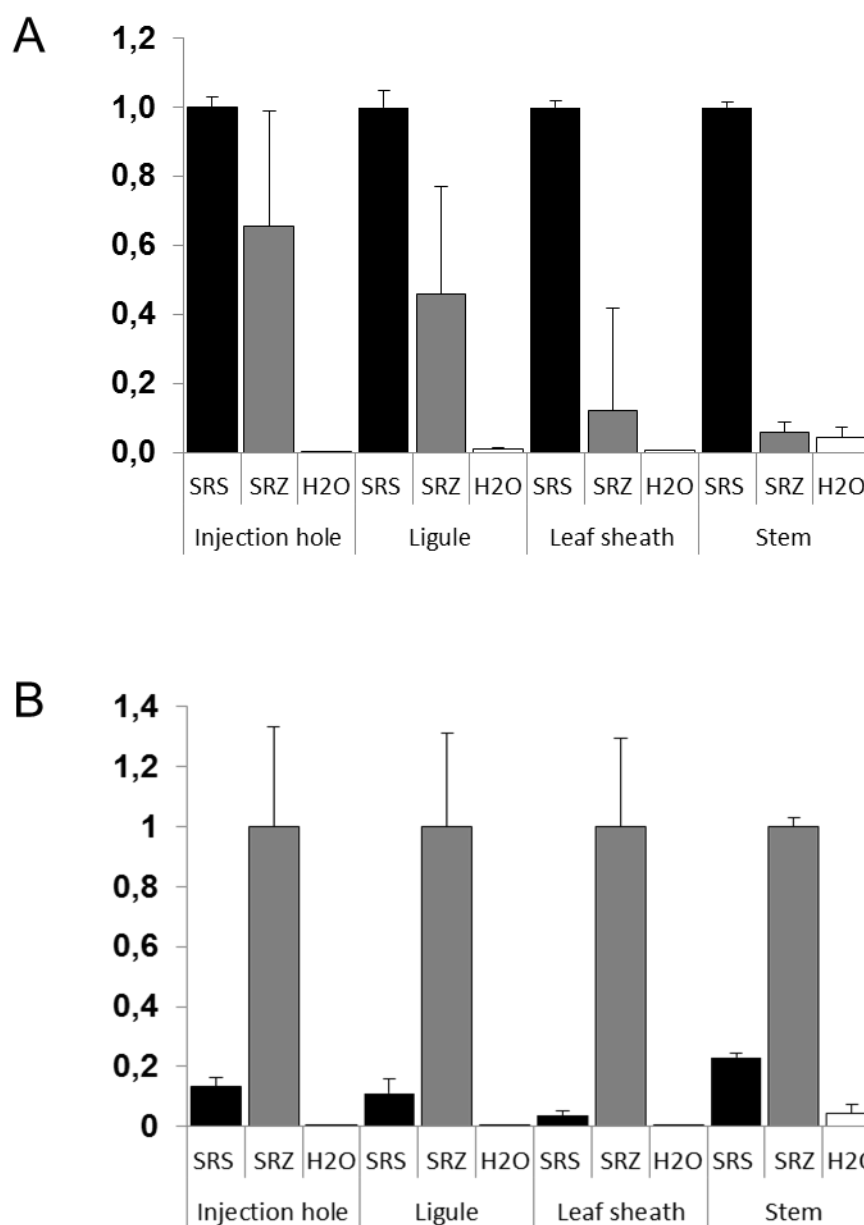


**Figure 10.** Quantification of fungal genomic DNA in sorghum and maize by quantitative PCR. (A) In sorghum, a high prevalence of DNA from SRS was observed in all tissues analysed, and a low concentration of SRZ DNA was found, relative to SRS-inoculated plants (B) In maize, SRZ was dominant in all tissues evaluated, and a lower quantity of SRS DNA relative to SRZ was found. SRS was also observed in maize nodes, what did not occur for SRZ in sorghum nodes.

In sorghum, quantitative PCR revealed a higher relative abundance of SRS in all tissues analysed, when compared to SRZ (Fig. 10A). The relative amount of genomic DNA of SRZ was already lower in the leaf blade and decreased even more in the other parts. In stems, DNA of SRZ could not be detected (Fig. 10A). This experiment

validated the visual impression gained by microscopy and confirmed that SRZ can colonize the inoculated leaf but is not able to reach the nodes and the apical meristem of sorghum plants. In maize, genomic DNA of SRZ was prevalent at the leaf inoculation point, and remained predominant in the ligule, leaf sheath and stems, when compared to SRS (Fig. 10B). In stems, a low quantity of SRS was detected, indicating a small but still measurable proliferation, which was also noticed by microscopic observations. Taken together, the quantification of fungal DNA showed that SRS is much less proliferative in maize than SRZ, but is able to reach stems, while the average amount of SRZ DNA in sorghum relative to SRS decreased from the inoculation point over the leaf sheath to the ligule and could not be detected in stems.

### **3.1.6 Transmission electron microscopy shows differences in SRS and SRZ cell wall thickness in maize**

Since both SRS and SRZ proliferated less well in their non-favored host, I wanted to know if there were differences in the region of contact between the fungus and plant or morphological differences in the fungal cell wall that were visible by transmission electron microscopy. Therefore, I collected infected maize and sorghum leaves at 3 dai and cut pieces of 0.5 x 0.5 cm that were fixed with glutaraldehyde and subjected to several steps of dehydration. Samples were then embedded in LR White resin and encapsulated. Ultra-thin cuts were obtained with an ultramicrotome and stained with uranyl acetate before microscopy. This experiment was performed at the Georg-August-Universität Göttingen, in cooperation with Dr. Michael Hoppert.

At 3 dai, intracellular growth of fungal hyphae was observed in sorghum (Fig. 11 and 12) and maize (Fig. 13), but some events of intercellular growth were also found (Fig.12B). Fungal hyphae were detected in epidermal cells (Fig. 13C), vascular bundles (Fig.11A-B; 12A, B; 13A) and mesophyll (Fig.11E- F; 12D, F; 13C, F). Fungal cell walls ranged in thickness, and variations were observed even within the same sample (Fig.11C-F). In some fungal cells, a white layer was immediately adjacent to the fungal cell wall (Fig.11E, 12F). This layer probably resulted from shrinking of the fungal cytoplasm during the process of samples preparation. Most fungal occurrences were characterized by a dark layer of fungal cell wall that was surrounded by a grey sheath (Fig. 11D, 12E). This grey layer indicates the interfacial

matrix that separates the fungal hypha from the plant plasma membrane (Fig. 13G). It was possible to observe vesicular-like structures within or connected to this sheath (Fig.12D).

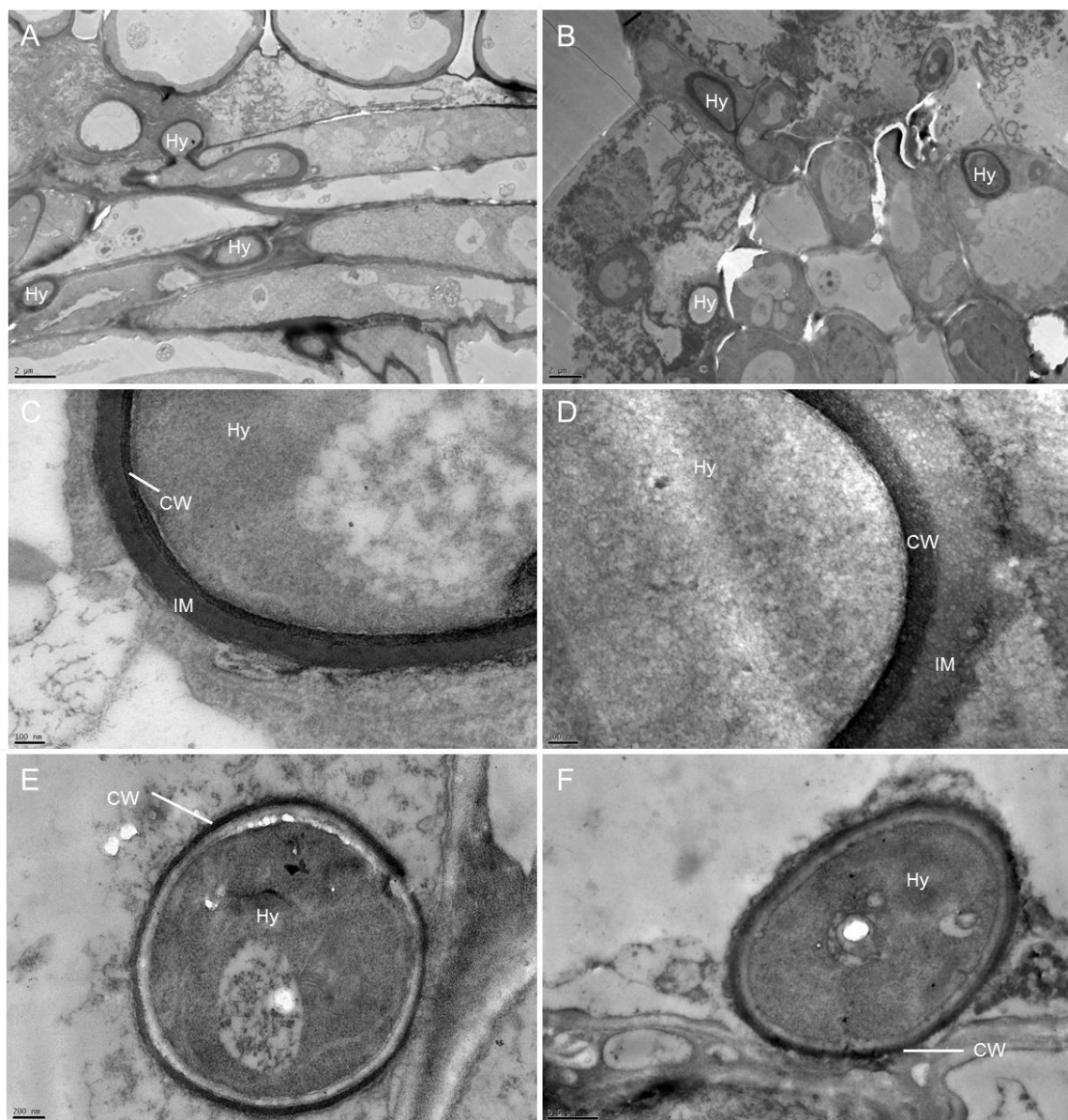


**Figure 11.** Electron micrographs of sections obtained from sorghum infected with SRS (A) Longitudinal section showing the fungus colonizing vascular bundles (B) Transverse section presenting fungal structures inside different cells of a vascular bundle (C) Magnification of the fungal cell wall showing the black layer and the grey interfacial matrix around, which is more evident in (D). (E) and (F) exhibit two different fungal hyphae, showing a white layer inside the cell wall and structures can be observed within the cell. Abbreviations are as follows: Chloroplast (C), Fungal cell wall (CW), Fungal hyphae (HY), Plant mitochondria (M), Plant nuclei (N), Vacuoles (V).

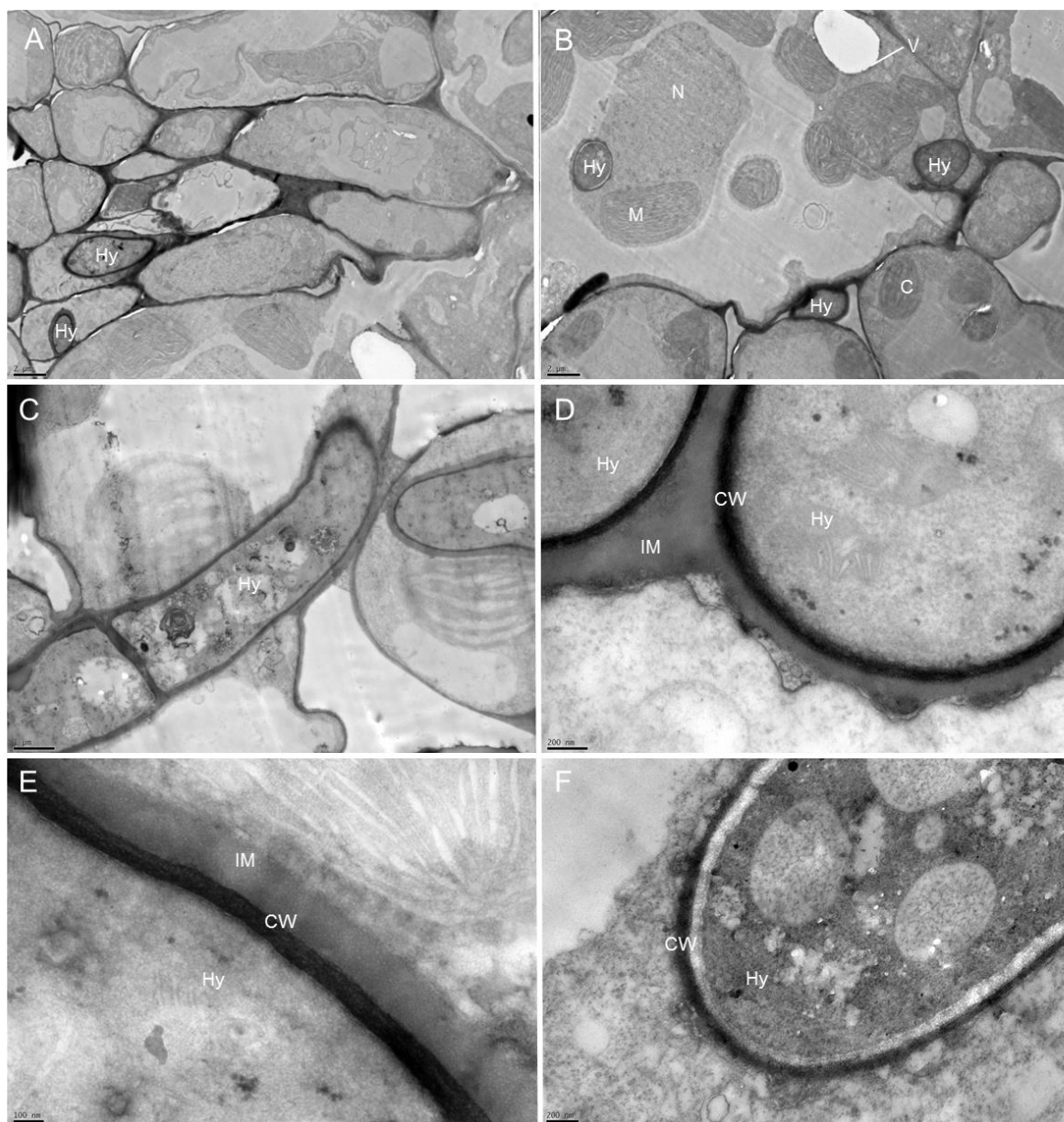


**Figure 12.** Electron micrographs of sections obtained from sorghum infected with SRZ. (A) Fungus growing inside vascular bundle cells. (B) Two hyphae are observed inside a huge bundle-sheath cell, but one hypha is also observed growing intercellularly in between three plant cells. (C) A longitudinal view of a hypha exhibiting a septum. (D) Two fungal hyphae showing the cell wall surrounded by the grey interfacial matrix. (E) Magnification of a fungal cell wall. (F) A fungal cell showing inner structures and the white layer connected to the cell wall. Abbreviations are as follows: Chloroplast (C), Fungal cell wall (CW), Fungal hyphae (HY), Plant mitochondria (M), Plant nuclei (N), Vacuoles (V).

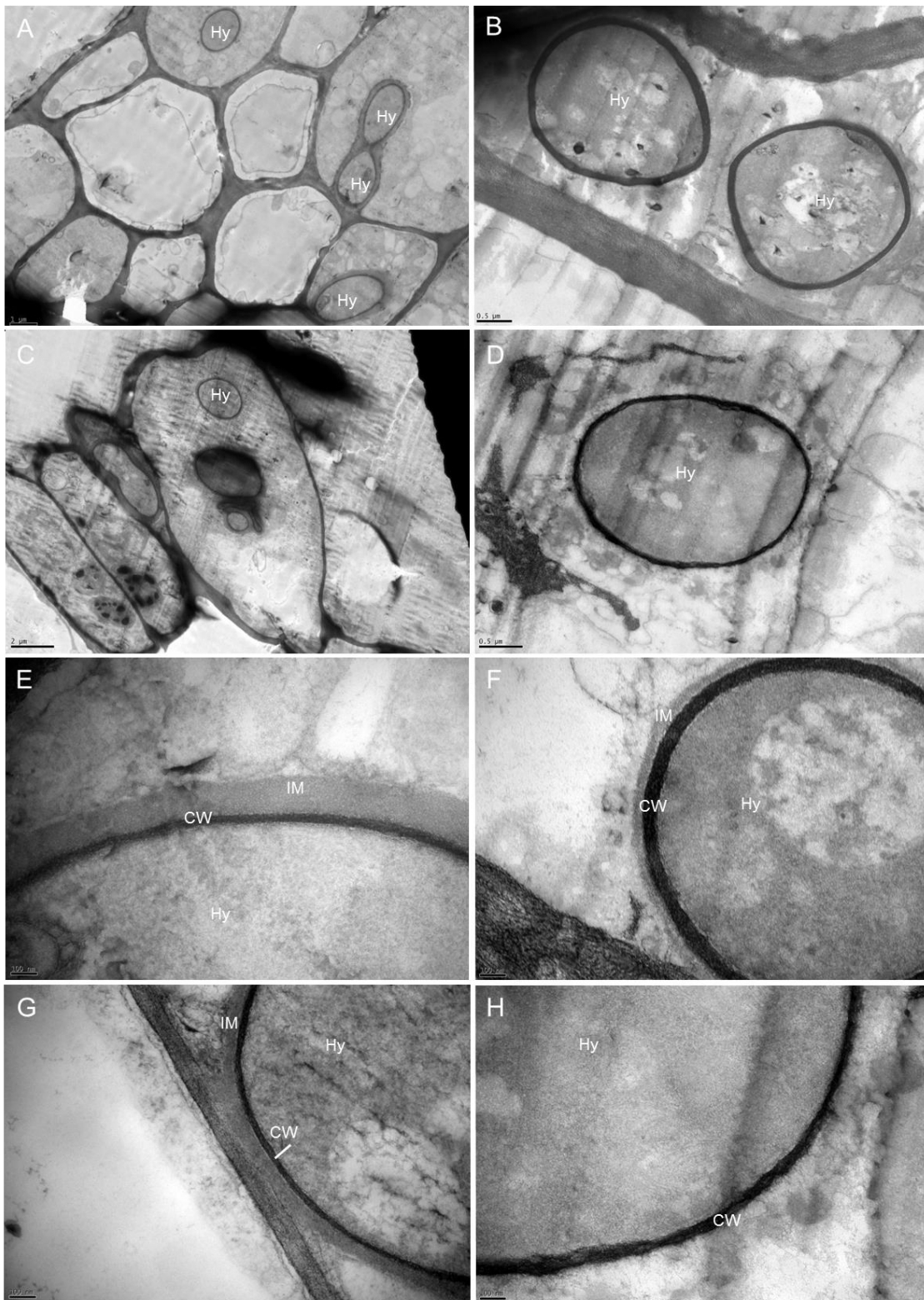


**Figure 13.** Electron micrographs of sections obtained from maize infected with *S. reilianum*. Shown are SRS (A, C, E, G) and SRZ (B, D, F, H). Fungal growth is observed in vascular bundles in (A) and epidermal cells in (C). Typical examples of fungal cell wall are shown in the remaining pictures. Differences in cell wall are apparent between SRS that shows a tick interfacial matrix and small cell wall (E, G) and SRZ that presents a tick cell wall and small or absent interfacial matrix (D, F, G). Abbreviations as in Fig.12.

In sorghum, it was not noticed evident differences in cell wall morphology and thickness of SRS and SRZ, since high variation occurred (Fig. 11 and 12). In maize, however, differences became more evident. SRS showed a big interfacial matrix (Fig. 13E, G), whereas in SRZ this layer was usually very thin (Fig. 13F) or absent (Fig. 13B, D, H).

### **3.1.7 No differences in appressorium morphology were observed between SRS and SRZ on maize, but differences appear on sorghum**

Since the study of fungal growth inside the plant showed differences for SRS and SRZ, I decided to investigate whether this variance would occur at early time points of the infection, during the appressoria development and penetration. For that, scanning microscopy of infected maize and sorghum leaves was performed at 1 dai, a time point when *S. reilianum* is known to have already formed penetration structures and is penetrating the plant epidermis. This experiment and the one described in 3.1.8 were done in cooperation with the group of Professor Dominik Begerow at Ruhr-Universität Bochum.

SRS-infected sorghum leaves showed typical appressoria penetrating the leaves (Fig. 14A). A good attachment of these structures to the leaf epidermis was observed in all samples (Fig. 14C). IN SRZ-infected sorghum, some appressoria presented a normal morphology and attachment, appearing to successfully enter the plant (Fig. 14B). However, in some cases, appressoria presented a distinct lip structure at the tip, that seemed to lay on top of the epidermis (Fig. 14D). It is not clear if these appressoria were able to penetrate the plant or not, and also the composition of the structure is unknown.

In maize, SRS-appressoria showed a similar morphology to the one observed in sorghum and seemed to normally penetrate the plant (Fig. 14E, G). In the same, hand, SRZ exhibited a normal morphology and the attachment was mostly observed at the appressorium head (Fig. 14F, H). The lip structure observed for SRZ in sorghum was never noticed in maize, indicating that it was specifically produced during the interaction of SRZ with sorghum.

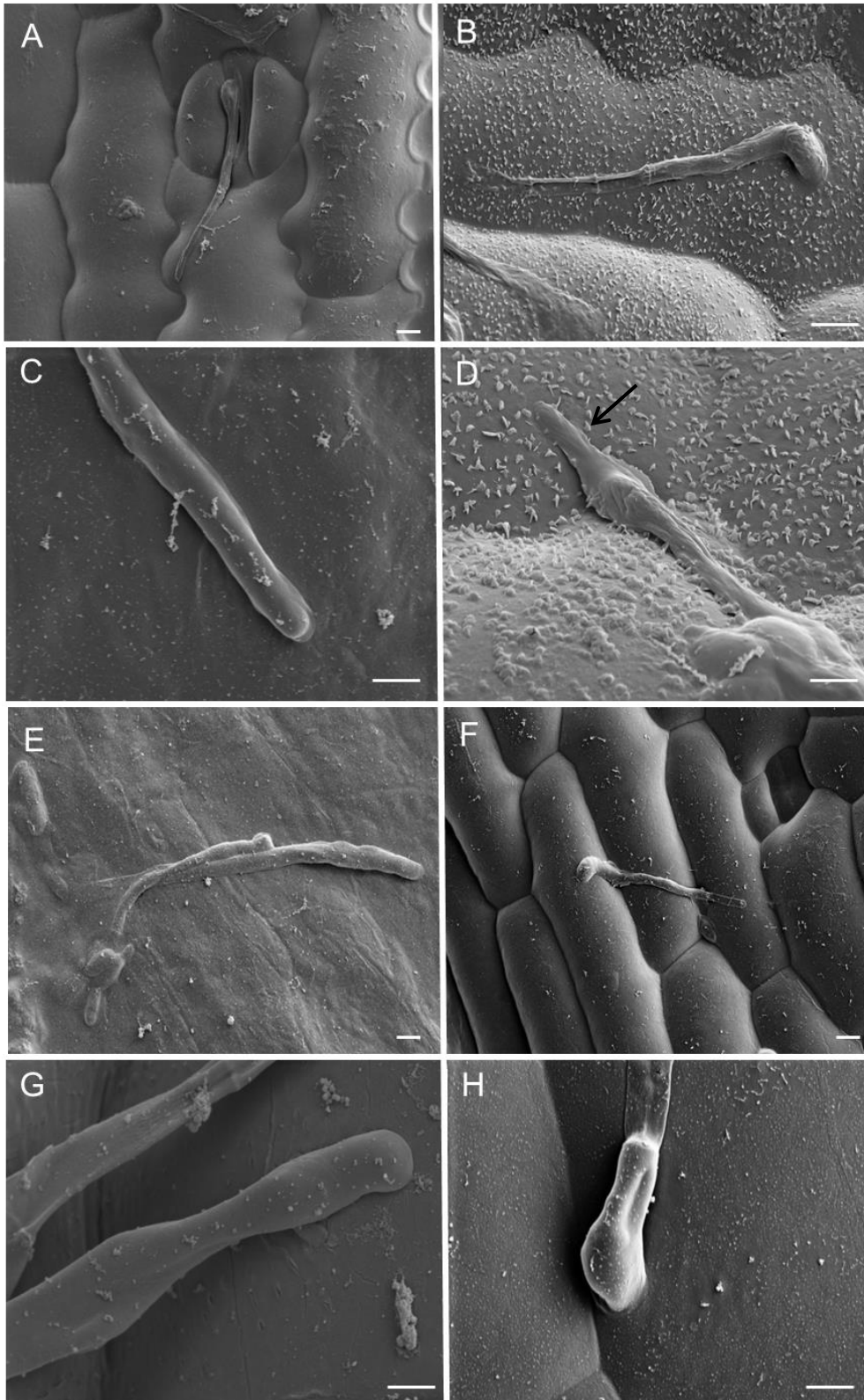


**Figure 14.** Scanning microscopy of sorghum and maize inoculated leaves collected at 1 dai. Sorghum is shown in A-D, and maize is shown in E-H. Penetrator structures of SRS (A, C, E, G) and SRZ (B, D, F, H) are visualized. Bars: 1 $\mu$ m. Arrow indicates lip structure at SRZ-appressorium.

### **3.1.8 SRS seems to form a more tight physical interaction with sorghum than SRZ**

Due to the different proliferation behavior of SRS and SRZ in sorghum, I decided to examine the contact zone between fungus and plant by scanning electron microscopy. For that, sorghum leaves collected at 3 dai were subjected to a procedure of freezing and breaking in order to expose a transverse view of the structures. Visualization of fungal structures by scanning microscopy showed that hyphae of SRS had a very good connection between fungus and plant, and a big interfacial matrix layer was observed between fungal hyphae and plant plasma membrane (Fig. 15A, C). For SRZ, this layer was much smaller or absent and the hyphae seemed to break out and easily separate from the plant, indicating a weaker attachment (Fig. 15B, D).

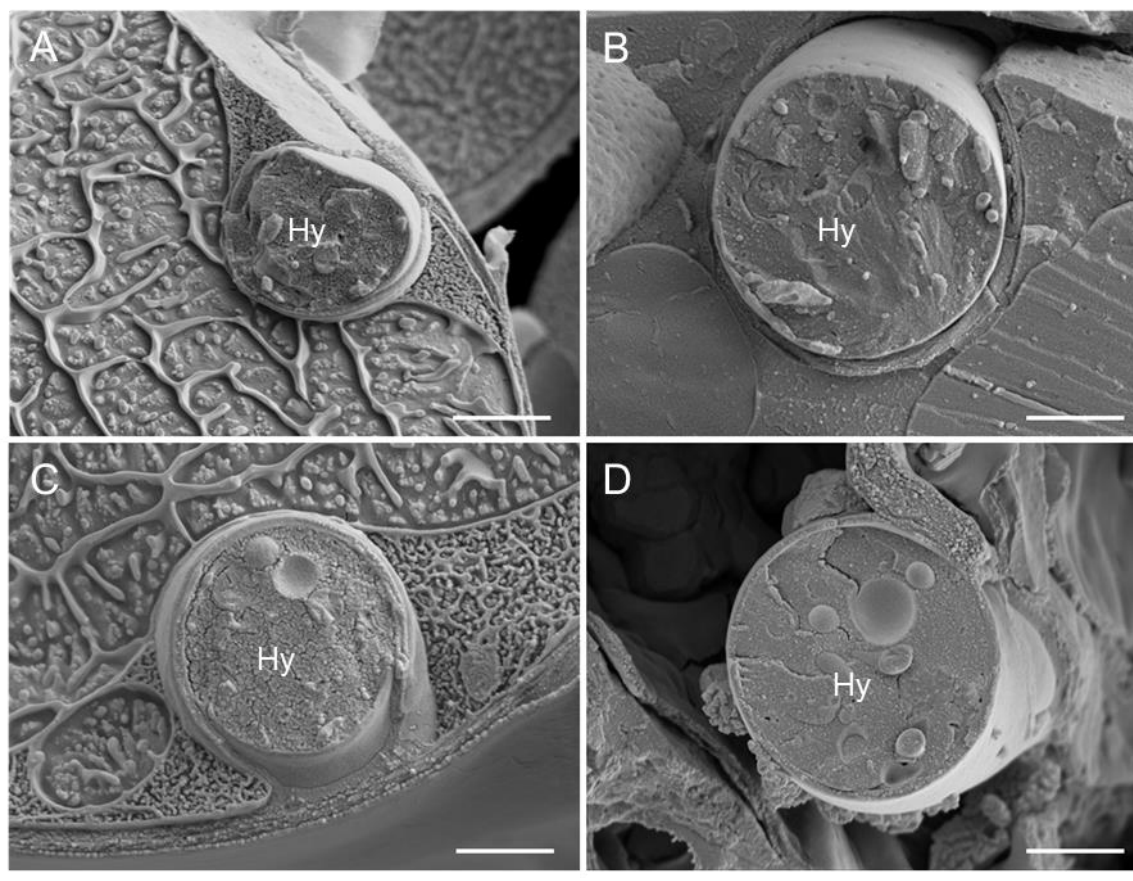


**Figure 15.** Scanning microscopy of infected sorghum leaves at 3 dpi. Transverse cuts of plant cells and fungal hyphae are presented, showing cell walls of SRS (A, C) or SRZ (B, D). Bars: 1 $\mu$ m  
Hy=Hyphae

## **3.2 The plant side: defense responses in maize and sorghum**

### **3.2.1 H<sub>2</sub>O<sub>2</sub> accumulates at penetrating hyphae of SRZ in sorghum**

To figure out the reasons that make SRZ unsuccessful in sorghum and SRS in maize, I decided to investigate possible differences in defense responses and started evaluating the occurrence of reactive oxygen species (ROS). Infected leaf samples were collected at 1, 2, and 3 dai and co-stained with 3,3'-diaminobenzidine (DAB, which stains H<sub>2</sub>O<sub>2</sub> and peroxidases) and calcofluor (to visualize fungal hyphae and appressoria on the leaf surface). As a control, uninfected samples were infiltrated with H<sub>2</sub>O<sub>2</sub> and stained with DAB. DAB staining resulted in an evenly distributed intense brown color across the whole leaf, proving that peroxidases were present all throughout the tissue.

Fungal penetration structures were visible at 1 dai for both *formae speciales* of *S. reilianum* in maize and sorghum. Interestingly, in sorghum, I found 1.5 times as many penetrating structures for SRS (398) than for SRZ (266) on comparable leaf areas. Furthermore, a strong accumulation of H<sub>2</sub>O<sub>2</sub> at the majority (61 ± 6%, n=266) of penetration sites of SRZ was observed as a brownish dot at the contact region between appressorium and plant cells (Fig. 16, Fig. 17B). In contrast, for infection sites of SRS, this H<sub>2</sub>O<sub>2</sub> accumulation was much lower (20 ± 10%, n=398) (Fig. 16, Fig.17A).

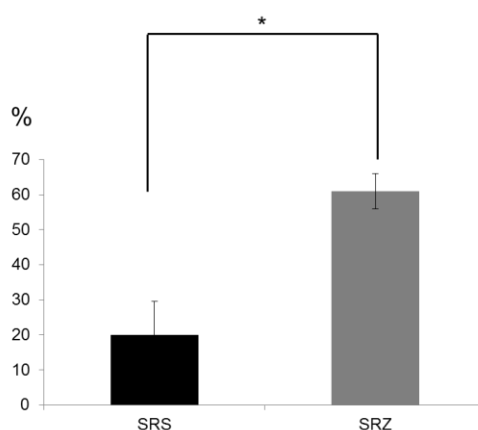


**Figure 16.** Accumulation of H<sub>2</sub>O<sub>2</sub> in sorghum infected with SRS or SRZ showing the percentage of appressoria presenting H<sub>2</sub>O<sub>2</sub>. Appressoria were counted for 4 plants per treatment and the experiment was repeated 4 times. Significant differences were observed for SRS and SRZ infected plants (t-test with p-value <0,05).

At 2 dai, when fungal hyphae had extended into the plant tissue, most penetrating hyphae of SRS showed no (Fig. 17C) or only weak DAB staining. In contrast, penetrating hyphae of SRZ were strongly stained by DAB, but surprisingly they continued to grow, indicating that  $H_2O_2$  was not sufficient to stop or kill the fungus (Fig. 17D). At 3 dai, hyphae of both SRS and SRZ as well as some plant cells showed DAB stain distributed at several regions, indicating a second phase of  $H_2O_2$  generation that was similar for both strains.

In maize, the vast majority of penetration structures did not show  $H_2O_2$  production either at 1 (Fig 17E, F), 2 (Fig.17G, H) or 3 dai. When the deposition occurred, it was weak and occasional, being similar for SRS and SRZ. The results point out that  $H_2O_2$  is not involved in host specificity on maize.

### **3.2.2 Sorghum cells are reinforced against SRS colonization**

Considering that I observed a distinct production of  $H_2O_2$  in sorghum, I started to wonder if cell reinforcement was also involved in defense. This defense is also a very early response and could contribute to stop the fungal spread. Reinforcement of plant cells occurs mainly by the deposition of callose and lignin, so I decided to investigate the deposition of both polymers. Callose deposition in infected leaves was observed at 1 and 2 dai using aniline blue staining, which stains callose in fluorescent blue under UV-illumination. For lignin observation in leaves and stems, phloroglucinol/HCl (PGH) test was used, which makes the lignified structures appear in a red-orange color.

At 1 dai, microscopic analysis of sorghum leaves inoculated with SRZ and SRS after staining with aniline blue revealed discrete fluorescence at the penetration points, that appeared around infection structures as a collar (data not shown). At 2 dai, sorghum samples infected with SRZ showed a much stronger fluorescence in plant cells at sites of attempted cell-to-cell crossing by hyphae (Fig. 18B, C, D). For sorghum leaf samples inoculated with SRS, the presence of fluorescence was very rare, occurring only occasionally in the region of contact between plant cell and

fungus or not at all (Fig. 18A). Therefore, results indicate an involvement of callose in the defense responses against SRZ in this host.

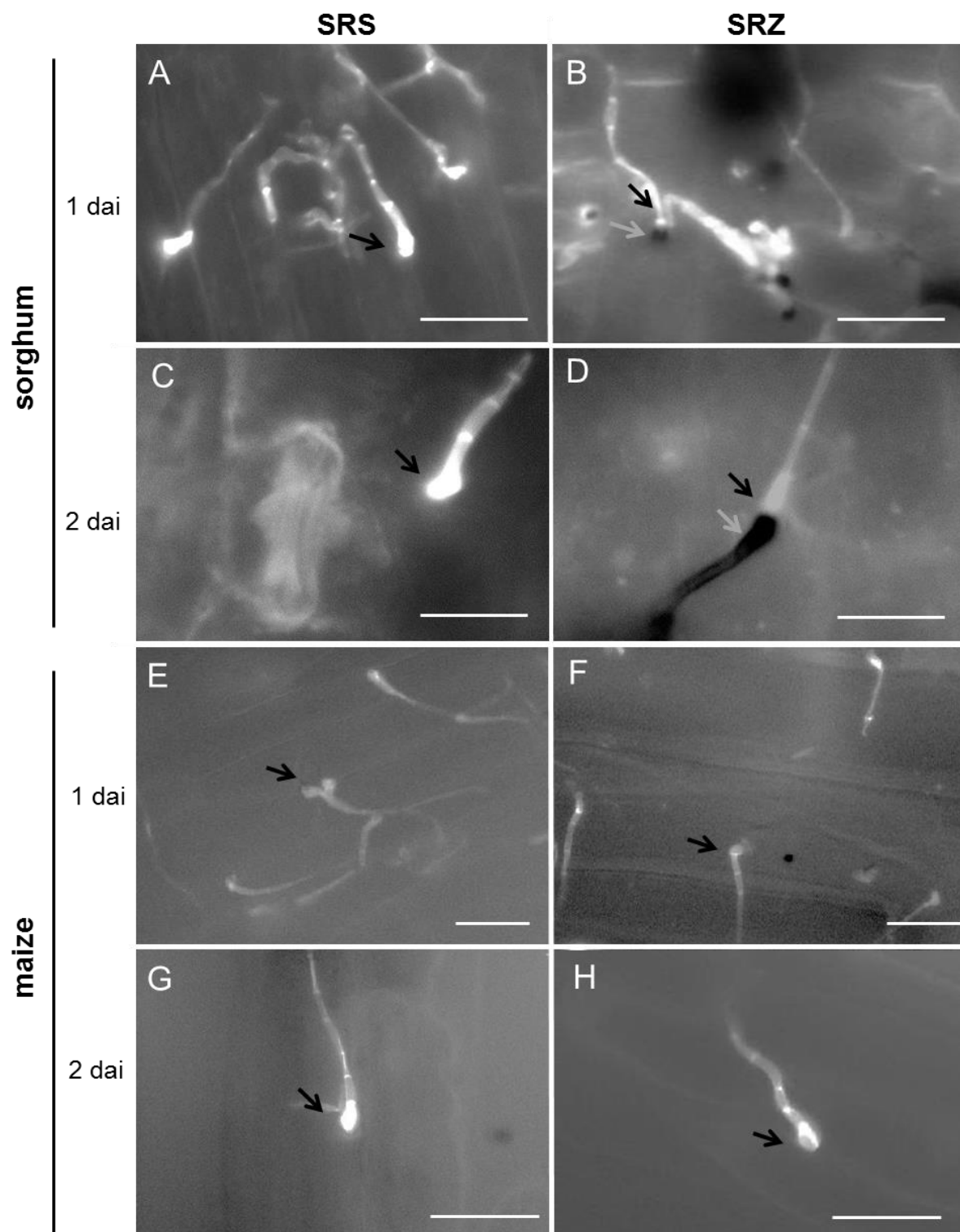


**Figure 17.** H<sub>2</sub>O<sub>2</sub> accumulation at *S. reilianum* infection sites. Sorghum (A-D) and maize (E-H) plants were inoculated with SRS (A, C, E, G) or SRZ (B, D, F, H). Shown are samples collected at 1 dai (A, B, E, F) and 2 dai (C,D,G,H) and stained with DAB-calcofluor for the presence of H<sub>2</sub>O<sub>2</sub>. Black arrows indicate fungal penetration structures, grey arrows show H<sub>2</sub>O<sub>2</sub> accumulation. Bars: 20  $\mu$ m

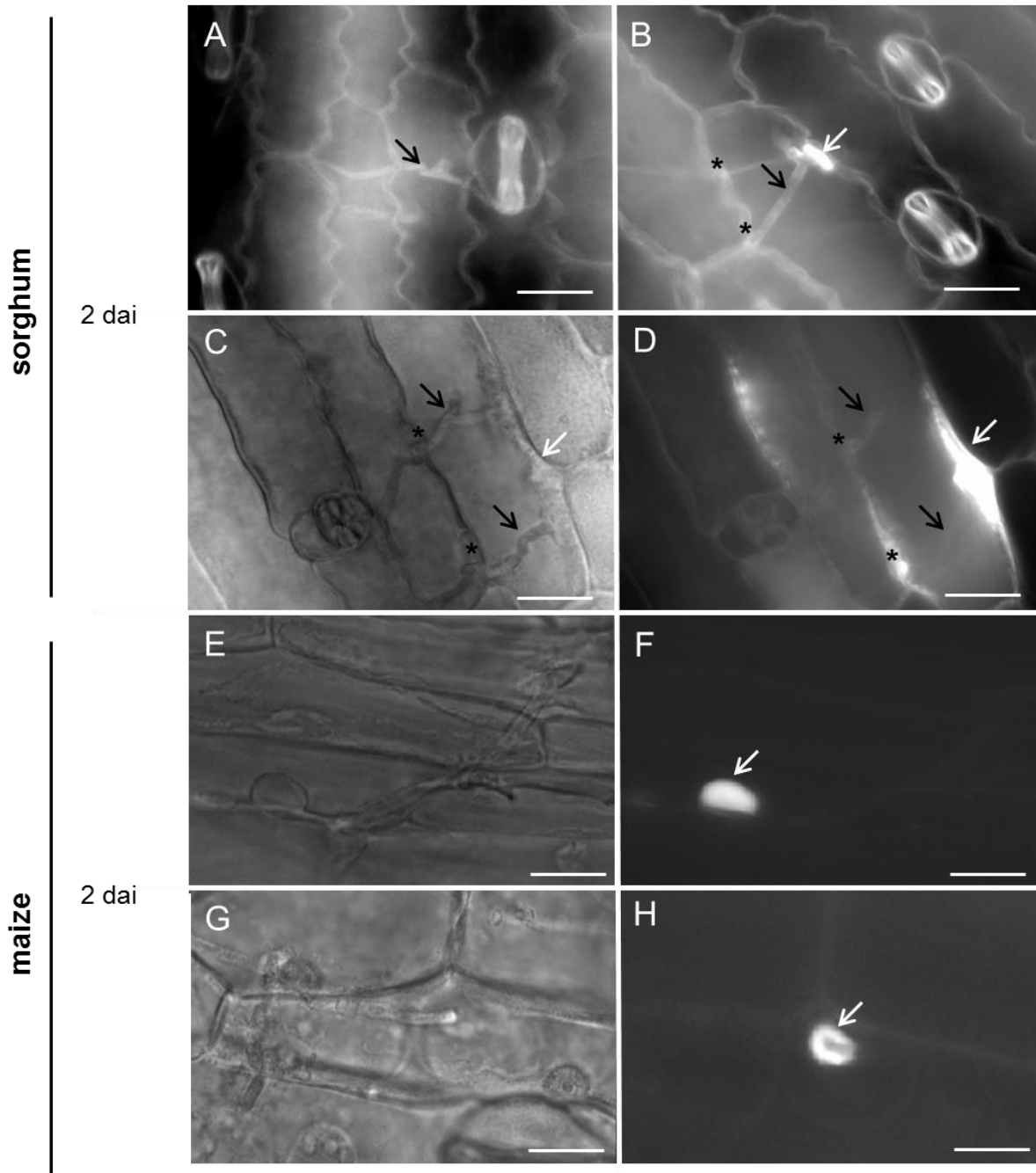


**Figure 18.** Black and white pictures showing callose deposition in infected plants. Sorghum (A-D) and maize (E-H) leaves were collected at 2 dai. Sorghum infected with SRS showed no or weak callose deposition (A), while strong levels of callose were observed for SRZ (B,C,D). In maize, callose was observed only in the penetration region and was similar for SRZ (E,F) and SRS (G,H). Images produced with DAPI filter appear in A,B,D,F,H, while bright filter is shown in C,E,G. White arrows indicate callose deposition, black arrows point to fungal hiphae. Bars: 20  $\mu$ m

In maize, a weak callose deposition was observed at 1 and 2 dai, being very similar for SRS and SRZ. This deposition was observed mainly around the hyphal tips, being deposited in the form of a collar at 2 dai (Fig.18E-H). As observed for H<sub>2</sub>O<sub>2</sub>, callose does not seem to be produced specifically against one strain in maize, since the levels of this polymer were low and similar for both SRS and SRZ.

Lignin deposition was analysed in hand-made cross sections of leaves and nodes at 9 dai. Due to the red color of phytoalexins in sorghum leaves and the difficulty to obtain good quality for leaf transverse cuts, lignin could not convincingly be detected in these samples. I was especially interested in checking lignin deposition in maize stems. The deposition of lignin in this part seemed likely, since microscopy showed that SRS can reach the stem in maize but does not continue further to produce spores in ears. However, only a very weak staining was observed in vascular bundles, showing phloroglucinol staining mainly in xylem cells. No visual differences were found when comparing uninfected samples, SRS and SRZ in sorghum (Fig. 19A-C) and maize (Fig. 19D-F). Apparently, lignification does not appear to be a major defense against *S. reilianum* in maize or sorghum stems.

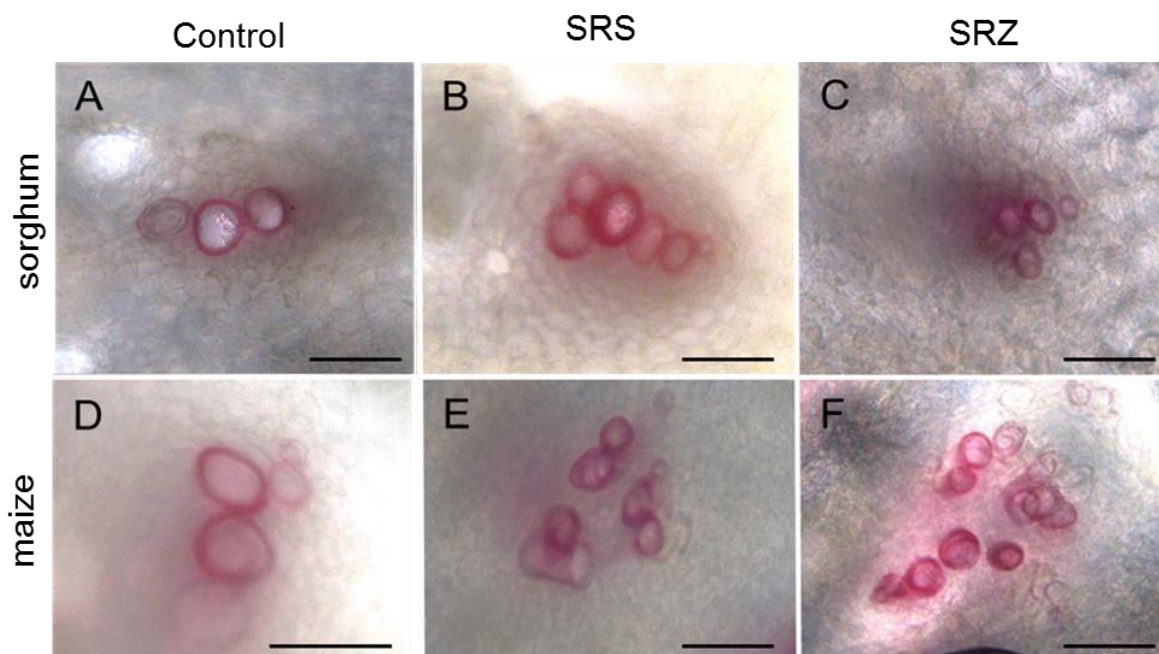


**Figure 19.** Lignin deposition in stems of sorghum and maize. Stems were collected at 9 dai and transverse cuts were stained with phloroglucinol/HCl. No differences were observed between sorghum (A-C) and maize (D-F) for control (A, D), SRS (B, E) and SRZ (C, F) inoculated plants. Bars: 100  $\mu$ m

### **3.2.3 No plant cell death is observed when plants are inoculated with *S. reilianum***

I then examined the occurrence of plant cell death in maize and sorghum. A programmed cell death usually occurs in plant cells at or close to the infection site, and is an efficient mechanism of protection against biotrophs, since they need living host cells for proliferation. Control, SRS, and SRZ inoculated maize and sorghum leaves were collected at 3 and 9 dai and stained with lactophenol trypan blue, which stains dead cells in blue. In all samples analysed, only vascular bundles and fungal hyphae were stained and no dead epidermal or mesophyll cells could be observed. However, sorghum samples infected with SRZ showed the characteristic red color of phytoalexins (Fig. 20F), which might mask a potential staining with trypan blue, making it difficult to analyse these samples. Comparing the samples, it was not possible to visualize meaningful differences between infected and control samples (Fig. 20). Therefore, excessive cell death does not appear to be induced by colonization of sorghum and maize by *S. reilianum*.

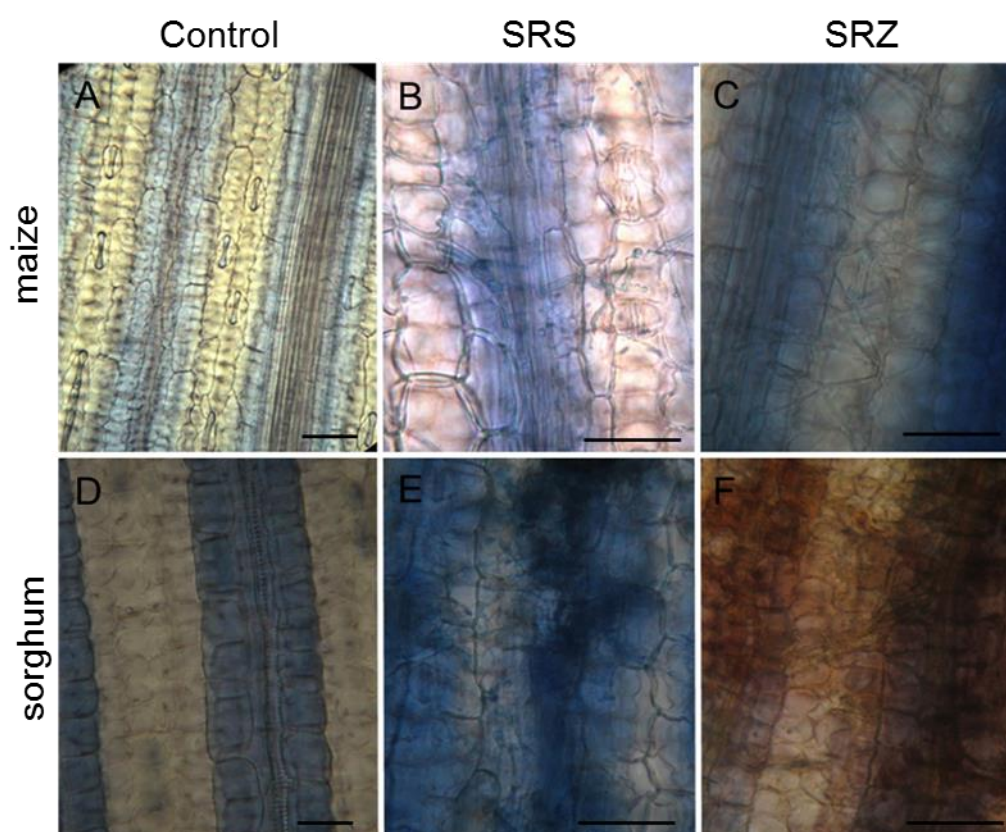


**Figure 20.** Trypan blue staining of infected leaves at at 9 dai. Maize (A-C) and sorghum (D-F) plants are shown for control (A, D), SRS (B, E) and SRZ (C, E). Bars: 50  $\mu$ m.

### 3.2.4 Phytoalexin deposition is a late response during the interaction of sorghum with SRZ

It is known that sorghum produces 3-deoxyanthocyanidins when infected with SRZ, but not with SRS (Zuther et al., 2012). However, many open questions remained, and I tried to address some of them during my PhD. My first question was why phytoalexins would be deposited against SRZ, but not SRS. We wondered if this would be a result of PAMP-triggered immunity or effector trigger-immunity response. To verify if just a PAMP would be sufficient to induce phytoalexins, I infiltrated 3 day old sorghum leaves with a solution of pure chitin in water, a very well know PAMP of fungi. Infiltration of chitin was enough to induce a strong phytoalexin deposition in sorghum leaves within 3 dai (Fig. 21A).

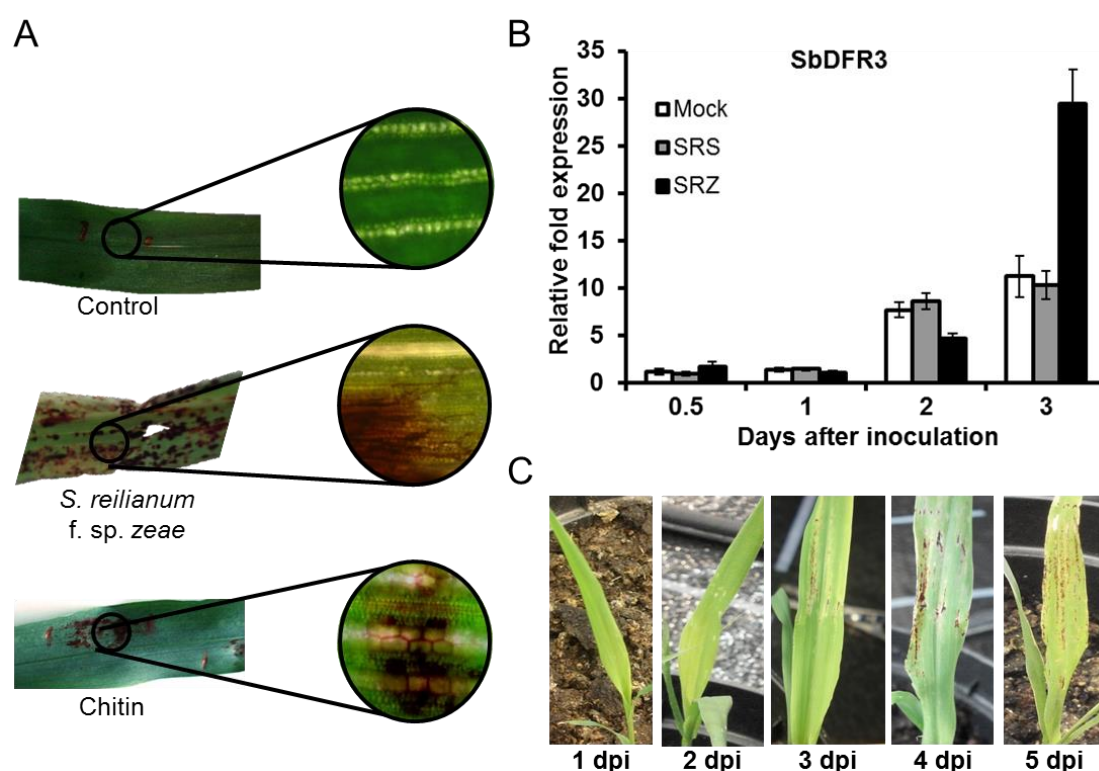


**Figure 21.** Deposition of 3-deoxyanthocyanidins in sorghum. (A) Control leaves infiltrated with water (top), infected with SRZ (middle) or infiltrated with chitin (bottom) (B) qRT-PCR of *SbDFR3* gene in samples inoculated with water (Mock), SRS or SRZ from 0,5 to 3 days after inoculation, relative to sorghum actin gene. (C) Sorghum leaves infected with SRZ show the emergence of phytoalexins visible by their red color at 3 dai, which gets more intense at later time points.

Apparently, the fungal PAMP chitin can elicit phytoalexin deposition in sorghum. However, it is not known why SRS does not trigger this defense, since both SRS and SRZ must have chitin in their cell wall. To find out if phytoalexins production was an early or late response, which could indicate an induction dependent on other defense responses (e.g. ROS), I also wanted to determine the exact time point when phytoalexins would start to be deposited on sorghum leaves. Visual inspection of SRZ-inoculated sorghum leaves showed clearly visible red dots at 3 to 4 dai (Fig. 21C). To check if phytoalexins biosynthesis would start much earlier than the observed appearance of the red dots on inoculated leaves, I quantified the expression of the dihydroflavonol 4- reductase (DFR3) involved in synthesis of phytoalexins by qRT-PCR. Differences in *SbDFR3* expression were observed between SRZ compared to SRS and control, and started to become evident at 3 dai (Fig. 21B). Strong upregulation of *SbDFR3* only in response to inoculation with SRZ coincided well with the appearance of red spots of phytoalexins macroscopically observed at 3 dai (Fig. 21C).

### **3.2.5 Expression analysis of marker genes reveals differential plant responses for SRS and SRZ in maize and sorghum**

My microscopic investigation showed induction of plant defense responses, especially in sorghum after inoculation with SRZ. To confirm these findings and investigate other potential defense responses, I determined the expression of several plant defense marker genes at 3 days after plant inoculation. For that, leaf samples of 3 cm were collected from the region bellow the inoculation point from sorghum and maize plants inoculated with SRS, SRZ or water. RNA was isolated as described before. Using quantitative RT-PCR, I measured gene expression relative to expression of the reference genes actin, ubiquitin and GAPDH in sorghum, and ubiquitin, tubulin and GAPDH in maize.

In sorghum, as marker gene for callose deposition, I used the gene *Sb03g030800* that we identified as the best homolog of the glucan synthase-like 5 gene (*GSL5*) of *Arabidopsis thaliana*, which has been shown to be essential for callose formation in response to attack by the fungal pathogen *Blumeria graminis* (Jacobs et al., 2009). Quantitative RT-PCR showed no significant differences in induction between SRS

and SRZ samples (Fig. 22), indicating that this gene is not involved in specific defenses against the *formae speciales* of *S. reilianum*. A chitinase gene (Sb03g030100) showed significant upregulation in SRZ-infected relative to SRS-infected samples (Fig. 22). A pathogenesis-related protein 10 (PR10), encoded by the gene Sb01g037970 did not show differences between SRS and SRZ-infection (Fig. 22).

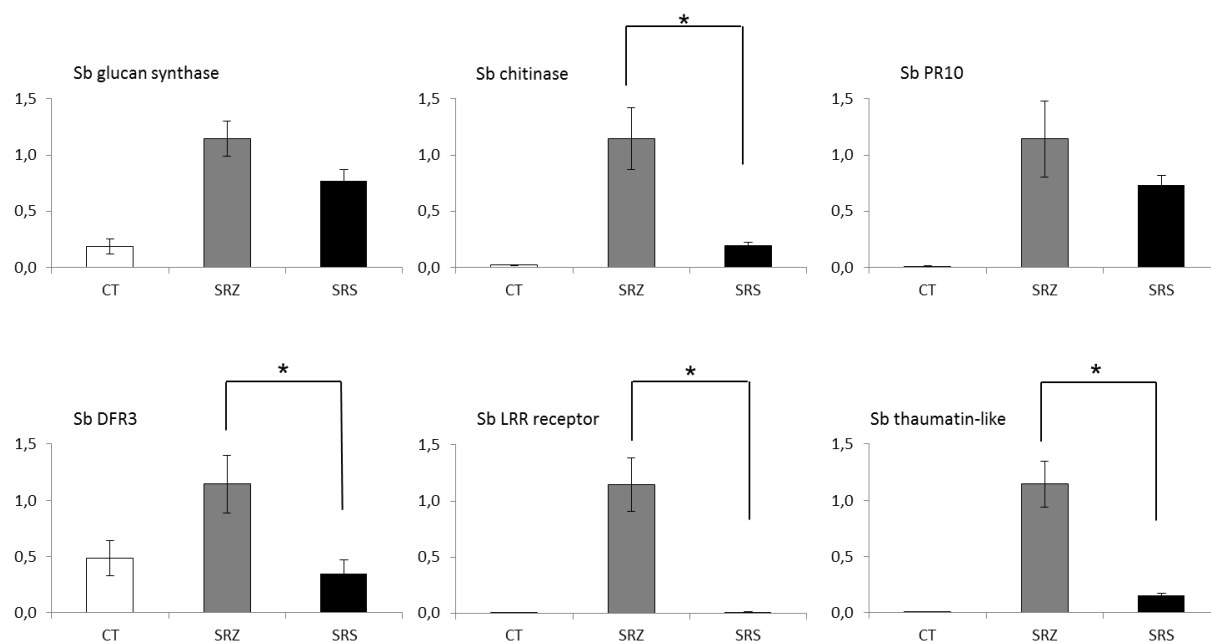


**Figure 22.** qRT-PCR of marker genes for plant defense responses in sorghum. Leaves were infected with water (CT), SRZ or SRS and collected at 3 dai. Expression levels of sorghum genes encoding a glucan synthase (Sb03g030800), a chitinase, (Sb03g030100), a PR10 (Sb01g037970), a DFR3 (Sb02g000220), a LRR receptor (Sb05g018800) and a thaumatin-like protein (Sb08g022440) were measured relative to the expression of genes encoding actin (Sb01g010030), ubiquitin (Sb02g003380) and GAPDH (Sb04g025120). Significance between SRZ and SRS-samples was measured by t-test ( $p \leq 0,05$ ).

The dihydroflavonol 4-reductase encoded by *SbDFR3* (Sb02g000220) that catalyzes an early essential step of luteolinidin biosynthesis in sorghum (Liu et al. 2010) was induced in plants infected with SRZ (Fig. 22, Fig. 21B). Similarly, a leucine-rich repeat-containing (LRR) extracellular glycoprotein precursor (Sb05g018800) was highly expressed upon SRZ infection, compared to SRS-infected samples. Furthermore, a gene encoding a thaumatin-like protein (Sb08g022440) showed significant upregulation in samples infected with SRZ (Fig. 22), demonstrating that

sorghum has the ability to recognize the different *formae speciales* of *S. reilianum* and trigger higher defense responses against SRZ.

In maize, differences in gene expression were not so pronounced. A glucan synthase gene (GRMZM2G430680) predicted to be involved in callose deposition did not show variation between control, SRS or SRZ samples (Fig. 23). The same occurred with a gene likely encoding a chitinase gene (GRMZM2G005633) that presented similar expression values in the two samples (SRS and SRZ, Fig. 23).

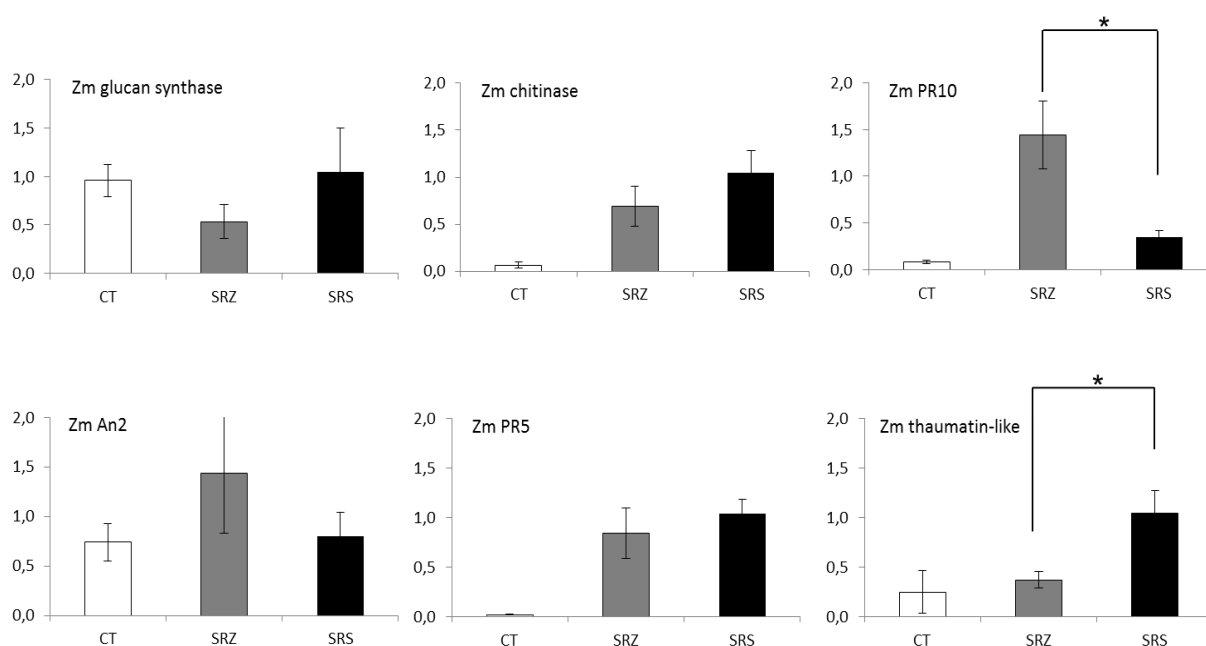


**Figure 23.** qRT-PCR of marker genes for plant defense responses in maize. Leaves were infected with water (CT), SRZ or SRS and collected at 3 dai. Expression levels of maize genes encoding a glucan synthase (GRMZM2G430680), a chitinase (GRMZM2G005633), a PR10 (GRMZM2G112538), a AN2 (GRMZM2G044481), a PR5 (GRMZM2G402631) and a thaumatin-like protein (GRMZM2G149809) were measured relative to the expression of genes encoding ubiquitin (GRMZM2G409726), tubulin (GRMZM2G099167) and GAPDH (GRMZM2G046804). Significance between SRZ and SRS-samples was measured by t-test ( $p \leq 0,05$ ).

A gene with homology to PR10 encoding genes (GRMZM2G112538) was significantly upregulated for SRZ relative to SRS (Fig. 23), while a gene encoding an kauren synthase 2 (AN2, GRMZM2G044481) involved in kauralexin deposition, presented similar expression values in the three samples (CT, SRS, SRZ; Fig. 23). A gene with homology to PR5 (GRMZM2G402631) was similarly upregulated for SRS and SRZ, whilst a gene encoding a thaumatin-like protein (GRMZM2G149809)

presented a significant upregulation for SRS, when compared to SRZ (Fig. 23). In summary, different scenarios were observed in sorghum and maize. In sorghum, most evaluated marker genes with homology to enzymes involved in defense responses showed upregulation for SRZ-infection, while in maize no pattern could be established and both strains induced expression of different defense- related genes.

### **3.2.6 Maize transcriptome shows mild differences in gene regulation between SRZ and SRS-infected plants**

Since no pronounced differences in the tested plant defense responses ( $H_2O_2$ , callose, lignin, plant cell death and expression of marker genes) were observed in maize, I decided to investigate more globally which plant genes were differentially expressed in maize when infected with SRS or SRZ. To this end, I collected maize leaves inoculated with SRS, SRZ or water at 3 dai, isolated total RNA and sent the samples to Beckmann Genomics for Illumina next-generation sequencing. Obtained reads were mapped against the genome references of *Zea mays* (B73 genome; Schnable et al., 2009) and of *S. reilianum* SRZ2\_5-1 or *S. reilianum* SRS1\_H2-8 (unpublished) by Theresa Wollenberg using CLC genomics workbench version 6.

First, *S. reilianum*-inoculated samples were compared against mock-inoculated samples (Zm-SRS vs Zm-0 and Zm-SRZ vs Zm-0) by Steven Stadler using the Edge R package version 3.0 with dispersion value of 0.1, to calculate log fold changes, false discovery rate (FDR) and p-values. Differentially expressed genes with calculated p-values of  $\leq 0.05$  were considered as significantly regulated. Gene annotation was obtained from maize GDB (<http://www.maizegdb.org/>) or Plant GDB (<http://www.plantgdb.org/ZmGDB/>), when available. Genes lacking annotation were subjected to BlastP search against the non-redundant (nr) database at NCBI (<http://blast.ncbi.nlm.nih.gov/Blast.cgi>).

In SRS-infected samples compared to control (Zm-SRS vs Zm-0), 1450 maize genes were differentially regulated, most of them (1279; 88%) being upregulated and only a few (171; 12%) downregulated. In SRZ-infected samples (Zm-SRZ vs Zm-0), 1563 genes showed differential regulation when compared to control. Of these, 1443 (92%) were upregulated and 120 (8 %) genes were downregulated.

Compared to uninfected plants, infection with SRS and SRZ led to regulation of the same 698 genes (Fig. 24). Of these, 670 were upregulated and 28 downregulated in plants infected with SRZ compared to control plants. This was very similar for SRS, and only 3 genes that were up in SRZ infected samples showed downregulation for plants infected with SRS. These genes were GRMZM2G113378, GRMZM2G502350 and GRMZM2G333022, all encoding putative protein kinases. SRZ infection led to the exclusive regulation of 865 genes, of which most (773; 89%) were up and some (92; 11%) downregulated (Fig. 24). Similarly, of the 752 genes only regulated upon infection by SRS, most (612; 81%) were up and some (140; 19%) downregulated (Fig. 24). This shows that the presence of both fungi was clearly detected by the plant and resulted in a large set of genes commonly regulated by both fungi. In addition, presence of each fungus induced or downregulated a distinct set of genes whose expression was not altered upon leaf colonization by the other *f. sp.* of *S. reilianum*.

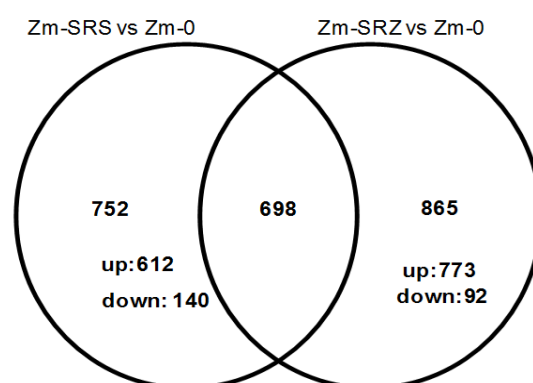


**Figure 24.** Venn diagram showing distribution of genes in the p-value-ranked expression list with a calculated p-value of  $\leq 0.05$  in maize. Comparison is shown among SRS-infected plants and control plants (Zm-SRS vs Zm-0) and SRZ-infected plants and control plants (Zm-SRZ vs Zm-0).

To identify the set of strain-specific significantly regulated maize genes, Edge R analysis was performed by Steven Stadler, comparing the SRS-inoculated maize samples with the SRZ-inoculated ones, setting the dispersion value to 0.1. This analysis led to a set of 500 differentially regulated genes with a calculated p-value  $\leq 0.05$ . Of these, 270 were upregulated for SRZ and 230 were upregulated for SRS.

To know whether the differentially expressed genes belonged to different functional processes, I performed a Gene Ontology (GO) Term Enrichment analysis using the tool AgriGO (Du et al., 2010b) and selecting the Singular Enrichment Analysis (SEA) method. For this analysis, the 500 significant genes ( $p$ -value  $\leq 0.05$ ) in the comparison of SRZ versus SRS-infected plants were included. For the 270 genes upregulated in SRZ-infected samples and the 230 upregulated in SRS-infected samples, 171 (63%) and 71 (31%) were annotated in the query list, respectively, and were used to calculate GO term enrichments.

In SRZ-specifically upregulated genes, 5 GO terms were enriched ( $FDR \leq 0.05$ ), two belonging to the main ontology biological process (BP) and three belonging to molecular function (MF), while cellular component (CC) was not represented. The enriched GO terms were: metabolic process (BP), oxidation reduction (BP), catalytic activity (MF), oxidoreductase activity (MF) and iron binding activity (MF) (Fig. 25). In SRS-infected samples, 6 GO terms were enriched ( $FDR \leq 0.05$ ), three of them belonging to the main ontology biological process (BP) and three belonging to molecular function (MF), while cellular component (CC) was also not represented. The enriched GO terms were: response to oxidative stress (BP), response to chemical stimulus (BP), cellular aromatic compound (BP), antioxidant activity (MF), oxidoreductase activity (MF) and iron binding (MF, Fig. 26).

This way, in biological process, SRZ induced processes of oxidation reduction, while SRS stimulated genes involved in response to stress and chemical stimulus. In molecular function, both SRS and SRZ upregulated iron binding and oxidoreductase activity, but more genes were present for SRZ-infected samples. The most enriched GO terms were found for SRZ-specifically upregulated samples: catalytic activity and oxidoreductase activity, which showed the highest levels of significance. Comparing SRS and SRZ-samples, similar processes were upregulated but different sets of genes were included in each one. All GO terms were represented by a much higher number of genes in the SRZ-induced gene set. This indicates that the compatible interaction resulted in a stronger and more focused transcriptional response in maize, with more genes associated to enriched GO terms than in the incompatible interaction.

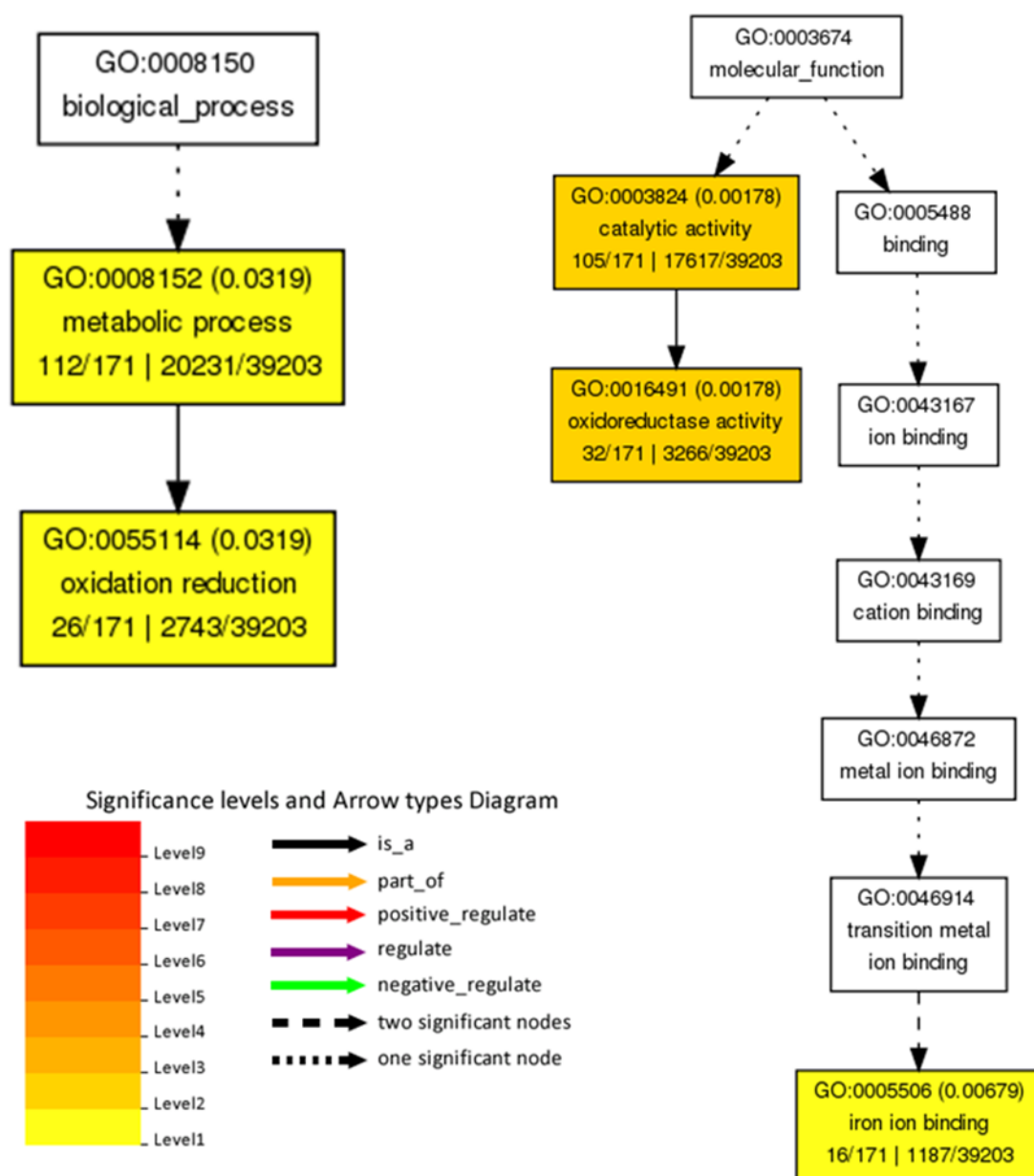


**Figure 25.** Pathway mapping of the significantly enriched GO terms among the SRZ-specific upregulated maize genes. (A) GO term map within the category “Biological process”. (B) GO term map within the “Molecular function” category. Boxes represent GO terms labeled with the GO ID, description and statistical information: number of submitted genes that belonged to this GO term / total number of genes submitted | total number of maize genes belonging to the GO term (background reference) / total number of genes annotated in the maize genome. The significant terms are shaded in color according to different levels of significance as indicated below the figure. Different arrows show the kind of regulation as indicated below the figure.

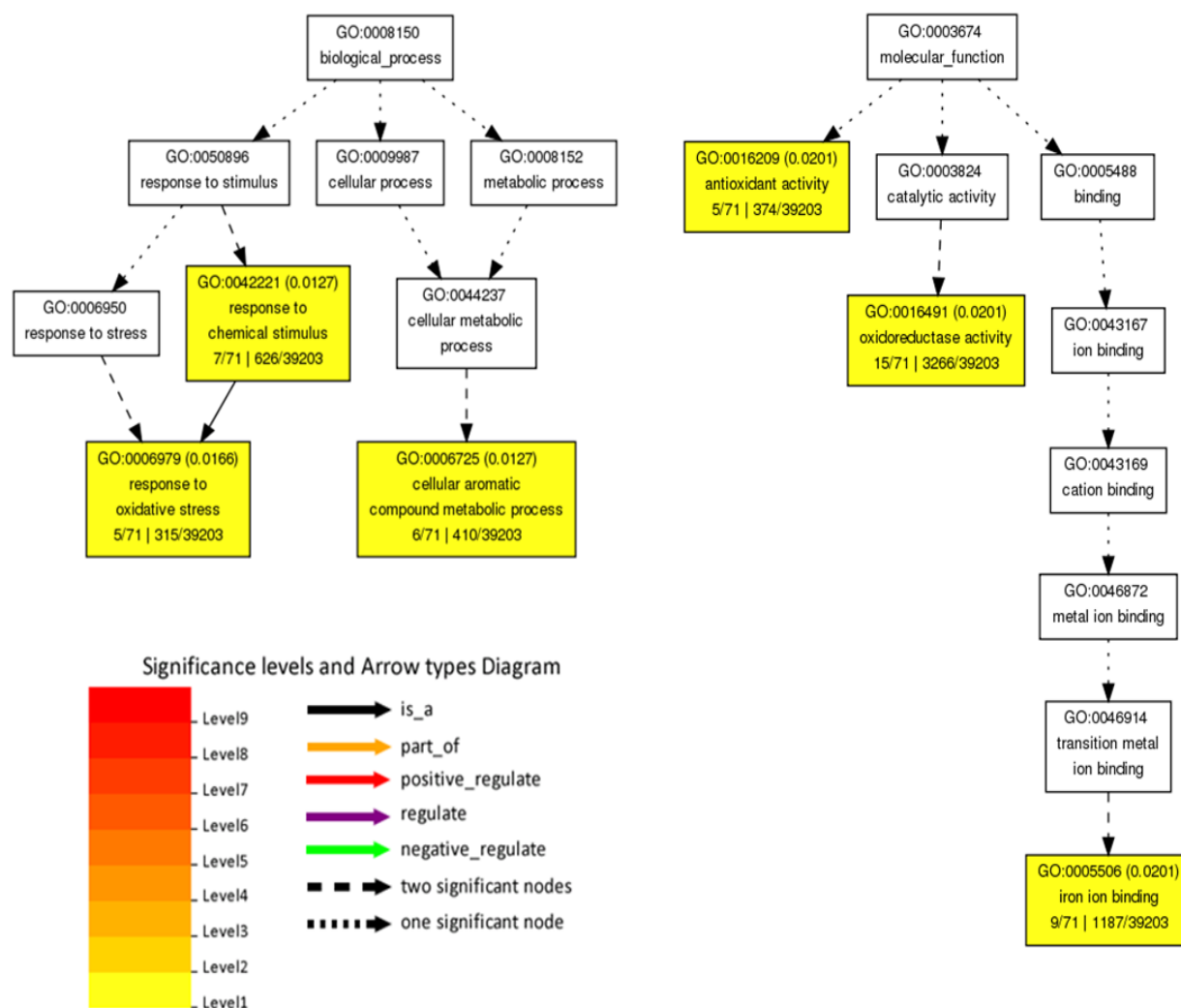


**Figure 26.** Pathway mapping of the significantly enriched GO terms among the SRS-specifically upregulated maize genes. (A) GO term map within the category “Biological process”. (B) GO term map within the “Molecular function” category. Boxes represent GO terms labeled with the GO ID, description and statistical information: number of submitted genes that belonged to this GO term / total number of genes submitted | total number of maize genes belonging to the GO term (background reference) / total number of genes annotated in the maize genome. The significant terms are shaded in color according to different levels of significance as indicated below the figure. Different arrows show the kind of regulation as indicated below the figure.

Since the GO term analysis was not very informative because many genes were not annotated in the query list, I decided to check the annotation of each gene, performing BLAST searches when annotation was not available. The evaluation showed that among the 230 genes upregulated in SRS-infected maize (Fig. 27A), some showed involvement in plant defenses (Fig. 27B, Supplemental Table S1). These genes were annotated as 4 peroxidases, 1 thaumatin-like, 1 calmodulin-

related, 1 protease inhibitor, 2 beta-glucosidases likely involved cell wall reinforcement, 1 toxin (dehydrin) and 2 genes encoding glutathione-S-transferases. Receptors and protein kinases were represented by 5 genes. Moreover, 8 membrane transporters, 3 hormone-related, 9 genes associated with metal binding, 2 genes implicated in cell wall remodeling and 10 genes involved with DNA-binding and transcription factors were upregulated, in addition to several enzymes. Interestingly, 11 pentatricopeptide repeat (PPR) proteins with unknown function were induced, in addition to 3 genes involved in thiamine biosynthesis (Fig. 27B).

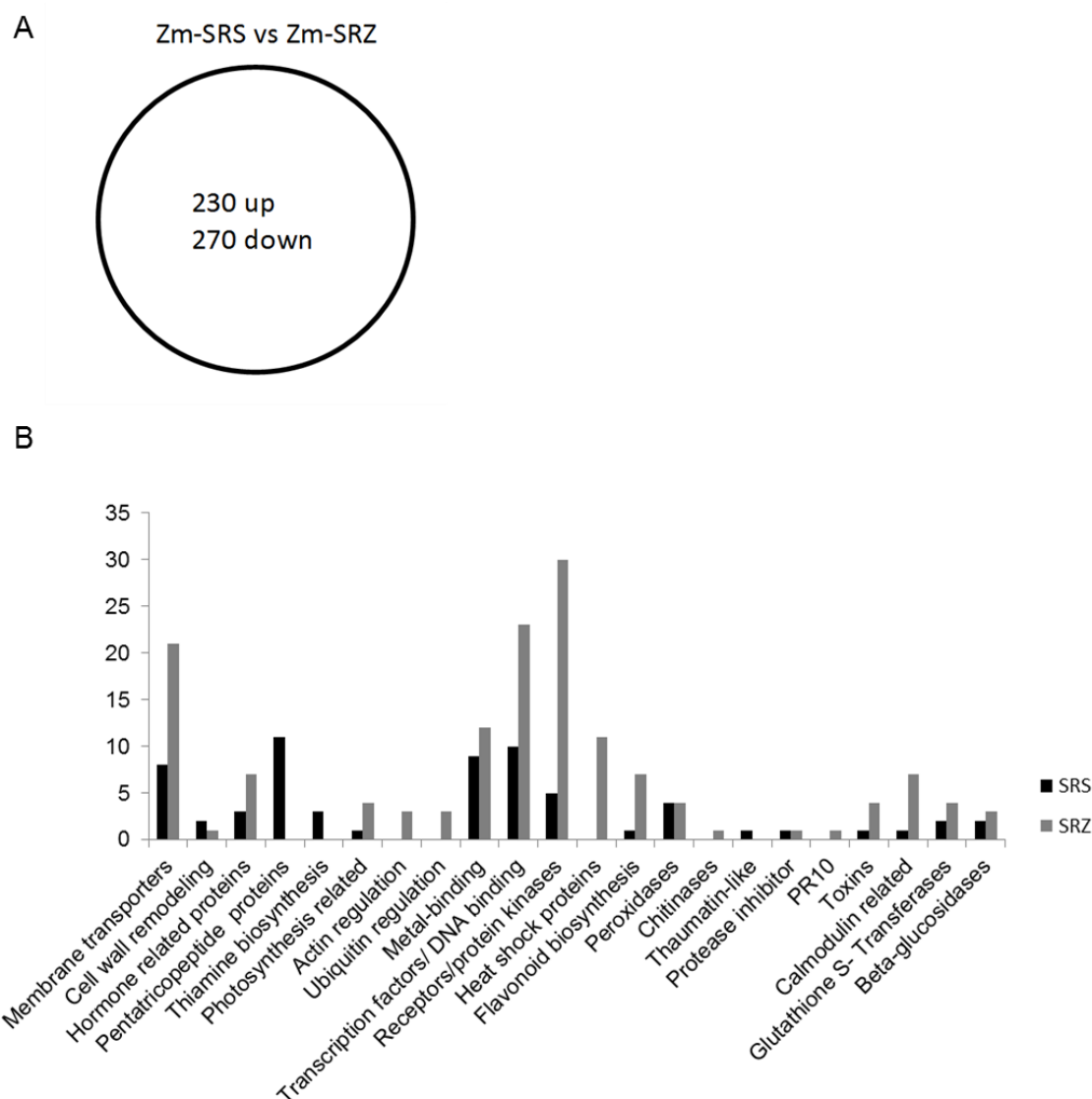


**Figure 27.** Distribution and annotation of the genes differentially regulated between SRS- and SRZ-infected samples. A- Diagram showing distribution of the 500 genes in the p-value-ranked expression list with a calculated p-value of  $\leq 0.05$  in the comparison among SRS-infected plants versus SRZ-infected plants (Zm-SRS vs Zm-SRZ). B- Annotation (X-axis) and number of genes (Y-axis) belonging to each function (212 genes are presented).

The remaining 270 genes were significantly highly expressed in SRZ-infected samples when compared to SRS-infected samples (Fig. 27A). Several of these genes were related to defense responses, and included 4 peroxidases, 1 chitinase, 1 PR10, 3 beta-glucosidases, 7 genes related to calmodulin, 1 protease inhibitor, 4 glutathione-S-transferases, 3 toxins (ricin-like and atrophin) and 7 genes related to flavonoid biosynthesis that include 2 terpene synthases involved in phytoalexin deposition. Furthermore, 30 genes coding for plant receptors or protein kinases were upregulated, as well as 11 heat shock proteins mainly belonging to the group of Hsp70. Twenty three genes associated to DNA binding or transcription factors, of which 5 belonging to the WRKY group, were also upregulated. Other genes included 21 membrane transporters, 7 hormone-related, 12 genes associated with metal-binding, 4 genes involved in photosynthesis and several enzymes, as well as genes involved in regulation of actin and ubiquitin (Fig. 27B, Supplemental Table S2).

This analysis shows that the presence of either SRS or SRZ in maize leaves leads to a transcriptional response in maize that includes the induction of a distinct set of defense genes. The marker genes tested by quantitative qRT-PCR were not among the significantly regulated genes in the transcriptome data and had p-values >0.05. However, RPKM values obtained in the transcriptome confirmed the expressions of *Zm thaumatin-like* and *Zm PR10* (Supplemental Table S3), which were the genes that showed differential upregulation in the qRT-PCR for SRS and SRZ, respectively. The remaining genes did not show significant changes between SRS and SRZ in qRT-PCR, but RPKM values correlated with what was observed, with exception of the gene *Zm AN2*, that was 3-fold upregulated for SRZ in the transcriptome data, but did not show differences in qRT-PCR. These differences between experiments, excepting *Zm AN2*, could be expected, since the calculation with Edge R resulted in the list of genes with the highest differences and excluded those with smaller but still reproducible differences, which means that additional differentially regulated genes might exist.

### **3.2.7 Transcriptome analysis in sorghum shows strong differences in gene regulation between SRZ- and SRS-infected plants**

In sorghum, several defense responses were observed in SRZ-inoculated plants by microscopy and qRT-PCR (Fig. 17, 18, 21, 22). To further investigate these differential responses, RNA-seq was carried out with RNA isolated from sorghum leaves at 3 days after inoculation with water, SRS, or SRZ. Sample collection and RNA extraction was performed as described for maize. Plant inoculation was done together with Theresa Wollenberg, sample collection and RNA extraction was done by Jan Utermark. For each replicate, 3 cm pieces of inoculated leaves of 10 plants were collected, frozen in liquid nitrogen, ground, and the powder was used to isolate total RNA. Equal RNA amounts of three biological replicates were pooled prior to Illumina next-generation sequencing by GATC Biotech.

Obtained reads were mapped against the genome references of *Sorghum bicolor* (Sbicolor\_79, Paterson et al., 2009) and the genomes of *S. reilianum* SRZ2\_5-1 and *S. reilianum* SRS1\_H2-8 (unpublished). The mapping and RPKM calculations were performed by Theresa Wollenberg using CLC genomics workbench version 6. Reads that did not map to the reference genomes were de-novo assembled using CLC genomics workbench version 6.

First, *S. reilianum*-inoculated samples were compared against mock-inoculated samples (Sb-SRS vs Sb-0, and Sb-SRZ vs Sb-0) by Steven Stadler using the Edge R package with the dispersion value set to 0.1 to calculate log fold changes, false discovery rate (FDR) and p-values. Differentially expressed genes with calculated p-values of  $\leq 0.05$  were considered as significantly regulated. Gene annotation was obtained from phytozome (<http://www.phytozome.net>), when available. Genes lacking annotation were subjected to BlastP search against the non-redundant (nr) database at NCBI (<http://blast.ncbi.nlm.nih.gov/Blast.cgi>) by Steven Stadler and Martin Kirchner.

In SRS-infected samples compared to control, 1916 genes were differentially regulated (p-value  $\leq 0.05$ ), of which most (1368; 71%) were upregulated and 548 (29%) were downregulated. The same ratio was found for SRZ-infected samples compared to control, however, twice as many genes were regulated: of the 4439

genes with differential regulation, 3122 (70%) were up and 1317 (30%) downregulated. Genes exclusively regulated by SRS and SRZ were 847 and 3370, respectively. In total, 1069 genes that were regulated by SRS were also regulated by SRZ infection (Fig. 28A). Of this set of genes regulated by SRS and SRZ, 765 showed upregulation for SRS, while 304 were downregulated. This was similar for SRZ, with the exception of 9 genes that showed differential regulation, being upregulated by SRZ, but downregulated by SRS. These genes presented the following annotation: 2 lipases, 1 peroxidase, 1 GTP-binding protein, 1 dhurrinase, 3 calcium-binding proteins and 1 uncharacterized protein.

In the comparison among SRS-infected plants and SRZ-infected plants, 2959 genes were differentially regulated with a calculated p-value of  $\leq 0.05$ , showing 832 (28%) genes upregulated for SRS, and 2127 (72%) upregulated for SRZ (Fig. 28B).

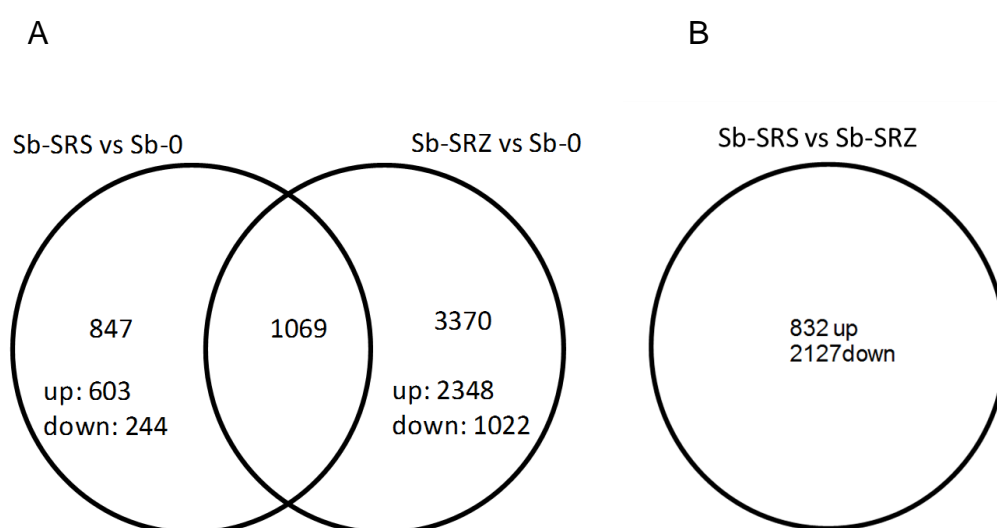


**Figure 28.** Venn diagram showing distribution of genes in the p-value-ranked expression list with a calculated p-value of  $\leq 0.05$  in sorghum. A-Comparison is shown among SRS-infected plants and control plants (Sb-SRS vs Sb-0) and SRZ-infected plants and control plants (Sb-SRZ vs Sb-0). B-Comparison between SRS-infected plants and SRZ-infected plants and control plants (Sb-SRS vs Sb-SRZ).

All 6 marker genes tested by qRT-PCR (Fig. 22) showed significance in the transcriptome data (p-values  $\leq 0.05$  in the comparison Sb-SRS vs Sb-SRZ infected samples), presenting upregulation for SRZ (Supplemental Table S3). This confirmed the expression results obtained by quantitative RT-PCR. Two genes (*Sb glucan*

*synthase* and *Sb PR10*) showed upregulation for SRZ in the transcriptome data, but did not show a significant difference in the qRT-PCR experiment (Fig. 22).

Similarly as in maize, Gene Ontology Term Enrichment (GO) was performed for significant genes (p-value  $\leq 0.05$ ) in the comparison of SRS- versus SRZ-infected plants, using AgriGO (Du et al., 2010b) and selecting the Singular Enrichment Analysis (SEA) method. Of the input genes that included 2127 genes upregulated for SRZ and 832 genes upregulated for SRS (Fig. 28B), 1755 (83%) and 712 (86%), respectively, were annotated in the query list. The analysis resulted in 111 and 97 significant GO terms for SRZ and SRS specific gene sets, respectively (Supplemental Table S4 and S5). Pathway maps were constructed for the three main ontologies using the AgriGO tool and are shown for sorghum genes upregulated by SRZ-infection (Figs. 29-31) and by SRS-infection (Figs. 32-34).

Solely 2 GO terms were significantly overrepresented in both gene sets: reproductive cellular process (12 genes for SRZ- and 7 for SRS-specifically upregulated genes) and lipid localization (7 genes for SRZ- and 13 for SRS-specifically upregulated genes). Therefore, different genes involved in the same processes are upregulated in sorghum upon infection with the different strains of *S. reilatum*, which indicates that reproductive cellular process and lipid localization may not be involved in host specificity.

In SRZ infected samples, several processes were activated (Figs. 29-31). In these samples, 57 GO terms were enriched for biological process, 53 for molecular function, and only 1 for cellular component (Supplemental Table S4). Inside the ontology biological process, several GO terms related to defense and immune responses were highly enriched (Fig. 29), such as defense response (128 genes), response to biotic stimulus (151 genes), defense response to fungus (39 genes), plant-type hypersensitive response (28 genes), innate immune response (59 genes), response to stress (322 genes), immune response (68 genes) and protein amino acid phosphorylation (215 genes). Furthermore, secondary metabolic process (90 genes), flavonoid biosynthetic process (31 genes), and phenylpropanoid biosynthetic process (31 genes) were also upregulated, which corresponds well with the accumulation of luteolinidin by sorghum when infected with SRZ (Fig. 21; Fig. 29). GO terms related to chitin recognition were also enriched, such as chitin metabolic process (13 genes), chitin binding (11 genes), and carbohydrate binding (69 genes), in addition to the GO

term chitinase activity (11 genes). This shows that sorghum recognizes the chitin of SRZ, an important fungal PAMP, and also induces chitinases to break down this compound. Chitin recognition could induce a PAMP-triggered immunity response that may result in the observed formation of H<sub>2</sub>O<sub>2</sub>, callose and phytoalexins (Figs. 17, 18, 21). This indicates a much stronger response to chitin for SRZ than observed for SRS. Supporting the several processes involved in defense response observed for biological process, the ontology molecular function showed several genes belonging to GO terms described as calcium ion binding (72 genes), calmodulin binding (31 genes), protein tyrosine kinase (205 genes), protein serine/threonine kinase activity (210 genes), protein kinase activity (221 genes), and receptor activity (43 genes), indicating a higher expression of defense related signaling components during colonization of sorghum by SRZ than by SRS (Fig. 30). Response to abscisic acid stimulus (74 genes) was also induced, revealing that sorghum also increases the production of hormones during colonization of SRZ. Other upregulated processes include catalytic activity (1056 genes), oxidoreductase activity (217 genes), and ATP binding (328 genes). Plasma membrane was the only GO term enriched for cellular component, presenting 152 genes. Taken together, the data show the modification of multiple processes in SRZ-infected plants, particularly the ones involved in defense responses, which possibly results in the complete inhibition of this strain inside sorghum inoculated leaves.

In SRS-infected samples, a very different distribution of enriched GO terms was found into the 3 main ontologies, which resulted in 52 GO terms in biological process, 4 GO terms in molecular function, and 40 GO terms in cellular component (Supplemental Table S5). They included GO terms related to DNA replication (8 genes), chromosome (39 genes), chromatin (23 genes), ribosome (96 genes), nucleosome (14 genes), translation (100 genes) and RNA binding (72 genes, Figs. 32-34). In addition, cell wall (40 genes) and cellular biosynthetic process (247 genes) were also enriched. The GO term H<sub>2</sub>O<sub>2</sub> catabolism was induced (6 genes, Fig. 32), suggesting that SRS could trigger detoxification of H<sub>2</sub>O<sub>2</sub> and therefore be able to escape this first layer of defense, which apparently does not happen with SRZ. These data indicate that SRS-infection strongly activates genes involved in cellular processes, increasing the division, multiplication and development of the host cells. This could be a benefit for the fungus, since boosting the plant metabolism would also increase nutritional possibilities for the pathogen.

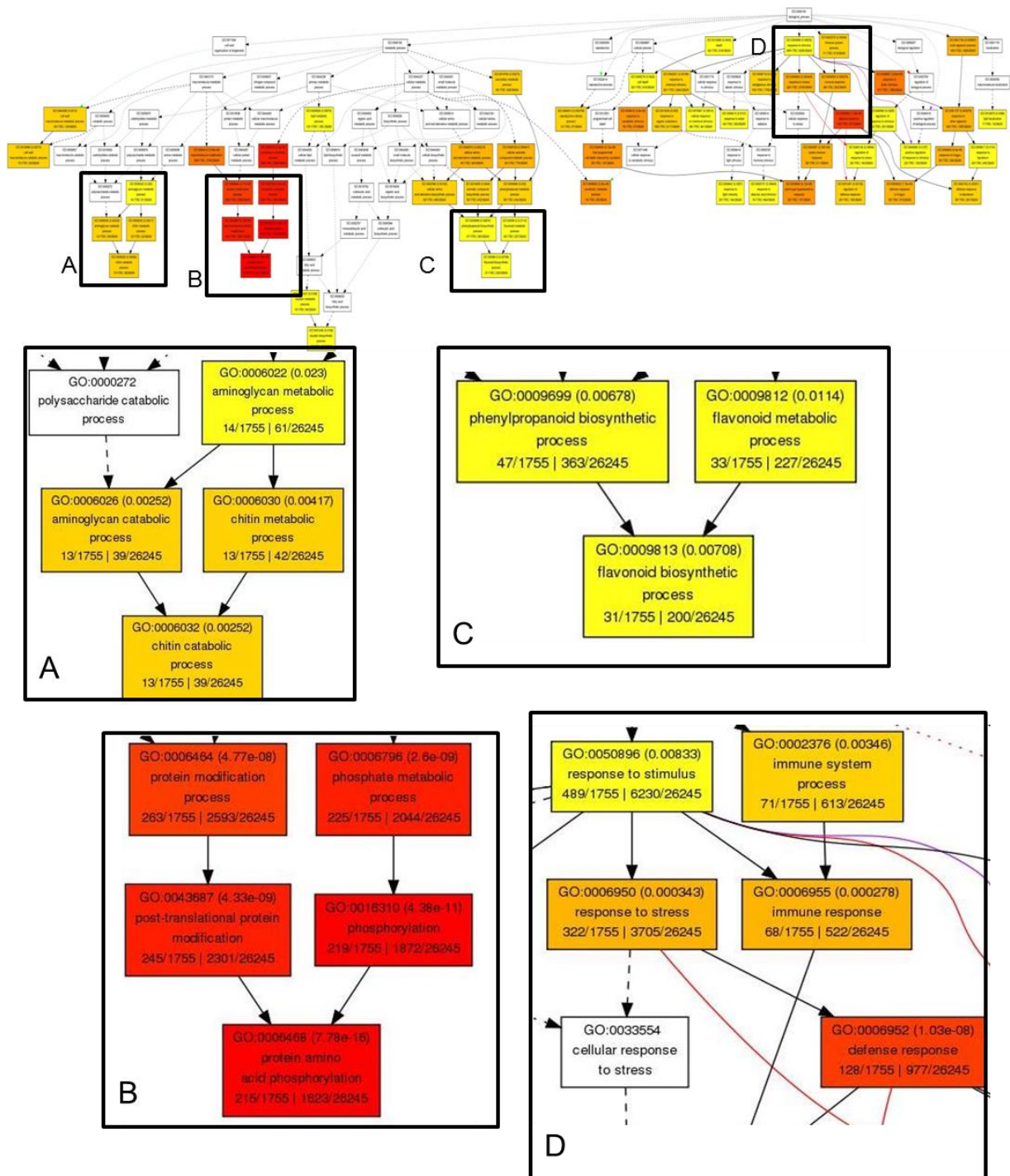


**Figure 29.** Pathway mapping of the significantly enriched GO terms among the SRZ-specifically upregulated maize sorghum within the category “Biological process”. Boxes represent GO terms labeled with the GO ID, description and statistical information: number of submitted genes that belonged to this GO term / total number of genes submitted | total number of maize genes belonging to the GO term (background reference) / total number of genes annotated in the sorghum genome. The significant terms are shaded in color according to different levels of significance, and different arrows show the kind of regulation as indicated below Figure 31.

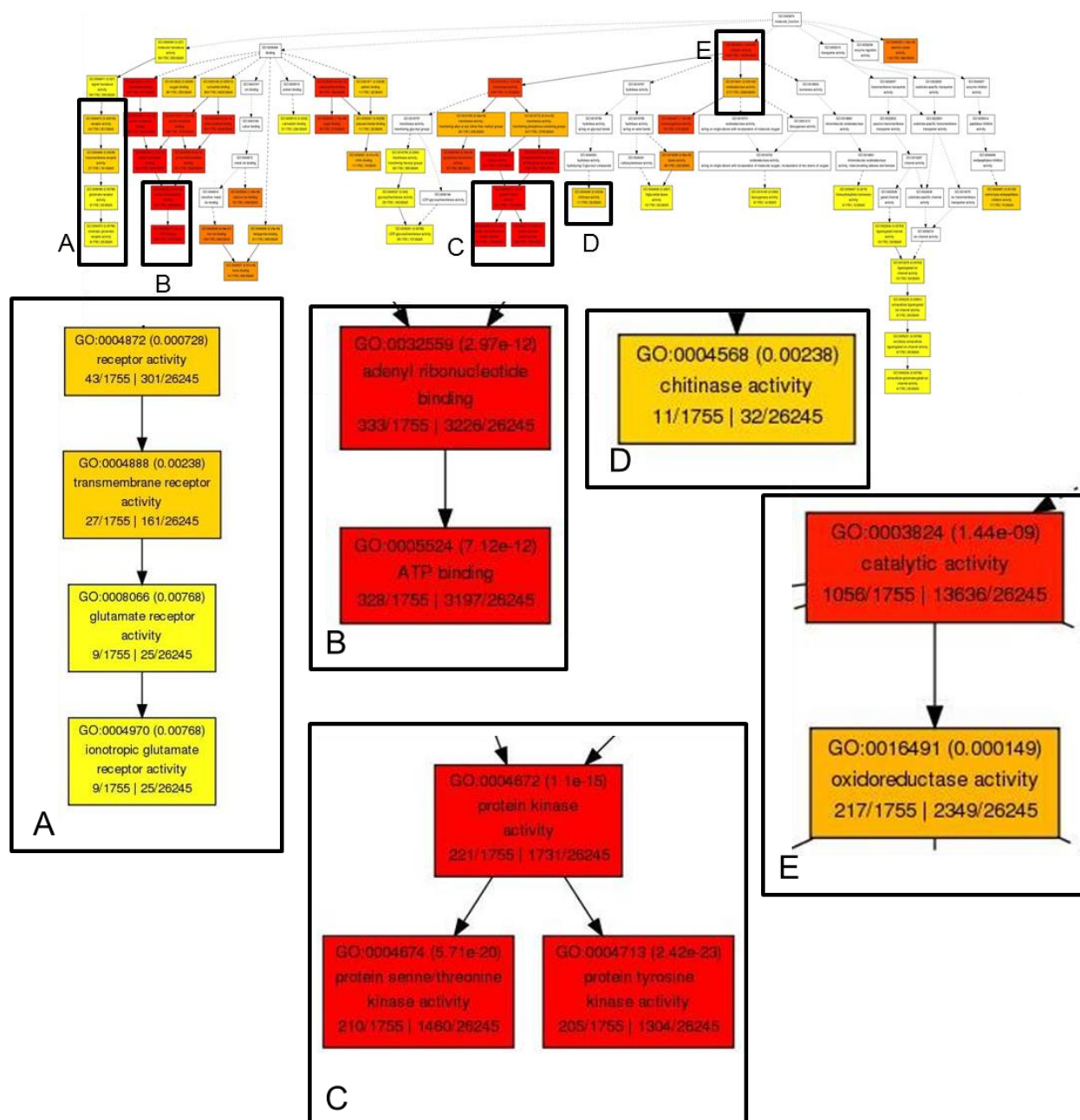


**Figure 30.** Pathway mapping of the significantly enriched GO terms among the SRZ-specific upregulated sorghum genes within the “Molecular function” category. Boxes represent GO terms labeled with the GO ID, description and statistical information: number of submitted genes that belonged to this GO term / total number of genes submitted | total number of maize genes belonging to the GO term (background reference) / total number of genes annotated in the sorghum genome. The significant terms are shaded in color according to different levels of significance, and different arrows show the kind of regulation as indicated below Figure 31.

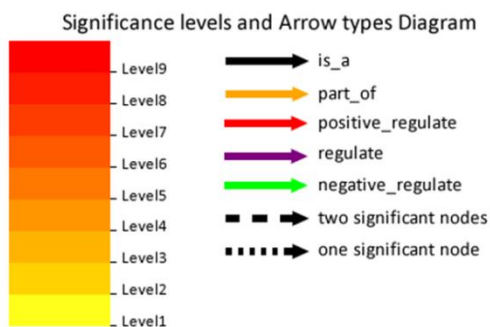
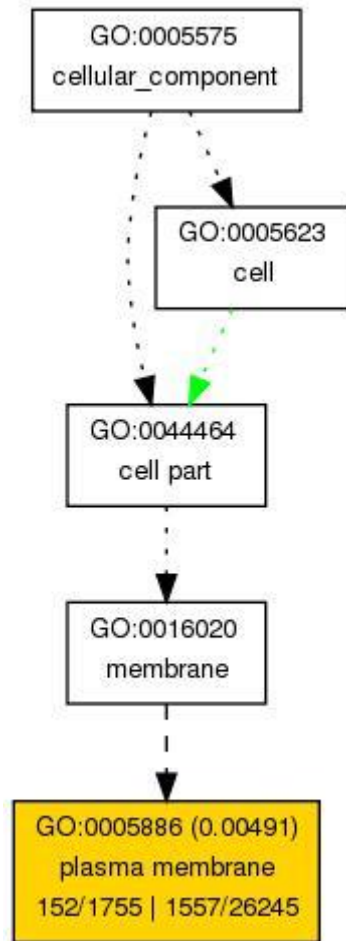


**Figure 31.** Pathway mapping of the significantly enriched GO terms among the SRZ-specifically upregulated sorghum genes within the category “Cellular component”. Boxes represent GO terms labeled with the GO ID, description and statistical information: number of submitted genes that belonged to this GO term / total number of genes submitted | total number of maize genes belonging to the GO term (background reference) / total number of genes annotated in the sorghum genome. The significant terms are shaded in color according to different levels of significance, and different arrows show the kind of regulation as indicated below the figure.

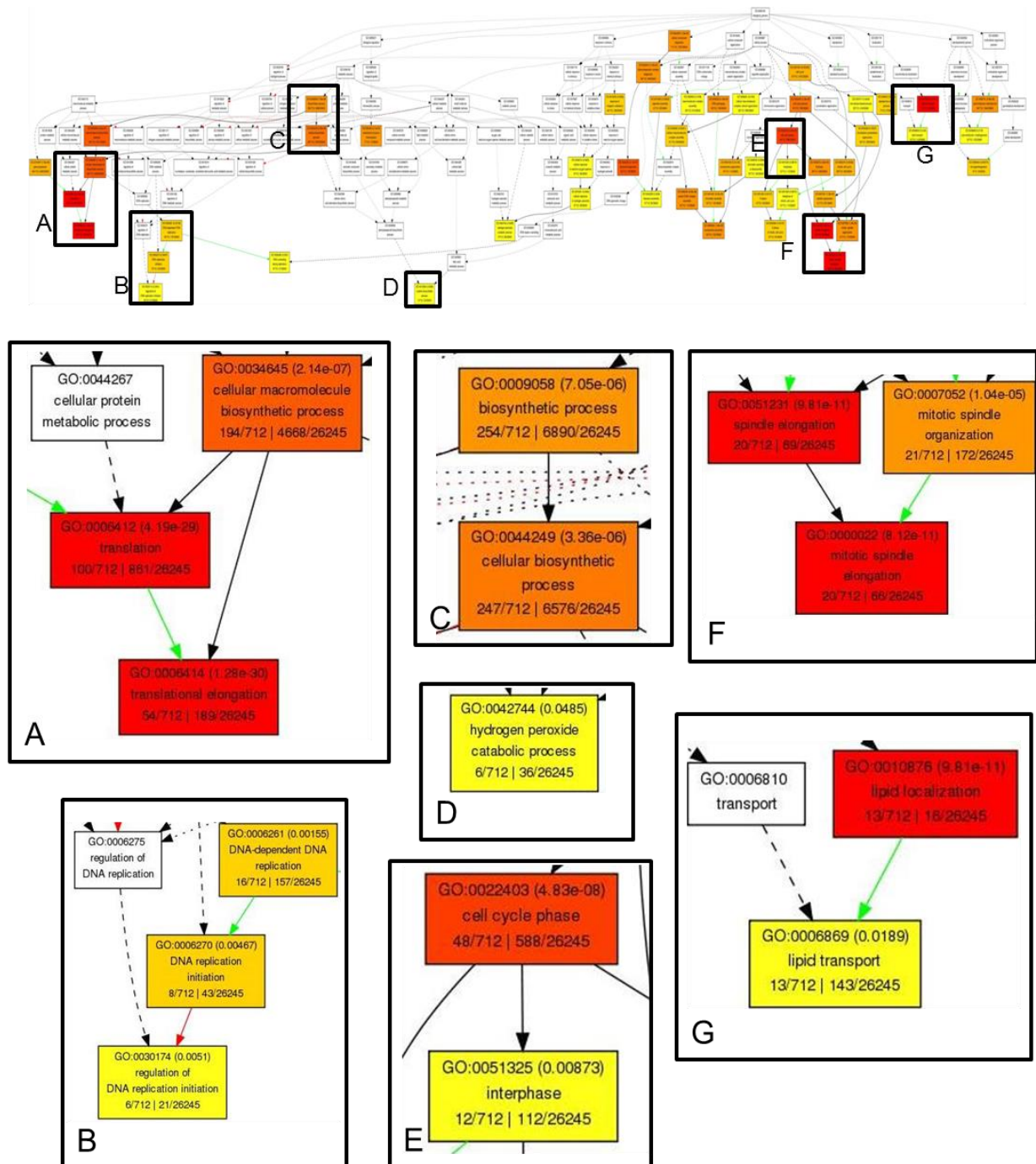


**Figure 32.** Pathway mapping of the significantly enriched GO terms among the SRS-specifically upregulated sorghum genes within the category “Biological process”. Boxes represent GO terms labeled with the GO ID, description and statistical information: number of submitted genes that belonged to this GO term / total number of genes submitted | total number of maize genes belonging to the GO term (background reference) / total number of genes annotated in the sorghum genome. The significant terms are shaded in color according to different levels of significance, and different arrows show the kind of regulation as indicated below Figure 33.

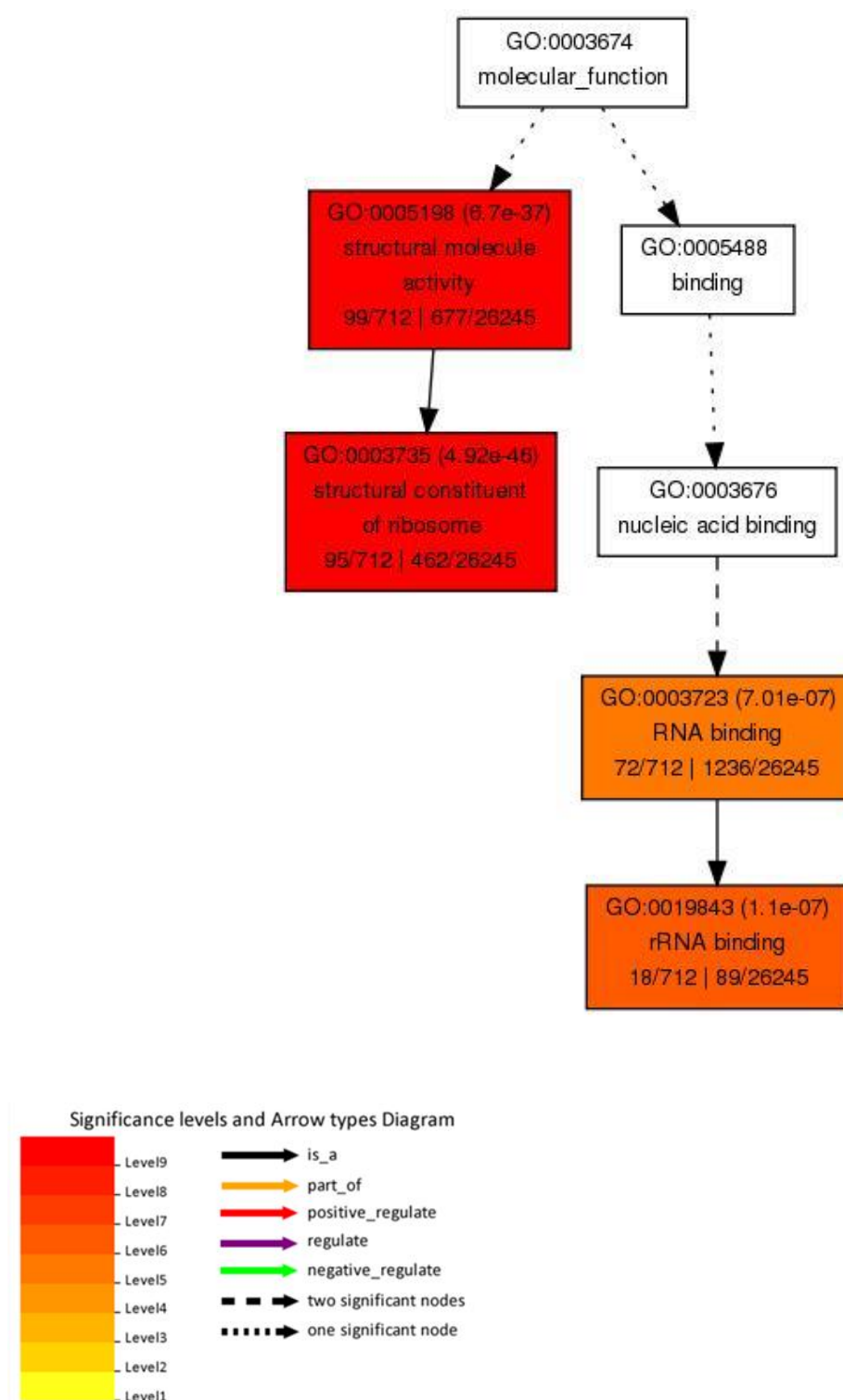


**Figure 33.** Pathway mapping of the significantly enriched GO terms among the SRS-specifically upregulated sorghum genes within the category “Molecular function” category. Boxes represent GO terms labeled with the GO ID, description and statistical information: number of submitted genes that belonged to this GO term / total number of genes submitted | total number of maize genes belonging to the GO term (background reference) / total number of genes annotated in the sorghum genome. The significant terms are shaded in color according to different levels of significance, and different arrows show the kind of regulation as indicated below Figure 33.

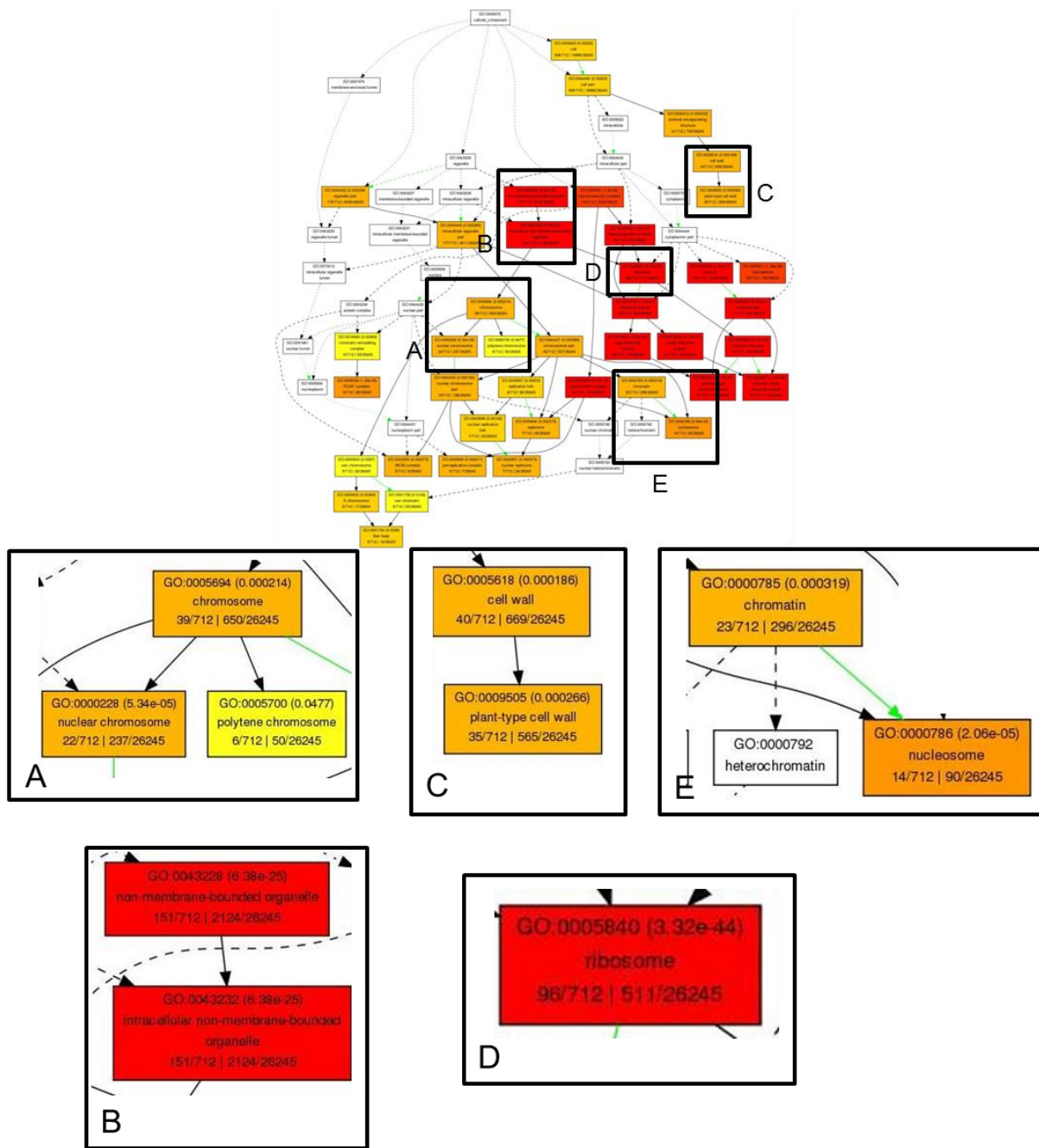


**Figure 34.** Pathway mapping of the significantly enriched GO terms among the SRS-specifically upregulated sorghum genes within the “Cellular component” category. Boxes represent GO terms labeled with the GO ID, description and statistical information: number of submitted genes that belonged to this GO term / total number of genes submitted | total number of maize genes belonging to the GO term (background reference) / total number of genes annotated in the sorghum genome. The significant terms are shaded in color according to different levels of significance, and different arrows show the kind of regulation as indicated below Figure 33.

### **3.3 Cell separation in sorghum: establishment of methods to isolate mesophyll and vascular bundle cells in sorghum leaves**

My experiments showed that both SRS and SRZ are able to penetrate the plant and grow on sorghum leaves. However, while SRS reaches the meristems and produces spores, SRZ is not so efficient colonizing vascular bundles and does not reach the meristems. Several defense reactions of sorghum were induced in leaves after inoculation with SRZ, but so far no tissue-specific defense reaction could be observed. Additionally, fungal genes involved in host colonization and necessary for the successful spread of SRS are still unknown. Transcriptome analysis of leaves infected with SRS and SRZ revealed differences in gene expression, but it is not clear whether and in which plant tissues specific defense reactions occur. To obtain insights into tissue-specific expression during fungal colonization, I wanted to compare gene expression in different cell types, which requires the collection of high-quality specific cell types for RNA extraction.

#### **3.3.1 Isolation of vascular bundles and mesophyll cells by laser microdissection (LMD)**

Laser microdissection is a method that uses a laser beam coupled into a microscope to cut and catapult cells of interest. The cells are visualized and selected using a computer monitor, and then the laser is activated, cutting and separating the cells from the slide. The cells are catapulted and collected inside a cap of a microcentrifuge tube. After that, cells can be used for RNA extraction.

The preparation of samples for LMD is a long procedure that includes sample collection and fixation, cryosectioning and several steps of slide dehydration. During establishment of the cryosection experiment, I tested different kinds of fixation methods, different sectioning procedures (such as cross sections and longitudinal sections) and also different thicknesses (between 8 and 15  $\mu\text{m}$ ). Prior to LMD, I performed a pre-experiment to quantify and verify the quality of the plant cells, using slides containing cross sections (20  $\mu\text{m}$ ) obtained by cryosectioning. Different sizes of vascular bundles were observed in sorghum leaves. Small vascular bundles

contained between 20 and 30 cells, while bigger ones presented about 90 cells. I also tested different kinds of staining, such as toluidine blue, WGA alexa fluoropropidium iodide, and DAPI to visualize plant and fungal cells after cryosectioning. The fluorescent staining resulted in high background fluorescence, probably due to the freezing procedure during cryosection and possible presence of tissue freezing medium still in the samples (Fig. 35A, C). Staining with toluidine blue allowed the perception of blue fungal hyphae inside the vascular bundles (Fig. 35B). SRZ-infected samples observed immediately after cryosectioning showed the presence of phytoalexins very closely connected to vascular bundles (Fig. 35D). With this experiment, I observed a good quality for vascular bundles and mesophyll cells, while epidermal cells seemed damaged, probably due to the freezing procedure. Therefore, only vascular bundles and mesophyll cells were selected for laser microdissection. After all the tests, I decided to use cross sections with 12  $\mu\text{m}$ , due to the best cellular morphology, easier identification of different cell types, and good performance during LMD.

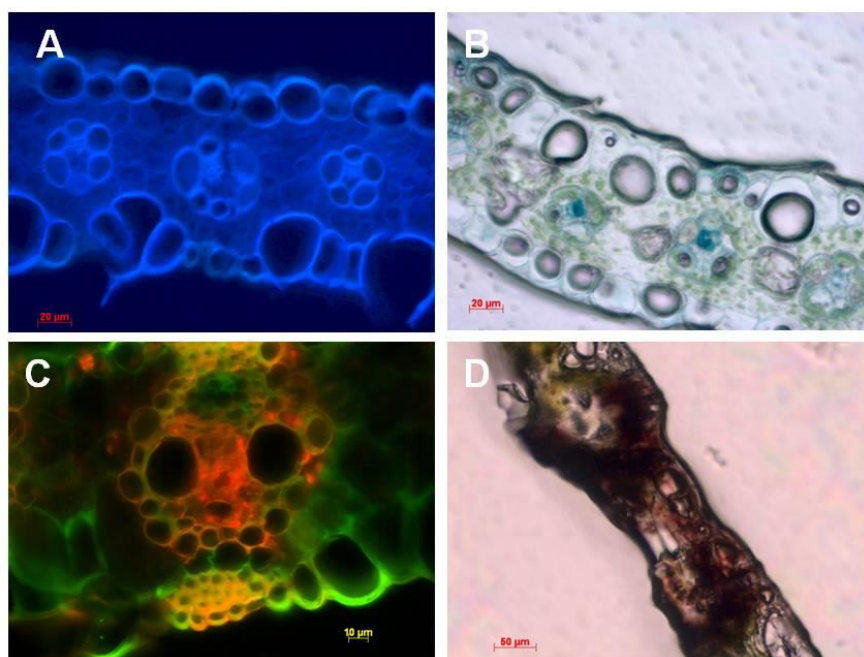


**Figure 35.** Cross sections (20  $\mu\text{m}$ ) of sorghum leaves showing different cell types. A. DAPI staining B. Toluidine blue showing hyphae of SRS inside vascular bundles of sorghum C. Alexa fluoropropidium iodide staining of a big vascular bundle D. Direct observation of a sample infected with SRZ, showing phytoalexins in red.

For LMD, conditions also had to be established to allow the best performance during cutting and catapulting. After several tests, the conditions selected were as follow:

autoLPC, speed 59, energy 50, focus 60. Examples of slides containing mesophyll cells and vascular bundle before and after LMD, as well as an example of collected vascular bundle inside the collection cap, are shown in Fig. 36. At least 3 groups containing 1500-2000 cells per cell type were individually collected and pooled to obtain about 6000 cells prior to RNA extraction. This amount of cells resulted in a concentration of about 1 ng/ $\mu$ l total RNA. Unfortunately, the total amount of fungal RNA obtained in the unavoidable background of plant RNA was too small for sequencing. Therefore, I started to look for alternative methods that would enable easier plant tissue separation and result in higher quantities of RNA for sequencing.

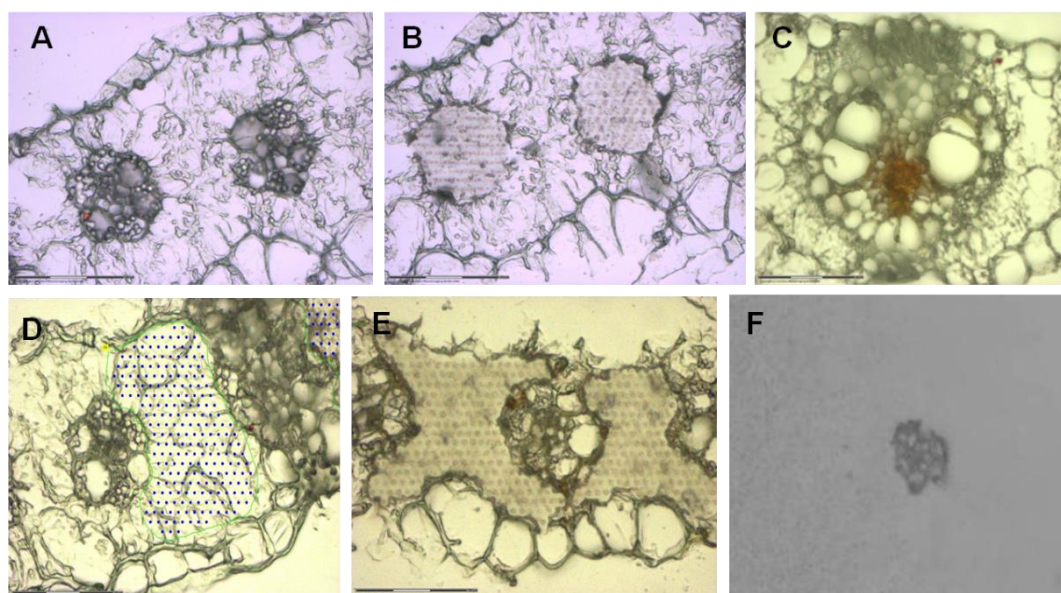


**Figure 36.** Samples before and after LMD. Two vascular bundles are shown prior (A) and after (B) LMD. A vascular bundle displays phytoalexin staining in the centrum (C), indicating the presence of SRZ. (D) A group of mesophyll cells selected for LMD, while the empty space is observed after LMD in (E). A vascular bundle collected inside a cap of a microcentrifuge tube is visualized in (F).

### **3.3.2 Vascular bundles and mesophyll cells isolation by mechanical and enzymatic methods**

Since with LMD I was not able to obtain good concentrations and quality of RNA, I decided to search for alternative methods for separation of vascular bundles and mesophyll cells. For collection of vascular bundles, an adaptation of the mechanical

method developed by Chang et al. (2012) was performed. This method is based in preparation of leaf slices that are added to a cold cell isolation medium, homogenized, filtered through a 500- $\mu\text{m}$  mesh, suspended, and then the cells are filtered using an 80- $\mu\text{m}$  nylon net, resulting in separated bundle strands. The method was modified and several filtrations had to be performed to allow the complete separation of vascular bundles, since in the beginning samples presented a high quantity of epidermal cells attached. In the end, large volumes of vascular strands were obtained, showing a good morphology (Fig. 37A, B). The samples were checked by fluorescence microscopy, where the quality was confirmed by the presence of nucleated plant cells (Fig. 37C) and large amounts of fungal hyphae (Fig. 37D).

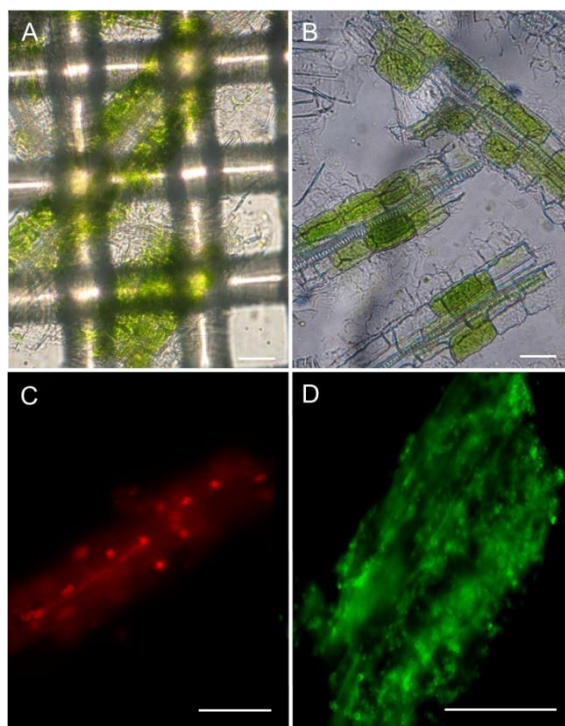


**Figure 37.** Vascular bundles isolated by a mechanical method. (A) Vascular strands on top of the nylon net (B) Separated vascular strands (C) Vascular bundle stained with propidium iodide, showing nuclei in red (D) vascular bundle stained with WGA Alexa Fluor showing fungal hyphae in green. Bars: 50  $\mu\text{m}$ .

For mesophyll separation, the protocol was adapted from Covshoof et al. (2012). The method uses leaf sections that are pressed and rolled with the assistance of a wallpaper seam roller. The fluid that emerges from the leaf is quickly removed by pipetting using buffer or DEPC water and dispensed into a 2 ml tube, being

immediately frozen. However, after pressing the leaf, it was still possible to see mesophyll cells attached, which indicated that they were not completely extracted (Fig. 38A, B). The sap showed the presence of mesophyll cells and fungal hyphae, but the cell quality was lower than expected, even after several repetitions (Fig. 38C, D). Therefore, this method was not as efficient as the method used for vascular bundle separation.

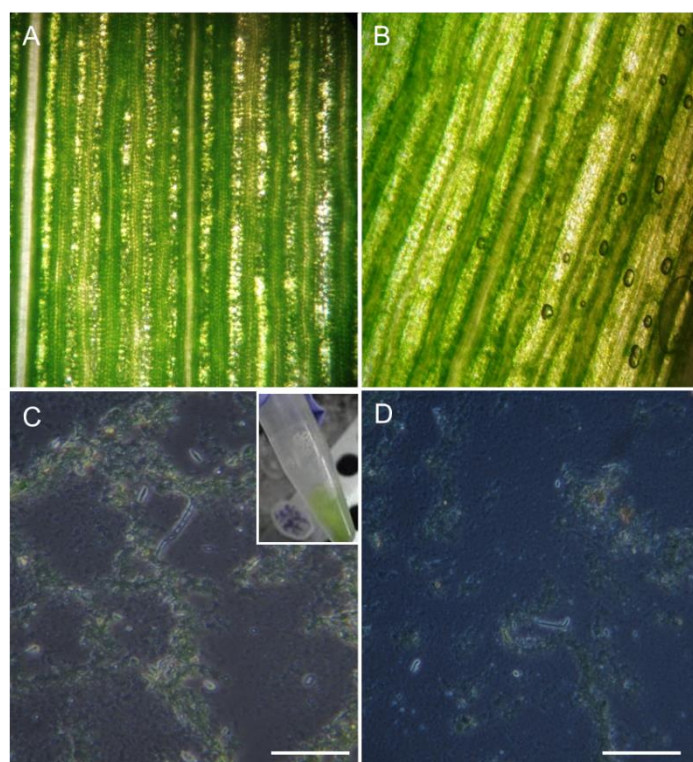


**Figure 38.** Separation of mesophyll cells in sorghum. (A) Leaf before rolling. (B) Leaf after rolling (C, D) Mesophyll cells and fungal hyphae. The collected sap is visualized in the inset picture. Bars: 50  $\mu\text{m}$

Compared with LMD, both methods presented the advantages of using larger amounts of plant material and being much faster, reducing the probability of RNA degradation. Indeed, these methods produced higher amounts of RNA that varied between 100 and 300 ng/ $\mu\text{l}$ . However, the quality of the RNA produced was insufficient for RNA-seq. Therefore, transcriptome of distinct cell types was not performed.

## **4. Discussion**

The vast majority of phytopathogenic fungi have a limited host range, infecting exclusively one or only a few distinct plant species. This is particularly true for the smut *S. reilianum*, which exists in two host adapted *formae speciales* that can infect sorghum (*f. sp. reilianum*, or SRS) or maize (*f. sp. zaeae*, or SRZ). To determine the mechanisms governing host specificity in *S. reilianum*, I compared the fate of SRS and SRZ during the colonization of maize and sorghum, investigating the fungal and the plant side.

### **4.1 The *Sporisorium reilianum*- maize pathosystem**

Maize infected with the two *ff. ssp.* of *S. reilianum* did not show very pronounced differences in fungal colonization, since both SRS and SRZ were able to spread from inoculated leaves to the nodes. Nevertheless, microscopic observation suggested smaller amounts of SRS hyphae in maize leaves (Fig. 9A), which was confirmed by quantitative PCR (Fig. 10B). Transmission electron microscopy revealed a thinner cell wall accompanied by a ticker interfacial matrix for SRS, compared to SRZ (Fig. 13E, G), where interfacial matrix was very thin or absent and the cell wall exhibited a larger thickness (Fig.13D, F, H).

The reasons that make SRS unable to induce sporulation on maize are currently unclear. This study shows that SRS is capable of colonizing the leaves and is able to follow its way until reaching the nodes and apical meristems, where sporulation is supposed to begin. However, although SRS reaches the floral meristems, it is only able to induce phyllody, thereby redefining floral meristem determinacy (Ghareeb et al., 2011). Microscopy of phyllodied cobs revealed the presence of considerable amounts of hyphae but no spores. It is uncertain how the fungus influences meristem determinacy, but several possibilities exist. The fungus could directly act on transcription or activity of maize meristem regulating transcription factors, or it could affect local hormone concentrations that indirectly affect maize morphogenesis (Ghareeb et al., 2011). Similar leafy-like structures were observed in *Arabidopsis* upon infection with the Aster Yellows phytoplasma. Recently, studies described the

effector protein SAP54, which is responsible for modulating the floral development, triggering the production of phyllody structures that attract the colonization by phytoplasma vectors (MacLean et al, 2011; MacLean et al., 2014). It is possible that *S. reilianum* has a functionally similar effector that is present in both SRZ and SRS but has a bigger influence on general disease symptoms because SRS does not proceed to the spore formation state in maize.

Sporulation is a complex process that widely differs among the fungal species and is dependent on several factors. Light, temperature, oxygen concentrations, quantity of inoculum, nutrient assimilation and the interaction with host tissues play an important role during this process (Su et al., 2012). Physical aspects do not seem to be responsible for the failure of SRS to sporulate in maize, since the conditions of cultivation were similarly kept during the infection with both strains. The concentration of nutrients is also essential for sporulation and different fungal species present specific requirements. Some fungi need specific concentrations of carbon and nitrogen to sporulate, others require the exhaustion of determined compounds, and for some the combination of many stimuli is necessary (Dahlerg and Etten, 1982). In the close relative *Ustilago maydis*, the sucrose transporter Srt1 was identified that enables the fungus to feed on the sucrose present in the plant apoplast, being essential for virulence (Wahl et al., 2010). *S. reilianum* presents a homologue of Srt1, and curiously the expression of this gene in maize is more than 3-fold higher for SRZ than for SRS, indicating that SRZ may better assimilate sucrose than SRS. Moreover, transcriptome analysis showed the upregulation of a few genes involved in photosynthesis for SRZ-infected samples, suggesting that SRZ could be able to trigger an increase in photosynthesis and therefore boost its own nutrition. In *U. maydis*, the lack of some proteins interferes with sporulation. An APSES transcription factor named Ust1 was described as a regulator of teliosporogenesis and its deletion abolished sporulation *in planta* (García-Pedrajas et al., 2010). Also in *U. maydis*, two proteins were described as involved in melanization, an important step during spore formation. The deletion of *lac1*, a laccase encoding gene, resulted in mutants showing reduced virulence on maize seedlings and fewer spores in adult plants, while mutants in *pks1*, which encodes a polyketide synthase, produced hyaline spores on maize (Islamovic et al., 2014). The velvet proteins Umv1 and Umv2 also play a role in sporulation. The *umv1* deletion mutants were not able to normally

proliferate and were blocked before the spore formation, while  $\Delta umv2$  mutants could slowly sporulate; therefore showing reduced virulence (Karakkatt et al., 2013). However, none of these genes seem to be missing or non-functional for SRS, since it is able to produce spores on sorghum and transcriptome shows the expression of the genes, indicating that genes involved in sporulation must be functional in SRS.

Quantitative PCR showed that SRS can reach meristems, but lower amounts of fungal DNA were found, when compared to SRZ (Fig. 10B). This may indicate that SRS does not proliferate as fast as SRZ, reaching the nodes at a late time point to trigger sporulation. In arbuscular mycorrhizal fungi, for example, sporulation reflects differences in fungal growth that are host-dependent (Bever et al., 1996). Alternatively, SRS may reach the nodes on time, but the amounts of hyphae could be insufficient to trigger sporulation, suggesting involvement of a quorum sensing mechanism. Quorum sense has been extensively studied in bacteria and has recently been described in fungi, where it is involved in several processes. In *Neurospora crassa*, measurement of the cell density is fundamental for the formation of conidial anastomosis tubes (Roca et al., 2005). In *Candida albicans*, the inoculum size defines the form of growth; small cell densities grow in the filamentous form, while high densities induce the yeast form. This is controlled by a quorum-sensing molecule, which inhibits the modification of yeast to filamentous growth (Hornby et al., 2001).

The occurrence of defense responses in maize leaves was investigated to elucidate the reasons that cause the distinct concentrations of SRZ and SRS-hyphae inside the plant. Curiously,  $H_2O_2$  and callose were produced at very low levels for both strains (Figs. 17 and 18), whereas increased lignification or plant cell death were not observed at all (Figs. 19 and 20). The next step was the quantification of the expression of defense marker genes in maize. From the 6 genes tested, 2 did not show changes when compared to uninfected samples (glucan synthase and chitinase), 2 of them (PR5 and chitinase) showed a similar upregulation for both strains, 1 (PR10) was upregulated for SRZ and 1 (thaumatin-like) was induced by SRS infection. A more complete investigation of differences between SRS- and SRZ-induced responses was done by transcriptome analysis of infected maize leaves, which resulted in 500 genes differentially regulated in the comparison of maize leaves colonized by SRS and SRZ. A GO term enrichment analysis of the strain-

specifically upregulated genes (270 for SRZ and 230 for SRS) revealed a high induction of equivalent terms for SRS and SRZ: significantly enriched GO-terms included oxidoreductase activity and iron ion binding, indicating that similar processes are stimulated by both SRS and SRZ. However, these similar processes were activated through different sets of genes and included a higher number of genes for SRZ. In SRS-infected samples, response to oxidative stress was increased, and from the 6 genes that belonged to this category, 5 belonged to the child GO term peroxidase activity, suggesting that SRS would be able to trigger detoxification of H<sub>2</sub>O<sub>2</sub>.

Since the GO term analysis was not very enlightening due to the low number of genes presenting an annotation in the query list, gene identity was checked by manual annotation using BLAST searches. Several genes upregulated in SRZ-infected samples presented involvement in defense, such as pathogen-related proteins, plant receptors and protein kinases. Also induced were transcription factors from the WRKY family that are important modulators in the regulation of plant-defense genes (Agarwal et al., 2011; Ishihama and Yoshioka, 2012). Heat shock proteins were upregulated exclusively in SRZ-infected samples and most of them belonged to the group of Hsp70 proteins that are thought to be involved in defense against oxidative stress (Duan et al., 2011; Byth-Illing and Bornman, 2014). Furthermore, expression of genes involved in actin regulation was also increased, pointing to a rearrangement of the plant cytoskeleton by the fungal infection. A rearrangement of the cytoskeleton upon fungal colonization was also observed in *Malva pusilla* infected with *C. gloesporioides f. sp. malvae* (Jin et al., 1999), and more recently, an increase in actin filaments was detected in the *Arabidopsis-Pseudomonas* pathosystem (Henty-Ridilla et al., 2013). Along with this, the upregulation of an E3 protein ligase, that is likely involved in the regulation of protein stability by ubiquitin (Trujillo and Shirasu, 2010), indicates an increase in ubiquitination in SRZ-infected maize.

The genes upregulated in SRS-infected maize mainly belonged to pathogen-related proteins, plant receptors, membrane transporters and DNA-binding or transcription factors. Interestingly, a group of 11 pentatricopeptide repeat-containing (PPR) proteins was upregulated in these samples. PPR proteins belong to a family characterized by repeats of a 35-amino acid motif. They are RNA-binders, being

implicated in RNA metabolism, stability, processing, editing and translation (Lurin et al., 2004; Saha et al., 2007; Fujii and Small, 2011; Yagi et al., 2014). In Arabidopsis, PGN, a PPR protein, is involved in resistance and its inactivation results in susceptibility to the necrotrophic pathogens *Botrytis cinerea* and *Alternaria brassicicola* (Laluk et al., 2011). Also in Arabidopsis, mutants for two genes encoding PPR proteins presented much more severe disease when infected with *Pseudomonas syringae* pv. *tomato* DC3000 or *Botrytis cinerea* (Park et al., 2014). Genes encoding PPR proteins generate trans-acting small interfering RNAs during the resistance response of soybean against *Phytophthora sojae* (Wong et al., 2014). These interfering RNAs, also known as phasiRNAs, are reported in Arabidopsis by their ability to suppress target transcript levels (Fei et al., 2013). In maize, the function of PPR proteins is still unknown, but my data suggest a possible involvement in defense against SRS. Additionally, 3 genes implicated in biosynthesis of thiamine were upregulated for SRS. Thiamine is reported as an activator of plant resistance, and its importance has been shown in several plants. In rice, Arabidopsis and plant crops, thiamine activates the expression of several PR proteins and protein kinases, increasing resistance to fungi, bacteria and viruses (Ahn et al., 2005). In grapevine, this vitamin enhances the production of H<sub>2</sub>O<sub>2</sub> and the expression of PR genes, and is connected with the modulation of phytoalexin biosynthesis (Boubakri et al., 2012; 2013). Thiamine was used to prime rice against *Rhizoctonia solani* and triggered an increase in H<sub>2</sub>O<sub>2</sub>, phenolic compounds, phenylalanine ammonia lyase and superoxide dismutase (Bahuguna et al., 2012). In Arabidopsis, priming with thiamine increased resistance to *Sclerotinia sclerotiorum* through modulation of the cellular redox status by the induction of ROS accumulation (Zhou et al., 2013).

No differences in plant defense could be found by microscopic experiments; however, transcriptome data indicates that distinct sets of genes are activated by SRS and SRZ already in the maize leaves. The expression of these different genes could be responsible for the less pronounced proliferation of SRS or a late arrival on the meristems, resulting in the observed lack of sporulation. Further studies will be necessary to understand the processes that are differentially regulated by SRS and SRZ, especially the involvement of the PPR proteins and thiamine. Additionally, an investigation of gene expression in apical meristems infected with SRS and SRZ will help to identify fungal and plant genes involved in host selection or sporulation in *S. reilianum*.

#### **4.2 The *Sporisorium reilianum*-sorghum pathosystem**

Noticeable differences regarding the behavior of SRS and SRZ were observed in sorghum. In leaves, extensive amounts of SRS-hyphae accumulated inside bundle sheath cells and vascular bundles (Fig. 7A, C). In contrast, the concentration of SRZ-structures started to decrease along the inoculated leaf, which was accompanied by the appearance of hyphae showing deformities inside the vascular bundles (Fig. 7B, D). Quantitative differences in proliferation of the two strains were confirmed by PCR analysis of fungal DNA, showing a prevalence of SRS in all parts analysed, while SRZ became undetectable in nodes (Fig. 10A). Accordingly, microscopic investigation of the growing point from inoculated plants showed that SRZ was indeed unable to reach the plant apical meristems (Fig. 7F), while meristematic tissues of plants inoculated with SRS were heavily colonized (Fig. 7E).

Several reasons seem to contribute for the differences in proliferation between SRS and SRZ in sorghum. According to Knogge (1996), host specificity can be controlled by toxins produced by the pathogen that target specific plant species. Fungal species from the genera *Cochliobolus* and *Alternaria* produce several host-selective toxins that are critical determinants for virulence in their respective hosts and act by disturbing plant biochemical processes, sometimes resulting in programmed cell death (Markham and Hille, 2001, Sindhu et al., 2008; Wight et al., 2009). *S. reilianum* is not known to produce toxins inducing cell death, and their biosynthesis seems unlikely, since this biotrophic fungus has to proliferate without causing damage to the plant, due to the necessity of keeping the tissues alive to complete its life cycle. On the other hand, plants can also deposit toxic compounds that can inhibit or kill pathogens. We have shown before that sorghum infected with SRZ leads to the induction of phytoalexins (3-deoxyanthocyanidins) that form readily visible red stains on plant leaves and fungal hyphae (Zuther et al., 2012). Phytoalexins are considered a good marker for resistance to biotic stress in sorghum (Dicko et al, 2005). Indeed, they are shown to confer resistance to *Colletotrichum sublineolum* in sorghum (Ibraheem et al., 2010), in addition to several other interactions, such as *Magnaporthe oryzae* in rice (Duan et al., 2014), *Alternaria brassicicola* in cruciferous crops (Pedras and Minic, 2014), *Phytophthora infestans* in *Nicotiana benthamiana* (Matsukawa et al., 2013), and the aphid *Myzus persicae* in Arabidopsis (Kettles et al., 2013). The 3-deoxyanthocyanidins induced by SRZ in sorghum were identified as

luteolinidin and apigeninidin, but only luteolinidin was able to restrict the growth of haploid *S. reilianum* cells *in vitro*. We proposed that spread of SRZ in sorghum might be precluded by an over-accumulation of luteolinidin at proliferation sites that is not induced by SRS (Zuther et al., 2012). It is impressive that SRS does not trigger phytoalexins in sorghum, since it is reported that many organisms and elicitors induce these compounds on sorghum, such as chitin (Fig. 21), carbohydrates and peptides extracted from conidia of *C. graminicola*, preparations of *Saccharomyces cerevisiae*, and even Kefir grains and fermented milk (Yamaoka et al., 1990; Wulff and Pascholati, 1998; Curti, 2010). Some pathogens developed enzymes to detoxify phytoalexins. This is the case of *Leptosphaeria maculans* and *Alternaria brassicicola* in crucifers (Pedras et al., 2008, 2009) and *Nectria haematococca* in pea (George and van Etten, 2001). It was thinkable that SRS could also have an enzyme that works in detoxification of phytoalexins, but SRS showed the same sensitivity to luteolinidin as SRZ *in vitro* (Zuther et al., 2012), making this scenario highly unlikely. Moreover, there are no additional genes encoding this sort of enzyme in SRS genome.

The deposition of luteolinidin was only observed at 3 days after inoculation, while in the interaction of sorghum with other fungi, such as *Helminthosporium maydis* and *Colletotrichum graminicola*, the accumulation of this compound was reported much earlier (Nicholson *et al.*, 1988; Zuther et al., 2012). This late deposition suggests that penetration and early leaf colonization might go unnoticed by sorghum. In this study, I show that SRZ is recognized in sorghum at least as soon as the fungal hyphae attempt penetration, since I observed 1.5 fold more penetration structures after inoculation with SRS than with SRZ (see 3.2.1). A reduced number of infection structures has also been observed in other similar systems. Spores of *Uromyces fabae* are able to germinate on non-host wheat leaves but over 98% of the germ tubes fail to produce appressoria necessary for penetration (Zhang et al. 2011). Similarly, *Colletotrichum sublineolum* shows a significantly lower number of appressoria on sorghum leaves from resistant and intermediate genotypes than of the susceptible ones (Basavaraju et al., 2009). Furthermore, the formation of an untypical lip-like structure bordering the tips of SRZ-appressoria was observed (Fig. 14D). While it is not clear what this lip-like structure is made of and whether appressoria that form such a structure are able to penetrate, it does show that

hyphae of SRZ behave differently on sorghum than on maize, which indicates presence of a very early interaction between host and pathogen.

An evident  $H_2O_2$  accumulation could be observed at penetration sites of SRZ (Fig. 17B, D), while hyphae of SRS were not or only to a much lower extent exposed to  $H_2O_2$  (Fig. 17A, C). This could indicate that either only SRZ is recognized by the plant leading to  $H_2O_2$  accumulation at penetration sites, or that both strains are recognized but SRS actively suppresses  $H_2O_2$  production at early time points. Of these two possibilities, the second is more likely, since some SRS-penetration events showed  $H_2O_2$  accumulation, which would not be expected if this strain had failed to induce it. As such, the green mold fungus *Penicillium digitatum* was shown to suppress  $H_2O_2$  accumulation in citrus, whereas the closely related *Penicillium expansum* triggers  $H_2O_2$  and does not induce disease (Macarasin et al., 2007). In *U. maydis*, a protein effector named Pep1 inhibits plant peroxidases involved in the oxidative burst. Deletion mutants lacking this effector induce strong  $H_2O_2$  production and the virulence is decreased (Hemetsberger et al., 2012). Also in *U. maydis*, deletion of Yap1, a transcription factor that induces generation of  $H_2O_2$ -degrading enzymes, leads to  $H_2O_2$ -accumulation at hyphal tips and to a reduction in fungal proliferation *in planta* (Molina and Kahmann, 2007). Since in both *formae speciales* of *S. reilianum* Pep1 and Yap1 are expected to be functional, the observed differences in  $H_2O_2$  accumulation may not affect fungal proliferation because PEP1 would inhibit peroxidases and Yap1 would induce  $H_2O_2$ -degrading enzymes at hyphal tips, thereby ensuring fungal proliferation. In SRZ, the observed higher amount of  $H_2O_2$  apparently did not lead to arrest of fungal growth, but perhaps helped to decrease fungal proliferation through the activation of other defense responses, since the fungus proliferated less well than SRS already in leaf tissues (Fig. 10A).

In addition to  $H_2O_2$ -accumulation, I observed callose depositions at 2 dai at sites of attempted cell-to-cell crossing of SRZ hyphae. The presence of thick callose depositions seemed effective in hindering fungal proliferation (Fig. 18B-D), but the same hyphae had before managed several cell-to-cell crossings without any or with only a minor amount of callose deposited at these sites (Fig. 18D, E, asterisks). This delayed response of callose deposition was unexpected, since callose deposition is a very early plant response and the timing of deposition has been implicated in the success of defense (Voigt et al., 2014). In Arabidopsis, callose formation in response

to wounding and penetrating fungal hyphae can be clearly observed at 1 dai (Jacobs et al., 2003). Possibly, SRZ has the ability to suppress early callose formation by secretion of fungal effector proteins. Alternatively, callose response might be much slower in sorghum than in *Arabidopsis*, as observed in the interaction of *C. sublineolum* with sorghum, where callose formation was also observed at 2 dai (Basavaraju et al., 2009).

To find out if other defense responses would also be induced by SRZ on sorghum, the expression of plant marker genes was measured. Genes encoding a DFR3 enzyme, a LRR receptor, a thaumatin-like and a chitinase showed a significant upregulation for samples infected with SRZ, indicating that sorghum readily responds against this strain and activates a pool of defense responses, which eventually stops the fungus in the inoculated leaves. A thaumatin-like gene was also upregulated by SRS in maize, suggesting that this group of pathogenesis-related proteins, in addition to the deposition of phytoalexins, could be used as marker genes for incompatible interactions in *S. reilianum*. According to Trudel et al (1998), some thaumatin-like proteins specifically bind  $\beta$ -glucan, what demonstrates an important role of these enzymes in plant defense against fungi.

Transcriptome analysis confirmed the differences observed by qRT-PCR and showed the activation of processes unknown before. Completely distinct gene sets were induced by SRS or SRZ. Mainly, SRS led to activation of genes involved in cellular processes, increasing the multiplication of plant cells. This indicates that SRS induces changes in the leaf development, triggering a metabolic reprogramming in sorghum. In the compatible interaction of *Ustilago maydis* and maize, microarray analysis of plant genes at different time points showed an increase in the GO terms related to cell wall metabolism, protein, transcription and RNA processing, which is similar to what I observed for SRS in sorghum (Doehlemann et al., 2008b). Although SRS mainly induces tumour formation in sorghum inflorescences, we observed before a few cases where tumours were produced in leaves and stem (J. Schirawski, personal communication). This is similar to what occurs in infections with *U. maydis* in maize, where tumours are known to contain free sugars that can be used by the fungus (Doehlemann et al., 2008b). Therefore, an increase in cellular processes is important for the compatibility of smuts with their hosts and could be advantageous for the fungus to acquire nutrients.

SRS-infected plants also showed expression of enzymes involved in catabolism of  $H_2O_2$ . An examination of the proteins encoded by the 6 genes that belonged to this GO term showed that all of them were peroxidases.  $H_2O_2$  is an important defense response, especially because it also triggers other defense responses, but high levels of this compound are toxic for the plant. To control that the oxidative burst does not cause damage to their own tissues, plants possess scavenging systems that include enzymes such as peroxidases, catalases, and superoxide dismutases (Polle, 1997). Therefore, SRS may be able to induce the scavenging system in sorghum, inducing the detoxification of  $H_2O_2$  through the activation of peroxidases, thereby decreasing this first layer of defense.

On the other hand, SRZ evoked dramatic defense responses in sorghum, inducing numerous proteins involved in immune responses, such as protein kinases, receptors, calcium-binding proteins, hormones, chitin-responsive proteins, proteins involved in secondary metabolism, phosphorylation, and catalysis. Several pathogenesis-related proteins showed induction, including glucanases and chitinases that are known for their potential to hydrolyze components of the fungal cell wall. The simultaneous activation of several defenses in sorghum was also observed during infection with *Fusarium proliferatum* and *Fusarium thapsinum*, where phytoalexins, peroxidases, beta-1,3-glucanases and chitinases were activated (Huang et al., 2004). The same occurred with sorghum infected with the necrotroph *Bipolaris sorghicola*, where phytoalexins, plant receptors, MAPK cascades, calcium signaling, transcription factors, peroxidases, PR proteins, phytoalexins and genes implicated in biosynthesis of lignin were upregulated (Mizuno et al., 2012, Yazawa et al., 2013). Transcriptome analysis of transgenic *Arabidopsis* infected with two isolates of *Blumeria graminis f. sp. hordei* showed a decrease in the expression of fungal candidate-effector proteins in the incompatible interaction. This was accompanied by high transcriptional reprogramming of the host, indicating that plant defenses may target the secretion of fungal effectors (Hacquard et al., 2013). The observation that many genes involved in defense are expressed against SRZ is particularly important. This knowledge could be used for the development of strategies to control SRS in sorghum through the generation of plants overexpressing specific plant defenses. Many examples are known where plant defense genes, such as chitinases,  $\beta$ -glucanases and other PR-proteins, were introduced or overexpressed in plants and increased the resistance

against pathogens (Zhu et al. 1994; Jach et al. 1995; Iwai et al., 2002; Gómez-Ariza et al., 2007).

The distinct responses encountered by SRS and SRZ may indicate the existence of different elicitors that could be present only in one of them. SRZ may have unknown avirulence genes (*avr*) that are recognized by resistance receptors in sorghum and trigger defense responses. In *Melampsora lini*, *Magnaporthe oryzae*, and *Cladosporium fulvum*, strains carrying different Avr proteins are only able to infect specific hosts (Ellis et al, 2007; Tosa et al., 2005; Sweigard et al., 1995; van der Does and Rep, 2007). However, since no resistant sorghum cultivars are known, gene for gene relationship does not seem to exist in the interaction of *S. reilianum* with its hosts (Lübberstedt et al., 1999). In addition, phenotypic analysis of meiotic progeny of SRS and SRZ showed a linear range in virulence on sorghum, indicating that virulence is a quantitative trait and not induced or hindered by the existence of a single Avr protein (T. Wollenberg and J. Schirawski, unpublished).

Alternatively, pathogen associated molecular patterns (PAMPs), such as chitin and  $\beta$ -1,3-glucan, could also be involved in the induction of defense responses observed for SRZ on sorghum. This is quite likely, since  $H_2O_2$ , callose, phytoalexins and the induction of PR proteins are very common responses during PAMP-triggered immunity and the infiltration of sorghum with chitin was sufficient to induce phytoalexins (Fig. 21). Supporting this idea, transcriptome data showed the upregulation of several GO terms involved in chitin recognition and chitinase enzymes for SRZ-infected samples, which means that sorghum actively recognizes the chitin from SRZ. Additionally, a sorghum receptor-like kinase 2 (Sb04g023810) was more than 3-fold upregulated in SRZ-infected samples, when compared to SRS. The protein encoded by this gene is the best homolog of BAK1 from Arabidopsis, which is the main regulator of several PRR receptors that are involved in PAMP-triggered immunity (Chinchilla et al., 2007; Monaghan and Zipfel, 2012).

However, how could a strain-specific response be explained, since both SRS and SRZ are supposed to present similar levels of chitin and  $\beta$ -1,3-glucan? Recent studies demonstrate that some plant pathogens developed the ability to trick the host through mechanisms that allow them to hide and escape from PAMP-recognition. These mechanisms are diverse and include the secretion of LysM domain-containing

effectors that can either protect chitin in the fungal cell wall (van den Burg et al., 2006) or sequester chitin fragments, avoiding them to reach plant receptors (de Jonge et al., 2010). A LysM-domain containing protein exists in *S. reilianum*, but its function is still unknown. A homologous gene occurs in the relative *U. maydis*, whose deletion generates hypervirulent strains and decrease several defense responses *in planta* (Stolle, 2013). Curiously, transcriptome data of infected sorghum shows an upregulation of 9-fold for this gene in SRZ compared to SRS, which suggests that this gene may have a similar avirulence function as the homolog in *U. maydis*. Future experiments generating gene deletions in SRZ will help to elucidate the involvement of this LysM- protein in host specificity and virulence of *S. reilianum*.

Other protection mechanisms employed by fungi against PAMP- recognition include the modification of chitin to the weaker elicitor chitosan (El Gueddariat et al., 2002), the production of  $\alpha$ -1,3-glucan to mask  $\beta$ -1,3-glucan in the cell wall (Fujikawa et al., 2009; Fujikawa et al., 2012) and the downregulation of  $\beta$ -1,3-glucan during initial stages after plant penetration (Oliveira-Garcia and Deising, 2013). Intriguingly, all genes encoding chitin synthases and several genes involved in the synthesis of  $\beta$ -1,3-glucan show higher expression for SRZ in sorghum, when compared to SRS. This suggests that SRS may be able to downregulate chitin and  $\beta$ -1,3-glucan during the early stages of infection, therefore escaping of being recognized by PRR receptors, and avoiding PAMP-triggered immunity. Further studies silencing or overexpressing chitin and glucan synthases, along with transcriptome analysis at later stages of colonization, will be helpful to show if the expression of these enzymes remain the same or suffer changes during SRS-colonization. This would help to confirm the possibility that SRS downregulates the cell wall components at early stages of colonization in sorghum.

Finally, the comparison of SRZ in sorghum and SRS in maize suggests a more efficient performance of SRS on its non-favored host, since it can reach apical meristems in maize, while SRZ on sorghum can only colonize infected leaves. SRS also seems to be more virulent on its host sorghum, considering that infections reach nearly 100% of virulence, while infections with SRZ on maize reach between 36% (Zuther et al., 2012) and 60% (this study) of virulence. Thus, most likely *S. reilianum* was originally a pathogen of sorghum (SRS) that during the evolution suffered a host shift and started to infect maize, giving rise to SRZ.

In this thesis, I presented new data about host specificity in smut fungi. Through a detailed analysis of the behavior of two *formae speciales* of *S. reilianum* in maize and sorghum, I showed that SRS and SRZ trigger different plant responses, and that the reasons that determine the lack of success of SRS in maize and SRZ in sorghum are most likely distinct. This study indicates that host specificity takes place at different time points in sorghum and maize, being defined at much earlier stages in sorghum. Taking together, the results demonstrate that host choice in *S. reilianum* is the result of a multilayered adaptation to either suppress or evade the different plant defense responses. Availability of the genome sequences of SRS and SRZ and the expression analysis of fungal genes that is currently underway will be extremely helpful to elucidate which fungal genes contribute to the complex plant-fungal interplay that determines host-specificity in *S. reilianum*.

## 5. References

- Agarwal P, Reddy MP, Chikara J** (2011) WRKY: Its structure, evolutionary relationship, DNA-binding selectivity, role in stress tolerance and development of plants. *Mol Biol Rep* **38**: 3883–3896
- Ahn I-P, Kim S, Lee Y-H** (2005) Vitamin B1 functions as an activator of plant disease resistance. *Plant Physiol* **138**: 1505–1515
- Ahuja I, Kissen R, Bones AM** (2012) Phytoalexins in defense against pathogens. *Trends Plant Sci* **17**: 73–90
- Alexander D, Goodman RM, Gut-Rella M, Glascock C, Weymann K, Friedrich L, Maddox D, Ahl-Goy P, Luntz T, Ward E** (1993) Increased tolerance to two oomycete pathogens in transgenic tobacco expressing pathogenesis-related protein 1a. *Proc Natl Acad Sci U S A* **90**: 7327–7331
- Almagro L, Gómez Ros L V., Belchi-Navarro S, Bru R, Ros Barceló A, Pedreño MA** (2009) Class III peroxidases in plant defence reactions. *J Exp Bot* **60**: 377–390
- Anderson JP, Gleason CA, Foley RC, Thrall PH, Burdon JB, Singh KB** (2010) Plants versus pathogens: An evolutionary arms race. *Funct Plant Biol* **37**: 499–512
- Antonovics J, Bever JD, Morton JB, Schultz PA** (1996) Host-dependent sporulation and species diversity of arbuscular mycorrhizal fungi in a mown grassland. *J Ecol* **84**: 71–82
- Bahuguna RN, Joshi R, Shukla A, Pandey M, Kumar J** (2012) Thiamine primed defense provides reliable alternative to systemic fungicide carbendazim against sheath blight disease in rice (*Oryza sativa* L.). *Plant Physiol Biochem* **57**: 159–167
- Bari R, Jones JDG** (2009) Role of plant hormones in plant defence responses. *Plant Mol Biol* **69**: 473–488
- Basavaraju P, Shetty NP, Shetty HS, de Neergaard E, Jørgensen HJL** (2009) Infection biology and defence responses in sorghum against *Colletotrichum sublineolum*. *J Appl Microbiol* **107**: 404–415
- Bauer R, Begerow D, Oberwinkler F, Piepenbring M, Berbee ML** (2000). Ustilaginomycetes. In: *Mycota VII, Part 2. Systematics and Evolution* (eds. D.J. McLaughlin, E.G. McLaughlin, and P.A. Lemke). Springer Verlag, Berlin, Heidelberg, New York: 57-83

- Bever JD, Morton J, Antonovics J, Schultz PA** (1996) Host-dependent sporulation and species diversity of mycorrhizal fungi in a mown grassland. *J. Ecol.* **75**: 1965–1977
- Boller T, Felix G** (2009) A renaissance of elicitors: perception of microbe-associated molecular patterns and danger signals by pattern-recognition receptors. *Annu Rev Plant Biol* **60**:379–406
- Boubakri H, Poutaraud A, Wahab MA, Clayeux C, Baltenweck-Guyot R, Steyer D, Marcic C, Mliki A, Soustre-Gacougnolle I** (2013) Thiamine modulates metabolism of the phenylpropanoid pathway leading to enhanced resistance to *Plasmopara viticola* in grapevine. *BMC Plant Biol* **13**: 31
- Boubakri H, Wahab MA, Chong J, Bertsch C, Mliki A, Soustre-Gacougnolle I** (2012) Thiamine induced resistance to *Plasmopara viticola* in grapevine and elicited host-defense responses, including HR like-cell death. *Plant Physiol Biochem* **57**: 120–133
- Byth-Illing HA, Bornman L** (2014) Heat shock, with recovery, promotes protection of *Nicotiana tabacum* during subsequent exposure to *Ralstonia solanacearum*. *Cell Stress Chaperones* **19**: 193–203
- Chang Y-M, Liu W-Y, Shih AC-C, Shen M-N, Lu C-H, Lu M-YJ, Yang H-W, Wang T-Y, Chen SC-C, Chen SM, et al** (2012) Characterizing Regulatory and Functional Differentiation between Maize Mesophyll and Bundle Sheath Cells by Transcriptomic Analysis. *Plant Physiol* **160**: 165–177
- Chinchilla D, Bauer Z, Regenass M, Boller T, Felix G** (2006) The Arabidopsis receptor kinase FLS2 binds flg22 and determines the specificity of flagellin perception. *Plant Cell* **18**: 465–476
- Ciuffetti LM, Tuori RP, Gaventa JM** (1997) A single gene encodes a selective toxin causal to the development of tan spot of wheat. *Plant Cell* **9**: 135–144
- Covshoff S, Furbank RT, Leegood RC, Hibberd JM** (2013) Leaf rolling allows quantification of mRNA abundance in mesophyll cells of sorghum. *J Exp Bot* **64**: 807–813
- Curti, M** (2010) Síntese de fitoalexinas em sorgo e soja, controle de oídio e produção de pepino, Cv. Hokushin, por leite fermentado, mananoligossacarídeo fosforilado e Kefir. Doctoral Thesis, Universidade Estadual de Maringa, 82 pp
- Dafoe NJ, Huffaker A, Vaughan MM, Duehl AJ, Teal PE, Schmelz EA** (2011) Rapidly Induced Chemical Defenses in Maize Stems and Their Effects on Short-term Growth of *Ostrinia nubilalis*. *J Chem Ecol* **37**: 984–991
- Dahlberg KR, Etten J** (1982) Physiology and biochemistry of fungal sporulation. *Annu Rev Phytopathol.* **20**: 281–301
- De Jonge R, van Esse HP, Kombrink A, Shinya T, Desaki Y, Bours R, van der Krol S, Shibuya N, Joosten MHAJ, Thomma BPHJ** (2010) Conserved fungal

- LysM effector Ecp6 prevents chitin-triggered immunity in plants. *Science* **329**: 953–955
- Dicko MH, Gruppen H, Barro C, Traore AS, Van Berkel WJH, Voragen AGJ** (2005) Impact of phenolic compounds and related enzymes in sorghum varieties for resistance and susceptibility to biotic and abiotic stresses. *J Chem Ecol* **31**: 2671–2688
- Doehlemann G, Wahl R, Horst RJ, Voll LM, Usadel B, Poree F, Stitt M, Pons-Kühnemann J, Sonnewald U, Kahmann R, et al** (2008b) Reprogramming a maize plant: Transcriptional and metabolic changes induced by the fungal biotroph *Ustilago maydis*. *Plant J* **56**: 181–195
- Doehlemann G, Wahl R, Vranes M, de Vries RP, Kamper J, Kahmann R** (2008a). Establishment of compatibility in the *Ustilago maydis*/maize pathosystem. *J. Plant Physiol.* **165**: 29–40
- Du Y, Chu H, Wang M, Chu IK, Lo C** (2010a) Identification of flavone phytoalexins and a pathogen-inducible flavone synthase II gene (*SbFNSII*) in sorghum. *J Exp Bot* **61**: 983–994
- Du Z, Zhou X, Ling Y, Zhang Z, Su Z** (2010b) agriGO: A GO analysis toolkit for the agricultural community. *Nucleic Acids Res.* doi: 10.1093/nar/gkq310
- Duan L, Liu H, Li X, Xiao J, Wang S** (2014) Multiple phytohormones and phytoalexins are involved in disease resistance to *Magnaporthe oryzae* invaded from roots in rice. *Physiol Plant.* doi: 10.1111/ppl.12192
- Duan YH, Guo J, Ding K, Wang SJ, Zhang H, Dai XW, Chen YY, Govers F, Huang LL, Kang ZS** (2011) Characterization of a wheat HSP70 gene and its expression in response to stripe rust infection and abiotic stresses. *Mol Biol Rep* **38**: 301–307
- EI Gueddari NE, Rauchhaus U, Moerschbacher BM, Deising HB** (2002) Developmentally regulated conversion of surface-exposed chitin to chitosan in cell walls of plant pathogenic fungi. *New Phytol* **156**: 103–112
- Ellis JG, Dodds PN, Lawrence GJ** (2007) Flax rust resistance gene specificity is based on direct resistance-avirulence protein interactions. *Annu Rev Phytopathol* **45**: 289–306
- Fei Q, Xia R, Meyers BC** (2013) Phased, secondary, small interfering RNAs in posttranscriptional regulatory networks. *Plant Cell* **25**: 2400–15
- Figuroa M, Alderman S, Garvin DF, Pfender WF** (2013) Infection of *Brachypodium distachyon* by Formae Speciales of *Puccinia graminis*: Early Infection Events and Host-Pathogen Incompatibility. *PLoS One.* doi: 10.1371/journal.pone.0056857
- Flor, HH (1942)** Inheritance of pathogenicity in a cross between physiologic races 22 and 24 of *Melampsora lini*. *Phytopathology*, **35**:5

- Food and Agriculture Organization of the United Nations (FAO)** <http://faostat.fao.org/> (accessed on 12 May 2014)
- Frederiksen RA** (1977) Head smuts of corn and sorghum. In: Proc. 32nd Annu. Corn Sorghum Res. Conf. H.D. Loden and D. Wilkinson, eds. American Seed Trade Association, Washington, DC. pp: 89-105
- Friesen TL, Stukenbrock EH, Liu Z, Meinhardt S, Ling H, Faris JD, Rasmussen JB, Solomon PS, McDonald BA, Oliver RP** (2006) Emergence of a new disease as a result of interspecific virulence gene transfer. *Nat Genet* **38**: 953–956
- Fujii S, Small I** (2011) The evolution of RNA editing and pentatricopeptide repeat genes. *New Phytol* **191**: 37–47
- Fujikawa T, Kuga Y, Yano S, Yoshimi A, Tachiki T, Abe K, Nishimura M** (2009) Dynamics of cell wall components of *Magnaporthe grisea* during infectious structure development. *Mol Microbiol* **73**: 553–570
- Fujikawa T, Sakaguchi A, Nishizawa Y, Kouzai Y, Minami E, Yano S, Koga H, Meshi T, Nishimura M** (2012) Surface  $\alpha$ -1,3-Glucan Facilitates Fungal Stealth Infection by Interfering with Innate Immunity in Plants. *PLoS Pathog.* doi: 10.1371/journal.ppat.1002882
- García-Pedrajas MD, Baeza-Montañez L, Gold SE** (2010) Regulation of *Ustilago maydis* dimorphism, sporulation, and pathogenic development by a transcription factor with a highly conserved APSES domain. *Mol Plant Microbe Interact* **23**: 211–222
- George HL, VanEtten HD** (2001) Characterization of pisatin-inducible cytochrome p450s in fungal pathogens of pea that detoxify the pea phytoalexin pisatin. *Fungal Genet Biol* **33**: 37–48
- Ghareeb H, Becker A, Iven T, Feussner I, Schirawski J** (2011) *Sporisorium reilianum* Infection Changes Inflorescence and Branching Architectures of Maize. *Plant Physiol* **156**: 2037–2052
- Gilchrist DG** (1998) Programmed cell death in plant disease: the purpose and promise of cellular suicide. *Annu Rev Phytopathol* **36**: 393–414
- Gillissen B, Bergemann J, Sandmann C, Schroeer B, Bölker M, Kahmann R** (1992) A two-component regulatory system for self/non-self recognition in *Ustilago maydis*. *Cell* **68**: 647–657
- Giraud T, Gladieux P, Gavrillets S** (2010) Linking the emergence of fungal plant diseases with ecological speciation. *Trends Ecol Evol* **25**: 387–395
- Glazebrook J** (2005) Contrasting mechanisms of defense against biotrophic and necrotrophic pathogens. *Annu Rev Phytopathol* **43**: 205–227

- Gómez-Ariza J, Campo S, Rufat M, Estopà M, Messeguer J, San Segundo B, Coca M** (2007) Sucrose-mediated priming of plant defense responses and broad-spectrum disease resistance by overexpression of the maize pathogenesis-related PRms protein in rice plants. *Mol Plant Microbe Interact* **20**: 832–842
- Graham TL** (1995) Cellular biochemistry of phenylpropanoid of soybean to infection by *Phytophthora sojae*. in *Handbook of Phytoalexin Metabolism and Action*. eds Daniel M, Purkayastha RP (Marcel Dekker, New York), pp 85–116.
- Graham TL, Graham MY** (1991) Cellular coordination of molecular responses in plant defense. *Mol Plant-Microbe Interact* **4**: 415–422
- Hacquard S, Kracher B, Maekawa T, Vernaldi S, Schulze-Lefert P, Ver Loren van Themaat E** (2013) Mosaic genome structure of the barley powdery mildew pathogen and conservation of transcriptional programs in divergent hosts. *Proc Natl Acad Sci U S A* **110**: E2219–28
- Halisky, PM** (1963) Head smut of sorghum, sudan grass, and corn, caused by *Sphacelotheca reiliana* (Kühn). *Clint. Hilgardia* **34**: 287-304
- Hammerschmidt R** (1999) Phytoalexins: What Have We Learned After 60 Years? *Annu Rev Phytopathol* **37**: 285–306
- Hanna WF** (1929) Studies in the physiology and cytology of *Ustilago zea* and *Sorosporium reilianum*. *Phytopathology* **19**:415-442
- Hejgaard J, Jacobsen S, Svendsen I** (1991) Two antifungal thaumatin-like proteins from barley grain. *FEBS Lett* **291**: 127–131
- Hemetsberger C, Herrberger C, Zechmann B, Hillmer M, Doehlemann G** (2012) The *Ustilago maydis* effector Pep1 suppresses plant immunity by inhibition of host peroxidase activity. *PLoS Pathog*. doi: 10.1371/journal.ppat.1002684
- Henty-Ridilla JL, Li J, Blanchoin L, Staiger CJ** (2013) Actin dynamics in the cortical array of plant cells. *Curr Opin Plant Biol* **16**: 678–687
- Hoffman CS, Winston F** (1987) A ten-minute DNA preparation from yeast efficiently releases autonomous plasmids for transformation of *Escherichia coli*. *Gene* **57**: 267–272
- Hornby JM, Jensen EC, Lisec AD, Tasto JJ, Jahnke B, Shoemaker R, Dussault P, Nickerson KW** (2001) Quorum Sensing in the Dimorphic Fungus *Candida albicans* Is Mediated by Farnesol. *Appl Environ Microbiol* **67**: 2982–2992
- Huang, LD, Backhouse, D** (2004) Effects of *Fusarium* species on defence mechanisms in sorghum seedlings. *N. Z. Plant Prot.* **57**: 121–124
- Hückelhoven R** (2007) Cell wall-associated mechanisms of disease resistance and susceptibility. *Annu Rev Phytopathol* **45**: 101–127

- Huffaker A, Kaplan F, Vaughan MM, Dafoe NJ, Ni X, Rocca JR, Alborn HT, Teal PEA, Schmelz EA** (2011) Novel acidic sesquiterpenoids constitute a dominant class of pathogen-induced phytoalexins in maize. *Plant Physiol* **156**: 2082–2097
- Ibraheem F, Gaffoor I, Chopra S** (2010) Flavonoid phytoalexin-dependent resistance to anthracnose leaf blight requires a functional yellow seed1 in *Sorghum bicolor*. *Genetics* **184**: 915–926
- Ishihama N, Yoshioka H** (2012) Post-translational regulation of WRKY transcription factors in plant immunity. *Curr Opin Plant Biol* **15**: 431–437
- Islamovic E, Garcia-Pedrajas MD, Chacko N, Andrews DL, Covert SF, Gold SE** (2014) Transcriptome analysis of a *Ustilago maydis* *ust1* deletion mutant uncovers involvement of laccase and polyketide synthase genes in spore development. *Mol Plant Microbe Interact*. <http://dx.doi.org/10.1094/MPMI-05-14-0133-R>
- Iwai T, Kaku H, Honkura R, Nakamura S, Ochiai H, Sasaki T, Ohashi Y** (2002) Enhanced resistance to seed-transmitted bacterial diseases in transgenic rice plants overproducing an oat cell-wall-bound thionin. *Mol Plant Microbe Interact* **15**: 515–521
- Iyengar RB, Smits P, van der Ouderaa F, van der Wel H, van Brouwershaven J, Ravestein P, Richters G, van Wassenaar PD** (1979) The complete amino-acid sequence of the sweet protein thaumatin I. *Eur J Biochem* **96**: 193–204
- Jach G, Gornhardt B, Mundy J, Logemann J, Pinsdorf E, Leah R, Schell J, Maas C** (1995) Enhanced quantitative resistance against fungal disease by combinatorial expression of different barley antifungal proteins in transgenic tobacco. *Plant J* **8**: 97–109
- Jacobs AK, Lipka V, Burton RA, Panstruga R, Strizhov N, Schulze-Lefert P, Fincher GB** (2003) An Arabidopsis Callose Synthase, *GSL5*, Is Required for Wound and Papillary Callose Formation. *Plant Cell* **15**: 2503–2513
- Jin S, Xu R, Wei Y, Goodwin PH** (1999) Increased expression of a plant actin gene during a biotrophic interaction between round-leaved mallow, *Malva pusilla*, and *Colletotrichum gloeosporioides* f. sp. *malvae*. *Planta* **209**: 487–494
- Johrde A, Schweizer P** (2008) A class III peroxidase specifically expressed in pathogen-attacked barley epidermis contributes to basal resistance. *Mol Plant Pathol* **9**: 687–696
- Jones JDG, Dangl JL** (2006) The plant immune system. *Nature* **444**: 323–329
- Kang SC, Sweigard JA, Valent B** (1995) The *PWL* host specificity gene family in the blast fungus *Magnaporthe grisea*. *Mol Plant-Microbe Interact* **8**: 939–948
- Karakat BB, Gold SE, Covert SF** (2013) Two members of the *Ustilago maydis* velvet family influence teliospore development and virulence on maize seedlings. *Fungal Genet Biol* **61**: 111–119

- Kawasaki T, Koita H, Nakatsubo T, Hasegawa K, Wakabayashi K, Takahashi H, Umemura K, Umezawa T, Shimamoto K** (2006) Cinnamoyl-CoA reductase, a key enzyme in lignin biosynthesis, is an effector of small GTPase Rac in defense signaling in rice. *Proc Natl Acad Sci U S A* **103**: 230–235
- Kerk NM, Ceserani T, Tausta SL, Sussex IM, Nelson TM** (2003) Laser capture microdissection of cells from plant tissues. *Plant Physiol* **132**: 27–35
- Kettles GJ, Drurey C, Schoonbeek HJ, Maule AJ, Hogenhout SA** (2013) Resistance of *Arabidopsis thaliana* to the green peach aphid, *Myzus persicae*, involves camalexin and is regulated by microRNAs. *New Phytol* **198**: 1178–1190
- Knogge W** (1996) Molecular basis of specificity in host/fungus interactions. *Eur J Plant Pathol* **102**: 807–816
- Koch E, Slusarenko A** (1990) *Arabidopsis* is susceptible to infection by a downy mildew fungus. *Plant Cell* **2**: 437–445
- Kuźniak E, Urbanek H** (2000) The involvement of hydrogen peroxide in plant responses to stresses. *Acta Physiol Plant* **22**: 195–203
- Laluk K, Abuqamar S, Mengiste T** (2011) The *Arabidopsis* Mitochondria-Localized Pentatricopeptide Repeat Protein PGN Functions in Defense against Necrotrophic Fungi and Abiotic Stress Tolerance. *Plant Physiol* **156**: 2053–2068
- Lamb C, Dixon RA** (1997) The Oxidative Burst in Plant Disease Resistance. *Annu Rev Plant Physiol Plant Mol Biol* **48**: 251–275
- Levine A, Tenhaken R, Dixon R, Lamb C** (1994) H<sub>2</sub>O<sub>2</sub> from the oxidative burst orchestrates the plant hypersensitive disease resistance response. *Cell* **79**: 583–593
- Lievens B, Houterman PM, Rep M** (2009) Effector gene screening allows unambiguous identification of *Fusarium oxysporum* f. sp. *lycopersici* races and discrimination from other formae speciales. *FEMS Microbiol Lett* **300**: 201–215
- Linthorst HJM** (1991) Pathogenesis-related proteins of plants. *CRC Crit Rev Plant Sci* **10**: 123–150
- Liu H, Du Y, Chu H, Shih CH, Wong YW, Wang M, Chu IK, Tao Y, Lo C** (2010) Molecular dissection of the pathogen-inducible 3-deoxyanthocyanidin biosynthesis pathway in sorghum. *Plant Cell Physiol* **51**: 1173–1185
- Liu JJ, Ekramoddoullah AKM, Yu X** (2003) Differential expression of multiple PR10 proteins in western white pine following wounding, fungal infection and cold-hardening. *Physiol Plant* **119**: 544–553
- Lo SC, Nicholson RL** (1998) Reduction of light-induced anthocyanin accumulation in inoculated sorghum mesocotyls. Implications for a compensatory role in the defense response. *Plant Physiol* **116**: 979–989

- Lo C, Coolbaugh RC, Nicholson RL** (2002) Molecular characterization and in silico expression analysis of a chalcone synthase gene family in *Sorghum bicolor*. *Physiol Mol Plant Pathol* **61**: 179–188
- Lübberstedt T, Xia XC, Tan G, Liu X, Melchinger AE** (1999) QTL mapping of resistance to *Sporisorium reilianum* in maize. *Theor Appl Genet* **99**: 593–598
- Luna E, Pastor V, Robert J, Flors V, Mauch-Mani B, Ton J** (2011) Callose deposition: a multifaceted plant defense response. *Mol Plant Microbe Interact* **24**: 183–193
- Lurin C, Andrés C, Aubourg S, Bellaoui M, Bitton F, Bruyère C, Caboche M, Debast C, Gualberto J, Hoffmann B, Lecharny A, Le Ret M, Martin-Magniette ML, Mireau H, Peeters N, Renou JP, Szurek B, Taconnat L, Small I** (2004) Genome-wide analysis of *Arabidopsis* pentatricopeptide repeat proteins reveals their essential role in organelle biogenesis. *Plant Cell* **16**: 2089–2103
- Macarisin D, Cohen L, Eick A, Rafael G, Belausov E, Wisniewski M, Droby S** (2007) *Penicillium digitatum* Suppresses Production of Hydrogen Peroxide in Host Tissue During Infection of Citrus Fruit. *Phytopathology* **97**: 1491–1500
- MacLean AM, Orlovskis Z, Kowitwanich K, Zdziarska AM, Angenent GC, Immink RGH, Hogenhout SA** (2014) Phytoplasma Effector SAP54 Hijacks Plant Reproduction by Degrading MADS-box Proteins and Promotes Insect Colonization in a RAD23-Dependent Manner. *PLoS Biol.* doi: 10.1371/journal.pbio.1001835
- MacLean AM, Sugio A, Makarova O V., Findlay KC, Grieve VM, Toth R, Nicolaisen M, Hogenhout SA** (2011) Phytoplasma Effector SAP54 Induces Indeterminate Leaf-Like Flower Development in *Arabidopsis* Plants. *Plant Physiol* **157**: 831–841
- Manning VA, Pandelova I, Dhillon B, Wilhelm LJ, Goodwin SB, Berlin AM, Figueroa M, Freitag M, Hane JK, Henrissat B, et al** (2013) Comparative genomics of a plant-pathogenic fungus, *Pyrenophora tritici-repentis*, reveals transduplication and the impact of repeat elements on pathogenicity and population divergence. *G3 (Bethesda)* **3**: 41–63
- Markham JE, Hille J** (2001) Host-selective toxins as agents of cell death in plant-fungus interactions. *Mol Plant Pathol* **2**: 229–239
- Martínez-Espinoza AD, García-Pedrajas MD, Gold SE** (2002) The Ustilaginales as plant pests and model systems. *Fungal Genet Biol* **35**: 1–20
- Martinez C, Roux C, Dargent R** (1999) Biotrophic Development of *Sporisorium reilianum* f. sp. *zeae* in Vegetative Shoot Apex of Maize. *Phytopathology* **89**: 247–253
- Matsukawa M, Shibata Y, Ohtsu M, Mizutani A, Mori H, Wang P, Ojika M, Kawakita K, Takemoto D** (2013) *Nicotiana benthamiana* calreticulin 3a is required for the ethylene-mediated production of phytoalexins and disease

- resistance against oomycete pathogen *Phytophthora infestans*. *Mol Plant-Microbe Interact* **26**: 880–92
- Mert-türk F** (2002) Phytoalexins : Defence or just a response to stress ? *J cell Mol Biol* **1**: 1–6
- Mizuno H, Kawahigashi H, Kawahara Y, Kanamori H, Ogata J, Minami H, Itoh T, Matsumoto T** (2012) Global transcriptome analysis reveals distinct expression among duplicated genes during sorghum-interaction. *BMC Plant Biol* **12**: 121
- Miya A, Albert P, Shinya T, Desaki Y, Ichimura K, Shirasu K, Narusaka Y, Kawakami N, Kaku H, Shibuya N** (2007) CERK1, a LysM receptor kinase, is essential for chitin elicitor signaling in Arabidopsis. *Proc Natl Acad Sci USA* **104**: 19613–19618
- Miyashita M, Nakamori T, Murai T, Yonemoto T, Miyagawa H, Akamatsu M, Ueno T** (2001) Structure-activity relationship study of host-specific phytotoxins (AM-toxin analogs) using a new assay method with leaves from apple meristem culture. *Zeitschrift fur Naturforsch - Sect C J Biosci* **56**: 1029–1037
- Molina L, Kahmann R** (2007) An *Ustilago maydis* gene involved in H<sub>2</sub>O<sub>2</sub> detoxification is required for virulence. *Plant Cell* **19**: 2293–2309
- Monaghan J, Zipfel C** (2012) Plant pattern recognition receptor complexes at the plasma membrane. *Curr Opin Plant Biol* **15**: 349–357
- Morisseau C, Ward BL, Gilchrist DG, Hammock BD** (1999) Multiple epoxide hydrolases in *Alternaria alternata* f. sp. *lycopersici* and their relationship to medium composition and host-specific toxin production. *Appl Environ Microbiol* **65**: 2388–2395
- Neuhaus J-M, Fritig B, Linthorst HJM, Meins F, Mikkelsen JD, Ryals J** (1996) A revised nomenclature for chitinase genes. *Plant Mol Biol Report* **14**: 102–104
- Nicholson RL, Jamil FF, Snyder BA, Lue WL, Hipskind J** (1988) Phytoalexin synthesis in the juvenile sorghum leaf. *Physiol Mol Plant Pathol* **33**:271–278
- Niderman T, Genetet I, Bruyère T, Gees R, Stintzi A, Legrand M, Fritig B, Möisinger E** (1995) Pathogenesis-related PR-1 proteins are antifungal. Isolation and characterization of three 14-kilodalton proteins of tomato and of a basic PR-1 of tobacco with inhibitory activity against *Phytophthora infestans*. *Plant Physiol* **108**: 17–27
- Oliveira-Garcia E, Deising HB** (2013) Infection structure-specific expression of  $\beta$ -1,3-glucan synthase is essential for pathogenicity of *Colletotrichum graminicola* and evasion of  $\beta$ -glucan-triggered immunity in maize. *Plant Cell* **25**: 2356–78
- Oliver RP, Lord M, Rybak K, Faris JD, Solomon PS** (2008) Emergence of tan spot disease caused by toxigenic *Pyrenophora tritici-repentis* in Australia is not associated with increased deployment of toxin-sensitive cultivars. *Phytopathology* **98**: 488–491

- Park CH, Kim S, Park JY, Ahn I-P, Jwa NS, Im KH, Lee YH** (2004) Molecular characterization of a pathogenesis-related protein 8 gene encoding a class III chitinase in rice. *Mol Cells* **17**: 144–150
- Park YJ, Lee HJ, Kwak KJ, Lee K, Hong SW, Kang H** (2014) MicroRNA400-guided cleavage of Pentatricopeptide repeat protein mRNAs Renders *Arabidopsis thaliana* more susceptible to pathogenic bacteria and fungi. *Plant Cell Physiol.* **55**: 1660-8
- Paterson AH, Bowers JE, Bruggmann R, Dubchak I, Grimwood J, Gundlach H, Haberer G, Hellsten U, Mitros T, Poliakov A, et al** (2009) The *Sorghum bicolor* genome and the diversification of grasses. *Nature* **457**: 551–556
- Pedras MSC, Minic Z** (2014) The phytoalexins brassilexin and camalexin inhibit cyclobrassinin hydrolase, a unique enzyme from the fungal pathogen *Alternaria brassicicola*. *Bioorganic Med Chem* **22**: 459–467
- Pedras MSC, Minic Z, Jha M** (2008) Brassinin oxidase, a fungal detoxifying enzyme to overcome a plant defense -purification, characterization and inhibition. *FEBS J* **275**: 3691–3705
- Pedras MSC, Minic Z, Sarma-Mamillapalle VK** (2009) Substrate specificity and inhibition of brassinin hydrolases, detoxifying enzymes from the plant pathogens *Leptosphaeria maculans* and *Alternaria brassicicola*. *FEBS J* **276**: 7412–7428
- Pedras MSC, Sarma-Mamillapalle VK** (2012) The cruciferous phytoalexins rapalexin A, brassalexin A and erucalexin: Chemistry and metabolism in *Leptosphaeria maculans*. *Bioorganic Med Chem* **20**: 3991–3996
- Pieterse CMJ, Leon-Reyes A, Van der Ent S, Van Wees SCM** (2009) Networking by small-molecule hormones in plant immunity. *Nat Chem Biol* **5**: 308–316
- Prom LK, Perumal R, Erattaimuthu SR, Erpelding JE, Montes N, Odvody GN, Greenwald C, Jin Z, Frederiksen, R, Magill CW** (2011) Virulence and Molecular Genotyping Studies of *Sporisorium reilianum* Isolates in *Sorghum*. *Plant Disease.* **95**: 523-529
- Reina-Pinto JJ, Yephremov A** (2009) Surface lipids and plant defenses. *Plant Physiol Biochem* **47**: 540–549
- Reineke G, Heinze B, Schirawski J, Buettner H, Kahmann R, Basse CW** (2008) Indole-3-acetic acid (IAA) biosynthesis in the smut fungus *Ustilago maydis* and its relevance for increased IAA levels in infected tissue and host tumour formation. *Mol Plant Pathol* **9**: 339–355
- Roca MG, Arlt J, Jeffree CE, Read ND** (2005) Cell biology of conidial anastomosis tubes in *Neurospora crassa*. *Eukaryot Cell* **4**: 911–919
- Saha D, Prasad AM, Srinivasan R** (2007) Pentatricopeptide repeat proteins and their emerging roles in plants. *Plant Physiol Biochem* **45**: 521–534

- Salzer P, Bonanomi A, Beyer K, Vögeli-Lange R, Aeschbacher RA, Lange J, Wiemken A, Kim D, Cook DR, Boller T** (2000) Differential expression of eight chitinase genes in *Medicago truncatula* roots during mycorrhiza formation, nodulation, and pathogen infection. *Mol Plant Microbe Interact* **13**: 763–777
- Sarh (1992)** Guía fitosanitaria para el cultivo del maíz. Serie Sanidad Vegetal. Secretaría de Agricultura y Recursos Hidráulicos, México DF. 14 pp.
- Selitrennikoff CP** (2001) Antifungal proteins. *Appl Environ Microbiol* **67**: 2883-2894
- Schirawski J, Heinze B, Wagenknecht M, Kahmann R** (2005) Mating type loci of *Sporisorium reilianum*: Novel pattern with three a and multiple b specificities. *Eukaryot Cell* **4**: 1317–1327
- Schirawski J, Mannhaupt G, Münch K, Brefort T, Schipper K, Doehlemann G, Di Stasio M, Rössel N, Mendoza-Mendoza A, Pester D, Müller O, Winterberg B, Meyer E, Ghareeb H, Wollenberg T, Münsterkötter M, Wong P, Walter M, Stukenbrock E, Güldener U, Kahmann R** (2010) Pathogenicity determinants in smut fungi revealed by genome comparison. *Science* **330**: 1546–1548
- Schittenhelm S** (2008) Chemical composition and methane yield of maize hybrids with contrasting maturity. *Eur J Agron* **29**: 72–79
- Schlumbaum A, Mauch F, Vögeli U, Boller T** (1986) Plant chitinases are potent inhibitors of fungal growth. *Nature* **324**: 365–367
- Schmelz EA, Kaplan F, Huffaker A, Dafoe NJ, Vaughan MM, Ni X, Rocca JR, Alborn HT, Teal PE** (2011) Identity, regulation, and activity of inducible diterpenoid phytoalexins in maize. *Proc Natl Acad Sci U SA* **108**: 5455–5460
- Schmidt SM, Houterman PM, Schreiver I, Ma L, Amyotte S, Chellappan B, Boeren S, Takken FLW, Rep M** (2013) MITEs in the promoters of effector genes allow prediction of novel virulence genes in *Fusarium oxysporum*. *BMC Genomics* **14**: 119
- Schnable PS, Ware D, Fulton RS, Stein JC, Wei F, Pasternak S, Liang C, Zhang J, Fulton L, Graves TA, Minx P, Reily AD, Courtney L, Kruchowski SS, Tomlinson C, Strong C, Delehaunty K, Fronick C, Courtney B, Rock SM, Belter E, Du F, Kim K, Abbott RM, Cotton M, Levy A, Marchetto P, Ochoa K, Jackson SM, Gillam B, Chen W, Yan L, Higginbotham J, Cardenas M, Waligorski J, Applebaum E, Phelps L, Falcone J, Kanchi K, Thane T, Scimone A, Thane N, Henke J, Wang T, Ruppert J, Shah N, Rotter K, Hodges J, Ingenthron E, Cordes M, Kohlberg S, Sgro J, Delgado B, Mead K, Chinwalla A, Leonard S, Crouse K, Collura K, Kudrna D, Currie J, He R, Angelova A, Rajasekar S, Mueller T, Lomeli R, Scara G, Ko A, Delaney K, Wissotski M, Lopez G, Campos D, Braidotti M, Ashley E, Golser W, Kim H, Lee S, Lin J, Dujmic Z, Kim W, Talag J, Zuccolo A, Fan C, Sebastian A, Kramer M, Spiegel L, Nascimento L, Zutavern T, Miller B, Ambroise C, Muller S, Spooner W, Narechania A, Ren L, Wei S, Kumari S, Faga B, Levy MJ, McMahan L, Van Buren P, Vaughn MW, Ying K, Yeh CT, Emrich SJ, Jia Y, Kalyanaraman A, Hsia AP, Barbazuk WB, Baucom RS, Brutnell TP,**

- Carpita NC, Chaparro C, Chia JM, Deragon JM, Estill JC, Fu Y, Jeddelloh JA, Han Y, Lee H, Li P, Lisch DR, Liu S, Liu Z, Nagel DH, McCann MC, SanMiguel P, Myers AM, Nettleton D, Nguyen J, Penning BW, Ponnala L, Schneider KL, Schwartz DC, Sharma A, Soderlund C, Springer NM, Sun Q, Wang H, Waterman M, Westerman R, Wolfgruber TK, Yang L, Yu Y, Zhang L, Zhou S, Zhu Q, Bennetzen JL, Dawe RK, Jiang J, Jiang N, Presting GG, Wessler SR, Aluru S, Martienssen RA, Clifton SW, McCombie WR, Wing RA, Wilson RK. (2009)** The B73 maize genome: complexity, diversity, and dynamics. *Science* **326**: 1112–1115
- Schulze-Lefert P, Panstruga R (2011)** A molecular evolutionary concept connecting nonhost resistance, pathogen host range, and pathogen speciation. *Trends Plant Sci* **16**: 117–125
- Serrano M, Coluccia F, Torres M, L'Haridon F, Métraux J-P (2014)** The cuticle and plant defense to pathogens. *Front Plant Sci* **5**: 274
- Sharma P, Jha AB, Dubey RS, Pessarakli M (2012)** Reactive Oxygen Species, Oxidative Damage, and Antioxidative Defense Mechanism in Plants under Stressful Conditions. *J Bot* **2012**: 1–26
- Shetty NP, Jensen JD, Knudsen A, Finnie C, Geshi N, Blennow A, Collinge DB, Jørgensen HJL (2009)** Effects of beta-1,3-glucan from *Septoria tritici* on structural defence responses in wheat. *J Exp Bot* **60**: 4287–4300
- Shimizu T, Nakano T, Takamizawa D, Desaki Y, Ishii-Minami N, Nishizawa Y, Minami E, Okada K, Yamane H, Kaku H, Shibuya N (2010)** Two LysM receptor molecules, CEBiP and OsCERK1, cooperatively regulate chitin elicitor signaling in rice. *Plant J* **64**: 204–214
- Shinya T, Motoyama N, Ikeda A, Wada M, Kamiya K, Hayafune M, Kaku H, Shibuya N (2012)** Functional characterization of CEBiP and CERK1 homologs in arabidopsis and rice reveals the presence of different chitin receptor systems in plants. *Plant Cell Physiol* **53**: 1696–1706
- Sindhu A, Chintamanani S, Brandt AS, Zanis M, Scofield SR, Johal GS (2008)** A guardian of grasses: specific origin and conservation of a unique disease-resistance gene in the grass lineage. *Proc Natl Acad Sci U S A* **105**: 1762–1767
- Song YY, Cao M, Xie LJ, Liang XT, Zeng R Sen, Su YJ, Huang JH, Wang RL, Luo SM (2011)** Induction of DIMBOA accumulation and systemic defense responses as a mechanism of enhanced resistance of mycorrhizal corn (*Zea mays* L.) to sheath blight. *Mycorrhiza* **21**: 721–731
- Stolle, Nancy (2013)** Funktionelle Charakterisierung eines LysM-Proteins von *Ustilago maydis*. Doctoral Thesis, Max Planck Institute for Terrestrial Microbiology, Marburg, 139 pp
- Stone BA, Evans NA, Bonig I, Clarke AE (1985)** The application of Sirofluor, a chemically defined fluorochrome from aniline blue for the histochemical detection of callose. *Protoplasma* **122**: 191–195

- Su Y-Y, Qi Y-L, Cai L** (2012) Induction of sporulation in plant pathogenic fungi. *Micology* **3**: 195-200
- Su Y, Xu L, Fu Z, Yang Y, Guo J, Wang S, Que Y** (2014) ScChi, encoding an acidic class III chitinase of sugarcane, confers positive responses to biotic and abiotic stresses in sugarcane. *Int J Mol Sci* **15**: 2738–2760
- Sweigard JA, Carroll AM, Kang S, Farrall L, Chumley FG, Valent B** (1995) Identification, Cloning, and Characterization of PWL2, a gene for host species specificity in the rice blast fungus. *Plant Cell* **7**: 1221–1233
- Takken F, Rep M** (2010) The arms race between tomato and *Fusarium oxysporum*. *Mol Plant Pathol* **11**: 309–314
- Thomma BPHJ, Nürnberger T, Joosten MHAJ** (2011) Of PAMPs and effectors: the blurred PTI-ETI dichotomy. *Plant Cell* **23**: 4–15
- Thordal-Christensen H, Zhang Z, Wei Y, Collinge DB** (1997) Subcellular localization of H<sub>2</sub>O<sub>2</sub> in plants. H<sub>2</sub>O<sub>2</sub> accumulation in papillae and hypersensitive response during the barley-powdery mildew interaction. *Plant J* **11**: 1187–1194
- Torres MA, Jones JDG, Dangl JL** (2006) Reactive oxygen species signaling in response to pathogens. *Plant Physiol* **141**: 373–378
- Tosa Y, Osue J, Eto Y, Oh H-S, Nakayashiki H, Mayama S, Leong SA** (2005) Evolution of an avirulence gene, AVR1-CO39, concomitant with the evolution and differentiation of *Magnaporthe oryzae*. *Mol Plant Microbe Interact* **18**: 1148–1160
- Troch V, Audenaert K, Wyand RA, Haesaert G, Höfte M, Brown JKM** (2014) *Formae speciales* of cereal powdery mildew: Close or distant relatives? *Mol Plant Pathol* **15**: 304–314
- Trudel J, Grenier J, Potvin C, Asselin A** (1998) Several thaumatin-like proteins bind to beta-1,3-glucans. *Plant Physiol* **118**: 1431–1438
- Trujillo M, Shirasu K** (2010) Ubiquitination in plant immunity. *Curr Opin Plant Biol* **13**: 402–408
- Vallet C** (1996) Histochemistry of Lignin Deposition during Sclerenchyma Differentiation in Alfalfa Stems. *Ann Bot* **78**: 625–632
- Van den Burg HA, Harrison SJ, Joosten MHAJ, Vervoort J, de Wit PJGM** (2006) *Cladosporium fulvum* Avr4 protects fungal cell walls against hydrolysis by plant chitinases accumulating during infection. *Mol Plant Microbe Interact* **19**: 1420–1430
- Van der Does HC, Rep M** (2007) Virulence genes and the evolution of host specificity in plant-pathogenic fungi. *Mol Plant Microbe Interact* **20**: 1175–1182

- Van H** (2000) Isolation and Characterization of Thaumatin I and II, the Sweet-Tasting Proteins from *Thaumatococcus daniellii* Benth. *Eur J Biochem* **225**: 221–225
- Vanholme R, Demedts B, Morreel K, Ralph J, Boerjan W** (2010) Lignin biosynthesis and structure. *Plant Physiol* **153**: 895–905
- Van Loon LC, Pierpoint WS, Boller T, Conejero V** (1994) Recommendations for naming plant pathogenesis-related proteins. *Plant Mol Biol Report* **12**: 245–264
- Van Loon LC, Rep M, Pieterse CMJ** (2006) Significance of inducible defense-related proteins in infected plants. *Annu Rev Phytopathol* **44**: 135–162
- Van Loon LC, van Kammen A** (1968) Polyacrylamide disc electrophoresis of the soluble leaf proteins from *Nicotiana tabacum* var. “Samsun” and “Samsun NN”-I. *Phytochemistry* **7**: 1727–1735
- Ványk K** (2002) The smut fungi of the world. A survey. *Acta Microbiol Immunol Hung* **49**: 163–175
- Vigers AJ, Roberts WK, Selitrennikoff CP** (1991) A new family of antifungal proteins. *Mol Plant-Microbe Interact.* **4**:315–323
- Voigt CA** (2014) Callose-mediated resistance to pathogenic intruders in plant defense-related papillae. *Front Plant Sci* **5**: 168
- Underwood W** (2012) The Plant Cell Wall: A Dynamic Barrier Against Pathogen Invasion. *Front Plant Sci.* doi: 10.3389/fpls.2012.00085
- Wahl R, Wippel K, Goos S, Kämper J, Sauer N** (2010) A novel high-affinity sucrose transporter is required for virulence of the plant pathogen *Ustilago maydis*. *PLoS Biol* **8**: e1000303 doi:10.1371/journal.pbio.1000303
- Wharton PS, Nicholson RL** (2000) Temporal synthesis and radiolabelling of the sorghum 3-deoxyanthocyanidin phytoalexins and the anthocyanin, cyanidin 3-dimalonyl glucoside. *New Phytol* **145**: 457–469
- Whetten R, Sederoff R** (1995) Lignin Biosynthesis. *Plant Cell* **7**: 1001–1013
- Wight WD, Kim K-H, Lawrence CB, Walton JD** (2009) Biosynthesis and role in virulence of the histone deacetylase inhibitor depudecin from *Alternaria brassicicola*. *Mol Plant Microbe Interact* **22**: 1258–1267
- Wilson, JM and Frederiksen, RA** (1970) Histopathology of the interaction of *Sorghum bicolor* and *Sphacelotheca reiliana*. *Phytopathology.* **60**, 828-833
- Wojtaszek P** (1997) Oxidative burst: an early plant response to pathogen infection. *Biochem J* **322**: 681–692
- Wong J, Gao L, Yang Y, Zhai J, Arikiti S, Yu Y, Duan S, Chan V, Xiong Q, Yan J, et al** (2014) Roles of small RNAs in soybean defense against *Phytophthora sojae* infection. *Plant J.* doi: **10.1111/tpj.12590**

- Worldometers.** [http:// www.worldometers.info/](http://www.worldometers.info/) (accessed on 12 May 2014)
- Wulff NA, Pascholati SF (1998)** Preparacoes de *Saccharomyces cerevisiae* elicitoras de fitoalexinas em mesocotilos de sorgo. *Sci. Agric.* **55**: 138-143
- Yagi Y, Hayashi S, Kobayashi K, Hirayama T, Nakamura T (2013)** Elucidation of the RNA Recognition Code for Pentatricopeptide Repeat Proteins Involved in Organelle RNA Editing in Plants. *PLoS One*. doi: 10.1371/journal.pone.0057286
- Yamaoka N, Lyons PC, Hipskind J, Nicholson RL (1990)** Elicitor of sorghum phytoalexin synthesis from *Colletotrichum graminicola*. *Physiol. Mol. Plant Pathol.* **37**: 255–270
- Yazawa T, Kawahigashi H, Matsumoto T, Mizuno H (2013)** Simultaneous Transcriptome Analysis of Sorghum and *Bipolaris sorghicola* by Using RNA-seq in Combination with De Novo Transcriptome Assembly. *PLoS One*. doi: 10.1371/journal.pone.0062460
- Zhang H, Wang C, Cheng Y, Wang X, Li F, Han Q, Xu J, Chen X, Huang L, Wei G (2011)** Histological and molecular studies of the non-host interaction between wheat and *Uromyces fabae*. *Planta* **234**: 979–991
- Zhou J, Sun A, Xing D (2013)** Modulation of cellular redox status by thiamine-activated NADPH oxidase confers *Arabidopsis* resistance to *Sclerotinia sclerotiorum*. *J Exp Bot* **64**: 3261–3272
- Zhu Q, Maher EA, Masoud S, Dixon RA, Lamb CJ (1994)** Enhanced Protection Against Fungal Attack by Constitutive Co-expression of Chitinase and Glucanase Genes in Transgenic Tobacco. *Bio/Technology* **12**: 807–812
- Zipfel C (2008)** Pattern-recognition receptors in plant innate immunity. *Curr Opin Immunol* **20**: 10–16
- Zipfel C, Robatzek S, Navarro L, Oakeley EJ, Jones JDG, Felix G, Boller T (2004)** Bacterial disease resistance in *Arabidopsis* through flagellin perception. *Nature* **428**: 764–767
- Zuther K, Kahnt J, Utermark J, Imkampe J, Uhse S, Schirawski J (2012)** Host specificity of *Sporisorium reilianum* is tightly linked to generation of the phytoalexin luteolinidin by *Sorghum bicolor*. *Mol Plant Microbe Interact* **25**: 1230–7

## 6. Appendix

### 6.1 List of Abbreviations

| <b>Abbreviation</b> | <b>Description</b>                              |
|---------------------|---|
| Δ                   | Deletion  |
| μl                  | Microliter                                      |
| ° C                 | Degree Celsius                                  |
| AFP                 | antifungal proteins                             |
| avr                 | Avirulence gene                                 |
| BAK1                | BRI1-ASSOCIATED RECEPTOR KINASE 1               |
| bp                  | Base pair                                       |
| CBE                 | Chlorazole black E                              |
| CEBiP               | Chitin elicitor bindin protein                  |
| cDNA                | Complementary DNA                               |
| CERK1               | CHITIN ELICITOR RECEPTOR KINASE 1               |
| DAB                 | 3,3'-Diaminobenzidine                           |
| dai                 | days after infection                            |
| DAPI                | 4',6-diamidino-2-phenylindole                   |
| DNA                 | Desoxyribonucleic acid                          |
| dNTP                | Deoxyribonucleotide                             |
| DTT                 | Dithiothreitol                                  |
| EDTA                | Ethylenediaminetetraacetic acid                 |
| ET                  | ethylene  |
| ETI                 | Effector-triggered immunity                     |
| ETS                 | Effector-triggered susceptibility               |
| f. sp.              | Forma specialis                                 |
| g                   | gramm   |
| GO                  | Gene ontology                                   |
| HR                  | hour  |
| HR                  | hypersensitive response                         |
| KDa                 | kilo dalton                                     |
| JA                  | jasmonic acid                                   |
| LMD                 | laser microdissection                           |
| LRR                 | Leucine rich repeat                             |
| M                   | Molar   |
| MAP                 | Mitogen-activated protein kinase                |
| ml                  | milliliter                                      |
| mM                  | milimolar                                       |
| mRNA                | messenger RNA                                   |
| NB-LRR              | nucleotide binding-leucine rich repeat proteins |
| NCBI                | National Center for Biotechnology information   |
| PAL                 | phenylalanine ammonia-lyase                     |
| PAMP                | Pathogen-associated molecular pattern           |

| <b>Abbreviation</b> | <b>Description</b>                                |
|---------------------|---|
| PBS                 | Phosphate buffer saline                           |
| PCR                 | Polymerase chain reaction                         |
| PD                  | Potato dextrose                                   |
| PRR                 | Pathogen recognition receptor                     |
| PTI                 | Pathogen-triggered immunity                       |
| qRT-PCR             | Quantitative real time RT-PCR                     |
| R                   | resistance gene                                   |
| RNA                 | Ribonucleic acid                                  |
| ROS                 | Reactive oxygen species                           |
| rpm                 | Rounds per minute                                 |
| RT-PCR              | Reverse transcription polymerase chain reaction   |
| s                   | second  |
| SA                  | Salicylic acid                                    |
| SAR                 | Systemic acquired resistance                      |
| SEM                 | scanning electron microscopy                      |
| sr                  | Sporisorium reilianum                             |
| SRS                 | <i>S. reilianum f. sp. reilianum</i>              |
| SRZ                 | <i>S. reilianum f. sp. zeaе</i>                   |
| TAE                 | Tris-Acetate + Na <sub>2</sub> -EDTA              |
| TBE                 | Tris-Borate + Na <sub>2</sub> -EDTA               |
| TE                  | Tris-EDTA   |
| TEM                 | Transmission electron microscopy                  |
| TLP                 | Thaumatococcus-like protein                       |
| Tris                | Tris(hydroxymethyl)aminomethane                   |
| WGA-AF              | Wheat germ agglutinin conjugated with Alexa Fluor |

## 6.2 Supplemental tables

**Supplemental Table S1-** Genes significantly upregulated for SRS in the comparison SRZ versus SRS infected plants ( $p \leq 0.05$ )

| Zm gene       | SRS-SRZ logFC | Annotation  |
|---------------|---------------|---|
| GRMZM2G368827 | 9.713162392   | Sugar efflux transporter  |
| GRMZM2G177900 | 9.463509278   | beta-binding protein 4-like [Musca domestica]                         |
| GRMZM2G138291 | 8.859981318   | hypothetical protein ACA1_123390 [Acanthamoeba castellanii str. Neff] |
| GRMZM2G100776 | 8.757847887   | 60 kDa jasmonate-induced protein-like [Zea mays]                      |
| GRMZM2G158953 | 8.714880153   | Zea mays uncharacterized  |
| GRMZM2G373578 | 8.670593326   | putative serine peptidase S28 family protein                          |
| GRMZM2G524813 | 8.45253228    | Zea mays uncharacterized  |
| GRMZM2G410978 | 8.22646222    | putative nuclease HARBI1  |
| GRMZM2G346449 | 8.22646222    | TPA: hypothetical protein ZEAMMB73                                    |
| GRMZM2G121333 | 8.131633371   | putative hydrolase  |
| GRMZM2G141260 | 8.098586132   | Zea mays alpha-1,4-glucan-protein synthase [                          |
| GRMZM5G899825 | 8.064764111   | hypothetical protein ZEAMMB73_339325                                  |
| GRMZM2G359369 | 8.064764111   | uncharacterized protein LOC103651017 isoform X1                       |
| GRMZM2G441115 | 8.030130105   | putative MADS-box transcription factor family protein                 |
| GRMZM2G386281 | 8.030130105   | TPA: hypothetical protein ZEAMMB73_464562                             |
| GRMZM2G120475 | 7.95826332    | hypothetical protein [Zea mays]                                       |
| GRMZM2G365768 | 7.95826332    | Putative pentatricopeptide repeat family protein                      |
| GRMZM2G034290 | 7.920941262   | uncharacterized protein LOC100303814                                  |
| GRMZM2G078088 | 7.882627997   | hypothetical protein ZEAMMB73_871878                                  |
| GRMZM2G114119 | 7.843269433   | putative GLUTAMINE DUMPER 1-like                                      |
| GRMZM2G144158 | 7.843269433   | early flowering 4 isoform 2   |
| GRMZM2G177150 | 7.843269433   | putative glycerol-3-phosphate acyltransferase 1-like                  |
| GRMZM2G701044 | 7.80280693    | unknown   |
| GRMZM2G340686 | 7.76117677    | Zea mays protein FAR1-RELATED SEQUENCE 5-like                         |
| GRMZM2G047600 | 7.674129499   | Putative MYB DNA-binding domain superfamily protein                   |
| GRMZM2G146540 | 7.58149093    | expansin-A23-like   |
| GRMZM2G333892 | 7.58149093    | uncharacterized protein   |
| GRMZM2G017557 | 7.545930324   | O-methyltransferase ZRP4  |
| GRMZM2G019356 | 7.532841035   | uncharacterized protein LOC103638128                                  |
| GRMZM2G357688 | 7.532841035   | zinc finger protein 2   |
| GRMZM2G124744 | 7.482493166   | unknown   |
| GRMZM5G847462 | 7.482493166   | hypothetical protein  |
| GRMZM2G016102 | 7.482493166   | transposable element  |
| GRMZM2G122384 | 7.482493166   | hypothetical protein  |
| GRMZM2G438456 | 7.430324499   | putative pentatricopeptide repeat-containing protein                  |
| GRMZM2G471048 | 7.430324499   | hypothetical protein [Afipia felis]                                   |
| GRMZM2G459599 | 7.376198378   | Zea mays UPF0051 protein ABCI8, chloroplastic-like                    |
| GRMZM2G033598 | 7.376198378   | Zea mays rust resistance protein rp3-1 (                              |
| GRMZM2G117465 | 7.319962166   | putative protein kinase superfamily protein                           |
| GRMZM2G332201 | 7.070142211   | glutathione transferase   |
| GRMZM2G170969 | 7.315791626   | protease inhibitor/seed storage/LTP family protein precursor          |
| GRMZM2G358365 | 7.200452862   | TPA: hypothetical protein   |
| GRMZM2G172807 | 7.200452862   | hypothetical protein  |
| GRMZM2G127499 | 7.136768317   | hypothetical protein ZEAMMB73_857263                                  |
| GRMZM2G431504 | 7.136768317   | anthocyanidin reductase-like [Setaria italica]                        |
| GRMZM2G100543 | 7.078196207   | hypothetical protein  |
| GRMZM2G158657 | 7.070142211   | carotenoid cleavage dioxygenase                                       |
| GRMZM5G801879 | 7.070142211   | uncharacterized LOC103632436  |
| GRMZM2G455784 | 7.070142211   | uncharacterized protein LOC100279321                                  |

| Zm gene          | SRS-SRZ<br>logFC | Annotation  |
|------------------|------------------|---|
| GRMZM2G176330    | 7.070142211      | putative zinc finger protein                                |
| GRMZM2G141325    | 7.000289592      | meiosis 5   |
| GRMZM2G075463    | 7.000289592      | hypothetical protein  |
| AC200866.4_FG003 | 7.000289592      | none  |
| GRMZM2G322434    | 7.000289592      | Zea mays BAC clone Z418K17                                  |
| GRMZM2G124028    | 6.926881983      | hypothetical protein  |
| GRMZM2G443302    | 6.926881983      | hypothetical protein ZEAMMB73_155088                        |
| GRMZM2G153811    | 6.926881983      | unknown [Zea mays]  |
| GRMZM2G066862    | 6.849538044      | expansin-A17-like   |
| GRMZM2G100192    | 6.849538044      | hypothetical protein [Zea mays]                             |
| GRMZM2G126349    | 6.76781158       | hypothetical protein ZEAMMB73_073716                        |
| GRMZM2G131763    | 6.76781158       | no hit  |
| GRMZM2G060309    | 6.76781158       | hypothetical protein ZEAMMB73_494259                        |
| GRMZM2G021433    | 6.76781158       | uncharacterized protein LOC100278949 isoform X2             |
| GRMZM2G127982    | 6.76781158       | hypothetical protein ZEAMMB73_681975                        |
| GRMZM2G700262    | 6.76781158       | hypothetical protein ZEAMMB73_417095                        |
| GRMZM2G067833    | 6.681175949      | hypothetical protein ZEAMMB73_338922                        |
| GRMZM2G099875    | 6.681175949      | CRR4  |
| GRMZM2G316789    | 6.681175949      | short chain dehydrogenase                                   |
| GRMZM2G107866    | 6.681175949      | nitrate and chloride transporter                            |
| GRMZM2G038707    | 6.681175949      | alpha-L-fucosidase [Flavobacterium chungangense]            |
| GRMZM2G329584    | 6.681175949      | uncharacterized protein LOC103638751                        |
| GRMZM2G561503    | 6.653856612      | uncharacterized   |
| GRMZM2G106092    | 6.589003476      | hypothetical protein ZEAMMB73_392507                        |
| GRMZM5G874198    | 6.589003476      | uncharacterized protein LOC100383658                        |
| GRMZM2G133538    | 6.589003476      | putative pentatricopeptide repeat-containing protein        |
| GRMZM5G850922    | 6.589003476      | hypothetical protein  |
| GRMZM2G024038    | 6.589003476      | hypothetical protein ZEAMMB73                               |
| GRMZM2G450939    | 6.589003476      | replication protein A 70 kDa DNA-binding subunit C-like     |
| GRMZM2G332391    | 6.589003476      | Zea mays dynactin subunit 1-like                            |
| GRMZM2G158518    | 6.589003476      | Zea mays uncharacterized LOC103645088                       |
| GRMZM2G064880    | 6.589003476      | Mitogen-activated protein kinase kinase 2 [Triticum urartu] |
| GRMZM2G482662    | 6.559719079      | Zea mays uncharacterized LOC103626799                       |
| GRMZM2G037306    | 6.490537837      | transposon Misfit putative TNP2-like protein                |
| GRMZM2G090226    | 6.490537837      | Phi_1   |
| GRMZM2G343828    | 6.490537837      | putative O-Glycosyl hydrolase superfamily protein           |
| GRMZM2G514245    | 6.490537837      | unknown   |
| GRMZM2G009200    | 6.490537837      | Zea mays ethylene-responsive transcription factor RAP2-9    |
| GRMZM2G111917    | 6.490537837      | unknown   |
| GRMZM5G838894    | 6.490537837      | uncharacterized protein LOC100384134                        |
| GRMZM2G439542    | 6.490537837      | phosphoenolpyruvate/phosphate translocator 3,               |
| GRMZM2G034651    | 6.490537837      | pre-mRNA-splicing factor 18-like                            |
| GRMZM2G498835    | 6.246909404      | uncharacterized LOC100275533                                |
| GRMZM2G032095    | 5.953211875      | probable 3-ketoacyl-CoA synthase 2-like                     |
| GRMZM2G114320    | 5.692982079      | Zea mays uncharacterized LOC103626989                       |
| GRMZM2G146981    | 5.677405649      | putative nuclease, ribosomal protein like                   |
| GRMZM2G448511    | 5.662751277      | dehydrin 13   |
| GRMZM2G071698    | 5.64427451       | uncharacterized   |
| AC186231.4_FG002 | 5.534651576      | early nodulin 75  |
| GRMZM2G100747    | 5.412401161      | thaumatin-like 1a   |
| GRMZM2G440853    | 5.33968771       | Zea mays protein FAR1-RELATED SEQUENCE 5-like               |
| GRMZM2G314064    | 5.288760461      | WUSCHEL-related homeobox 6-like                             |
| GRMZM2G438824    | 5.196547379      | maize jasmonate induced protein                             |
| GRMZM2G116279    | 5.196547379      | putative xylose isomerase family protein                    |
| GRMZM2G539489    | 5.192300204      | uncharacterized protein                                     |
| GRMZM2G386091    | 5.135786481      | unknown   |
| GRMZM2G074097    | 5.073964874      | thiazole biosynthetic enzyme 1-1                            |
| GRMZM2G108900    | 4.992235879      | unknown   |
| GRMZM2G053315    | 4.831743686      | probable flavin-containing monooxygenase 1                  |
| GRMZM2G110553    | 4.75414001       | hypothetical protein ZEAMMB73_094684                        |

| Zm gene          | SRS-SRZ<br>logFC | Annotation   |
|------------------|------------------|--|
| GRMZM2G489119    | 4.620844934      | hypotetical protein  |
| GRMZM2G141026    | 4.623692411      | O-methyltransferase ZRP4   |
| GRMZM2G113844    | 4.619628978      | monooxygenase/ oxidoreductase  |
| GRMZM2G180907    | 4.615981448      | unknown  |
| GRMZM2G066609    | 4.602671605      | hypothetical protein   |
| GRMZM5G869027    | 4.577644391      | 36.4 kDa proline-rich protein [Zea mays].                                |
| GRMZM2G149326    | 4.56946344       | hypothetical protein   |
| GRMZM2G071846    | 4.563205199      | adenine phosphoribosyltransferase  |
| GRMZM2G110439    | 4.560678662      | hypothetical protein   |
| GRMZM2G110447    | 4.528505611      | hypothetical protein   |
| GRMZM2G129396    | 4.503463603      | 22 kDa alpha zein gene cluster   |
| GRMZM2G325453    | 4.489218425      | ribosomal protein  |
| GRMZM2G176327    | 4.468829597      | putative MYB DNA-binding domain superfamily protein                      |
| GRMZM2G167076    | 4.433343657      | uncharacterized,   |
| GRMZM2G097916    | 4.433343657      | serine/threonine-protein kinase sepA-like                                |
| GRMZM2G036340    | 4.321327489      | GA 3-oxidase 1   |
| GRMZM2G010518    | 4.321327489      | hypothetical protein   |
| GRMZM2G006287    | 4.291449403      | Maternal protein pumilio   |
| GRMZM2G339725    | 4.281968925      | hypothetical protein   |
| GRMZM2G070603    | 4.241506422      | peroxidase 1   |
| GRMZM2G036996    | 4.216017828      | uncharacterized protein  |
| GRMZM2G159965    | 4.171731001      | uncharacterized protein  |
| GRMZM2G352234    | 4.157009044      | pentatricopeptide repeat-containing protein At3g58590                    |
| GRMZM2G563606    | 4.157009044      | uncharacterized  |
| GRMZM2G367235    | 4.136136088      | Zea mays glutathione S-transferase T3-like                               |
| GRMZM2G171078    | 4.112828991      | peroxidase 4 like  |
| GRMZM2G070620    | 4.072912806      | Putative cytochrome P450 superfamily protein                             |
| AC212739.3_FG005 | 4.067253144      | unknown  |
| GRMZM2G008032    | 4.067253144      | hypothetical protein   |
| GRMZM2G117216    | 4.067253144      | hypothetical protein   |
| GRMZM2G073982    | 4.067253144      | Putative AP2/EREBP transcription factor superfamily protein              |
| GRMZM2G166141    | 4.053288009      | germin-like protein 8-4  |
| GRMZM2G103945    | 4.052206079      | Aquaporin TIP4-1   |
| AC216870.3_FG003 | 4.050203715      | none   |
| GRMZM5G815214    | 4.034426268      | 36.4 kDa proline-rich protein  |
| GRMZM2G149123    | 4.033555278      | uncharacterized protein  |
| GRMZM2G154809    | 4.022636453      | uncharacterized protein  |
| GRMZM2G346312    | 4.005055749      | hypothetical protein   |
| GRMZM5G889769    | 3.983871949      | Thioredoxin reductase  |
| GRMZM2G125233    | 3.971540527      | aldose 1-epimerase-like  |
| GRMZM2G157536    | 3.971540527      | hypothetical protein   |
| GRMZM2G151567    | 3.95493775       | Putative leucine-rich repeat receptor-like protein kinase family protein |
| GRMZM2G126168    | 3.925300214      | unknown  |
| GRMZM2G143377    | 3.916855943      | putative pentatricopeptide repeat-containing protein                     |
| GRMZM2G052344    | 3.845058544      | putative RING zinc finger domain superfamily protein                     |
| GRMZM5G834254    | 3.845058544      | uncharacterized  |
| GRMZM2G028570    | 3.832097954      | sugar transporter ERD6-like 4  |
| GRMZM5G892777    | 3.816578193      | unknown  |
| GRMZM2G005100    | 3.81489787       | uncharacterized protein  |
| GRMZM2G341216    | 3.81489787       | pentatricopeptide repeat-containing protein At3g26540                    |
| GRMZM2G374405    | 3.81489787       | hypothetical protein   |
| GRMZM2G313007    | 3.81489787       | uncharacterized  |
| GRMZM2G323075    | 3.81489787       | uncharacterized  |
| GRMZM5G880028    | 3.793842893      | Putative calmodulin-binding family protein                               |
| GRMZM2G029314    | 3.758661658      | uncharacterized  |
| GRMZM5G855743    | 3.758661658      | hypothetical protein   |
| GRMZM2G404535    | 3.758661658      | none   |
| GRMZM2G067786    | 3.758661658      | hypothetical protein   |
| GRMZM2G096602    | 3.757873189      | pentatricopeptide repeat-containing protein At3g24000                    |
| GRMZM2G176354    | 3.757452032      | hypothetical protein   |
| GRMZM5G811624    | 3.757452032      | hypothetical protein   |

| Zm gene          | SRS-SRZ<br>logFC | Annotation  |
|------------------|------------------|---|
| GRMZM2G129879    | 3.751869913      | uncharacterized                                       |
| AC184780.3_FG003 | 3.727599895      | uncharacterized                                       |
| AC195351.3_FG003 | 3.700144134      | uncharacterized                                       |
| GRMZM2G087495    | 3.700144134      | pentatricopeptide repeat-containing protein           |
| AC233751.1_FG002 | 3.700144134      | glume architecture                                    |
| GRMZM2G009435    | 3.687676921      | hypothetical protein                                  |
| GRMZM2G082268    | 3.674127171      | uncharacterized                                       |
| GRMZM2G419875    | 3.654168988      | hypotetical protein                                   |
| GRMZM2G436787    | 3.644672494      | uncharacterized protein                               |
| GRMZM2G077664    | 3.630509862      | none  |
| GRMZM2G093111    | 3.608196519      | hypothetical protein                                  |
| GRMZM2G497978    | 3.599723807      | hypothetical protein                                  |
| GRMZM2G092867    | 3.594003089      | metal ion binding protein                             |
| GRMZM2G129249    | 3.593800477      | beta glucosidase aggregating factor                   |
| GRMZM2G587231    | 3.590410123      | uncharacterized                                       |
| GRMZM2G012566    | 3.574694143      | hypotetical protein                                   |
| AC208711.3_FG005 | 3.573764805      | hypothetical protein                                  |
| GRMZM2G458122    | 3.53910797       | pentatricopeptide repeat-containing protein           |
| AC188003.3_FG011 | 3.534927154      | none  |
| GRMZM2G402174    | 3.482883759      | uncharacterized                                       |
| GRMZM5G834568    | 3.478134789      | L-ascorbate peroxidase 2                              |
| GRMZM2G343149    | 3.473155891      | dnaJ domain containing protein                        |
| AC205154.3_FG005 | 3.466543728      | peroxidase 5-like                                     |
| GRMZM2G066343    | 3.40233141       | catalytic/ hydrolase                                  |
| GRMZM2G429940    | 3.395349259      | CBL-interacting serine/threonine-protein kinase 15    |
| GRMZM2G061126    | 3.372111184      | uncharacterized                                       |
| AC204292.4_FG002 | 3.363739523      | pentatricopeptide repeat-containing protein At1g20230 |
| GRMZM2G038174    | 3.339742591      | uncharacterized                                       |
| GRMZM2G007593    | 3.33685161       | uncharacterized                                       |
| GRMZM2G004988    | 3.326353245      | SSXT protein  |
| GRMZM2G474407    | 3.307635819      | uncharacterized                                       |
| GRMZM2G032514    | 3.278713658      | hypothetical protein                                  |
| GRMZM2G013588    | 3.274832438      | anconi anemia group I protein homolog isoform X1      |
| GRMZM2G108371    | 3.227712224      | uncharacterized                                       |
| GRMZM2G110192    | 3.205942679      | zeaxanthin 7,8(7',8')-cleavage dioxygenase            |
| GRMZM2G074307    | 3.205007526      | hypothetical protein                                  |
| GRMZM5G826596    | 3.192412261      | hypothetical protein                                  |
| GRMZM2G042995    | 3.185597958      | uncharacterized                                       |
| GRMZM2G060255    | 3.185087823      | universal stress protein family protein               |
| GRMZM2G426613    | 3.168001967      | putative RING zinc finger domain superfamily protein  |
| GRMZM2G069098    | 3.158304089      | putative MATE efflux family protein, testa 12 protein |
| GRMZM2G389645    | 3.136691385      | pentatricopeptide repeat-containing protein           |
| GRMZM2G125072    | 3.126663537      | ferredoxin  |
| GRMZM2G000221    | 3.106870792      | PVR3-like protein                                     |
| GRMZM2G022804    | 3.08350559       | uncharacterized                                       |
| GRMZM2G406400    | 3.081795155      | uncharacterized, transposon                           |
| GRMZM2G076239    | 3.072878163      | hydroxyacid oxidase                                   |
| GRMZM2G056513    | 3.053270472      | uncharacterized                                       |
| GRMZM2G395207    | 3.046675994      | ubiquitin-protein ligase/ zinc ion binding            |
| GRMZM5G810727    | 3.04663666       | beta-glucosidase precursor                            |
| GRMZM2G160354    | 3.039236261      | hypothetical protein                                  |
| GRMZM2G158175    | 3.035485005      | beta-carotene isomerase D27                           |
| GRMZM2G111764    | 3.034306352      | hypothetical protein                                  |
| GRMZM2G041980    | 3.030874037      | aquaporin   |
| GRMZM5G831102    | 3.000952015      | gibberellin receptor GID1L2                           |
| GRMZM2G018375    | 2.982959584      | thiazole biosynthetic enzyme 1-1                      |
| GRMZM2G092169    | 2.957372758      | uncharacterized                                       |
| GRMZM2G701047    | 2.950959535      | uncharacterized                                       |
| GRMZM2G159547    | 2.925484898      | putative MYB DNA-binding domain superfamily protein   |
| GRMZM2G487931    | 2.920276225      | none  |

**Supplemental Table S2-** Genes significantly upregulated for SRZ in the comparison SRZ versus SRS infected plants ( $p \leq 0.05$ )

| Zm gene          | SRZ-SRS<br>logFC | Annotation  |
|------------------|------------------|---|
| GRMZM2G502350    | 11.370782        | putative protein kinase superfamily protein                     |
| GRMZM2G379773    | 10.80944273      | proline-rich receptor-like protein kinase PERK5                 |
| GRMZM2G333022    | 10.48988519      | putative protein kinase superfamily protein                     |
| GRMZM2G473511    | 10.30510466      | putative protein kinase superfamily protein                     |
| GRMZM5G825193    | 10.24214577      | putative protein kinase superfamily protein                     |
| GRMZM2G450108    | 9.021340732      | probable serine/threonine-protein kinase dyrk2                  |
| GRMZM2G077914    | 8.960060895      | probable LRR receptor-like serine/threonine-protein kinase RKF3 |
| GRMZM2G085486    | 8.928416408      | sphingoid long-chain bases kinase 1-like isoform X2             |
| GRMZM2G065617    | 8.758861497      | probable glycosyltransferase                                    |
| GRMZM2G151083    | 8.685036188      | probable atrophim-1-like  |
| GRMZM2G063287    | 8.685036188      | Embryonic protein DC-8  |
| GRMZM2G177445    | 8.524983839      | TPR-containing protein kinase                                   |
| GRMZM2G168079    | 8.437765758      | Putative bZIP transcription factor superfamily protein          |
| GRMZM2G064750    | 8.392096275      | Ser/Thr receptor-like kinase1 precursor                         |
| GRMZM2G104622    | 8.193423533      | BAP2  |
| GRMZM2G113378    | 8.178332197      | putative protein kinase superfamily protein                     |
| GRMZM2G034611    | 8.026930605      | probable L-type lectin-domain containing receptor kinase        |
| GRMZM2G311401    | 7.899087312      | protein ZINC INDUCED FACILITATOR-LIKE 1-like                    |
| GRMZM2G382273    | 7.762188044      | uncharacterized protein   |
| GRMZM2G145412    | 7.762188044      | ZIM motif family protein  |
| GRMZM2G164909    | 7.762188044      | Heat shock factor protein 7                                     |
| GRMZM2G176430    | 7.762188044      | tonoplast dicarboxylate transporter-like                        |
| GRMZM2G149930    | 7.68853718       | hypothetical protein ZEAMMB73                                   |
| GRMZM2G104109    | 7.528895037      | peroxidase 1 precursor  |
| GRMZM2G157202    | 7.528895037      | hypothetical protein  |
| GRMZM2G147774    | 7.441920351      | cytochrome P450 72A15-like                                      |
| AC233903.1_FG002 | 7.34936399       | putative RING zinc finger domain superfamily protein            |
| GRMZM2G080594    | 7.34936399       | uncharacterized abhydrolase domain-containing protein           |
| GRMZM5G832498    | 7.250460106      | unknown [Zea mays]  |
| GRMZM2G438960    | 7.250460106      | potassium transporter 21-like                                   |
| GRMZM2G468111    | 7.250460106      | hypothetical protein  |
| GRMZM5G834477    | 7.144273546      | hypothetical protein  |
| GRMZM2G006981    | 7.144273546      | glycine-rich cell wall structural protein 1.0-like              |
| GRMZM2G399930    | 7.029645949      | uncharacterized   |
| GRMZM2G101472    | 7.029645949      | hypothetical protein  |
| GRMZM2G070392    | 7.029645949      | calmodulin-binding transcription activator 3-like               |
| AC217499.3_FG002 | 7.029645949      | uncharacterized   |
| GRMZM2G130608    | 7.029645949      | Zea mays DNA-directed RNA polymerase II subunit J               |
| GRMZM2G160840    | 7.029645949      | MYB DNA-binding domain superfamily protein                      |
| GRMZM2G378665    | 7.029645949      | E2F transcription factor-like E2FE isoform X3                   |
| GRMZM2G115070    | 6.905118518      | putative MYB DNA-binding domain superfamily protein             |
| GRMZM2G457694    | 6.905118518      | uncharacterized   |
| GRMZM2G403762    | 6.905118518      | Zea mays DNA ligase 1-like                                      |
| GRMZM2G336134    | 6.905118518      | hypothetical protein  |
| GRMZM2G369991    | 6.905118518      | 60S ribosomal protein L10a-1-like                               |
| GRMZM2G007113    | 6.905118518      | Zea mays cyclin2 (cyc2)   |
| GRMZM2G005758    | 6.768818216      | Zea mays serine/threonine-protein phosphatase 7                 |
| GRMZM2G009779    | 6.768818216      | putative inorganic phosphate transporter 1-13                   |
| GRMZM2G010494    | 6.768818216      | transketolase, chloroplastic-like                               |
| GRMZM2G345798    | 6.768818216      | IQ calmodulin-binding motif family protein                      |
| GRMZM2G361475    | 6.768818216      | putative peroxidase   |
| GRMZM2G170734    | 6.686023939      | chlorophyllase-2, chloroplastic-like                            |
| GRMZM2G125196    | 6.623683457      | putative alcohol dehydrogenase superfamily protein              |

| Zm gene          | SRZ-SRS<br>logFC | Annotation   |
|------------------|------------------|--|
| GRMZM2G463449    | 6.618284365      | unknown  |
| GRMZM2G137341    | 6.618284365      | putative AP2/EREBP transcription factor superfamily protein                        |
| GRMZM2G366532    | 6.618284365      | heat shock cognate 70KDa   |
| AC204711.3_FG003 | 6.618284365      | senescence-associated protein DIN1 precursor                                       |
| GRMZM2G021482    | 6.618284365      | probable glycerophosphoryl diester phosphodiesterase 2                             |
| GRMZM2G117956    | 6.618284365      | proline oxidase  |
| GRMZM2G472638    | 6.618284365      | hypothetical protein   |
| GRMZM2G006080    | 6.618284365      | receptor-like protein kinase FERONIA   |
| GRMZM2G046313    | 6.618284365      | RNA recognition motif protein 2 family protein                                     |
| GRMZM2G114356    | 6.618284365      | proline-rich protein precursor   |
| GRMZM2G432747    | 6.618284365      | uncharacterized  |
| GRMZM2G477864    | 6.618284365      | uncharacterized  |
| GRMZM2G093072    | 6.134457526      | probable LRR receptor-like serine/threonine-protein kinase RKF3                    |
| GRMZM2G000236    | 6.067545731      | 12-oxophytodienoate reductase 2  |
| GRMZM2G306679    | 5.921207595      | class I heat shock protein 3   |
| GRMZM2G075244    | 5.880865082      | cytochrome P450 734A1-like   |
| GRMZM2G078465    | 5.828530702      | indole-3-acetate beta-glucosyltransferase  |
| GRMZM2G336533    | 5.709080237      | putative NAC domain transcription factor superfamily protein                       |
| GRMZM2G113421    | 5.688695695      | probable LRR receptor-like serine/threonine-protein kinase RKF3                    |
| GRMZM2G097135    | 5.679051955      | putative IQ calmodulin-binding and BAG domain containing family                    |
| GRMZM2G157936    | 5.646987424      | heme oxygenase   |
| GRMZM2G314667    | 5.646987424      | hypothetical protein   |
| GRMZM2G155746    | 5.466937284      | uncharacterized  |
| GRMZM2G106303    | 5.398093622      | 12-oxo-phytyldienoic acid reductase1   |
| GRMZM2G018044    | 5.367718511      | protein ASPARTIC PROTEASE IN GUARD CELL 2-like                                     |
| GRMZM2G407223    | 5.259418028      | hypothetical protein   |
| GRMZM5G827496    | 5.204790025      | probable nitrite transporter At1g68570-like  |
| GRMZM2G541926    | 5.197216608      | unknown  |
| GRMZM2G104078    | 5.146118038      | putative NAC domain transcription factor superfamily protein                       |
| GRMZM2G086946    | 5.016322256      | unknown  |
| GRMZM2G320786    | 4.898567933      | putative laccase-9   |
| GRMZM2G021277    | 4.840717707      | aromatic-L-amino-acid decarboxylase-like   |
| GRMZM2G380377    | 4.830853841      | DRE-binding protein 4; Putative AP2/EREBP transcription factor superfamily protein |
| AC186602.4_FG003 | 4.810540765      | hypothetical protein   |
| GRMZM2G366389    | 4.790317552      | unknown  |
| GRMZM2G117246    | 4.754315713      | flavonol synthase/flavanone 3-hydroxylase-like                                     |
| GRMZM2G119150    | 4.742456978      | aminotransferase ALD1 homolog  |
| GRMZM2G096475    | 4.732926728      | late embryogenesis abundant protein  |
| GRMZM2G475059    | 4.676473438      | glutathione S-transferase GST31  |
| AC209257.4_FG006 | 4.650898622      | dehydration-responsive element-binding protein 2D-like                             |
| GRMZM2G126367    | 4.650898622      | esterase PIR7B-like  |
| GRMZM5G815323    | 4.650898622      | putative transcriptional adaptor family protein                                    |
| GRMZM2G061403    | 4.6480782        | glucan endo-1,3-beta-glucosidase GII-like isoform X1                               |
| AC191045.3_FG006 | 4.563923936      | unknown  |
| GRMZM2G031909    | 4.563923936      | putative cytochrome P450 superfamily protein                                       |
| GRMZM2G375249    | 4.563923936      | extensin-like protein precursor  |
| GRMZM2G003489    | 4.537158138      | hypothetical protein   |
| GRMZM2G364131    | 4.471367574      | hypothetical protein   |
| AC203173.3_FG002 | 4.471367574      | receptor-like protein kinase HSL1 LRR  |
| GRMZM2G002704    | 4.471367574      | Gibberellin 20 oxidase 2   |
| AC209987.4_FG010 | 4.441289896      | early nodulin-like protein 2-like  |
| GRMZM2G115716    | 4.357032629      | G-type lectin S-receptor-like serine/threonine-protein kinase At1g11410            |
| GRMZM2G173809    | 4.355474668      | ricin-like   |
| GRMZM2G080839    | 4.316574398      | reticuline oxidase-like protein  |
| GRMZM2G114619    | 4.306411883      | actin binding protein  |
| GRMZM2G179092    | 4.295844566      | terpene synthase 10  |
| GRMZM2G156877    | 4.284797593      | glutathione S-transferase GST8   |
| AC193374.2_FG008 | 4.281420751      | unknown  |
| GRMZM2G089949    | 4.263445306      | cyclic dof factor 2-like isoform X2  |
| GRMZM2G331518    | 4.247739895      | unknown  |
| GRMZM2G016890    | 4.243056491      | Beta-glucosidase, chloroplastic  |

| Zm gene          | SRZ-SRS logFC | Annotation   |
|------------------|---------------|--|
| GRMZM5G833699    | 4.240884462   | heat shock protein 82  |
| GRMZM2G144420    | 4.204397121   | putative calcium-transporting ATPase 13                                |
| AC202954.4_FG003 | 4.199176191   | unknown  |
| GRMZM2G091540    | 4.157957729   | IAA-amino acid hydrolase ILR1-like 4 isoform X1                        |
| GRMZM2G447447    | 4.157957729   | leucine-rich repeat receptor protein kinase EXS                        |
| GRMZM2G083855    | 4.141121378   | hypothetical protein   |
| GRMZM2G115730    | 4.122712754   | ENTH domain-containing protein C794.11c-like                           |
| GRMZM2G007729    | 4.114118813   | heat shock 22  |
| GRMZM2G372877    | 4.10797557    | C2 and GRAM domain-containing protein At1g03370-like                   |
| GRMZM2G007736    | 4.106345384   | probable alpha,alpha-trehalose-phosphate synthase                      |
| GRMZM2G121309    | 4.101509811   | IAA responsive Aux/IAA family member                                   |
| AC209784.3_FG007 | 4.101164297   | Heat shock 70 kDa protein  |
| GRMZM2G025720    | 4.100566368   | Hypothetical protein   |
| GRMZM2G305901    | 4.084644521   | E3 ubiquitin-protein ligase MBR1                                       |
| GRMZM2G320705    | 4.081617457   | uncharacterized  |
| GRMZM2G075461    | 4.053332331   | putative cytochrome P450 superfamily protein                           |
| GRMZM2G110345    | 4.045836749   | hypothetical protein   |
| GRMZM5G882446    | 3.985813486   | hypothetical protein   |
| GRMZM2G079440    | 3.980604377   | dehydrin DHN1  |
| GRMZM2G477205    | 3.962778489   | chaperone protein dnaJ   |
| GRMZM5G828219    | 3.944104107   | unknown  |
| GRMZM2G128315    | 3.919907279   | leucine-rich repeat receptor-like protein kinase                       |
| GRMZM2G002830    | 3.919907279   | ubiquitin carrier protein  |
| GRMZM2G048910    | 3.912162622   | Odorant 1 protein; Putative MYB DNA-binding domain superfamily protein |
| GRMZM2G428040    | 3.912162622   | hypothetical protein   |
| GRMZM2G166616    | 3.895393523   | 1-aminocyclopropane-1-carboxylic acid oxidase                          |
| GRMZM2G449447    | 3.894710446   | hypothetical protein   |
| GRMZM2G095280    | 3.892639257   | indole-3-acetate beta-glucosyltransferase                              |
| GRMZM2G108219    | 3.885851961   | anionic peroxidase   |
| GRMZM2G348257    | 3.867615885   | uncharacterized  |
| AC183907.3_FG001 | 3.862356264   | unknown  |
| GRMZM2G339452    | 3.862356264   | protein YLS9-like  |
| GRMZM2G021388    | 3.847223254   | aromatic-L-amino-acid decarboxylase-like                               |
| GRMZM2G169033    | 3.829259823   | Putative laccase   |
| GRMZM2G416184    | 3.818151657   | BTB/POZ domain-containing protein NPY1-like                            |
| GRMZM2G443445    | 3.813357643   | Mannitol dehydrogenase   |
| GRMZM2G052571    | 3.806136081   | Glutathione S-transferase  |
| GRMZM2G181536    | 3.802236997   | GTP-binding protein SAR2-like  |
| GRMZM2G042754    | 3.795386264   | probable esterase/lipase   |
| GRMZM2G373329    | 3.779951396   | U-box domain-containing protein 33-like                                |
| GRMZM2G179462    | 3.762335961   | low temperature-induced protein It101.2-like                           |
| GRMZM2G047713    | 3.759286952   | ricin-like   |
| GRMZM2G174001    | 3.756978792   | probable receptor-like protein kinase At1g67000 isoform                |
| GRMZM2G470075    | 3.749692678   | putative MATE efflux family protein                                    |
| GRMZM2G122072    | 3.747944009   | Uncharacterized, possible anthocyanidin 5,3-O-glucosyltransferase      |
| GRMZM2G010435    | 3.736619372   | cysteine protease 1  |
| AC205471.4_FG007 | 3.715546469   | hypothetical protein, nuclear  |
| GRMZM2G329029    | 3.715018916   | cytochrome P450 93A3-like  |
| GRMZM2G084779    | 3.698037605   | potassium ion uptake permease 1  |
| GRMZM2G154747    | 3.694781047   | plasma membrane associated protein                                     |
| GRMZM2G037431    | 3.684463372   | polygalacturonase  |
| GRMZM2G433557    | 3.676585726   | calmodulin binding protein isoform X1                                  |
| AC235534.1_FG007 | 3.669349433   | outer cell layer2  |
| GRMZM2G176489    | 3.665545793   | probable WRKY transcription factor 72                                  |
| GRMZM2G352866    | 3.665545793   | putative DUF26-domain receptor-like protein kinase family              |
| GRMZM5G898755    | 3.665545793   | nonspecific lipid-transfer protein 4 precursor                         |
| GRMZM2G339367    | 3.665545793   | salutaridine reductase-like isoform X1                                 |
| GRMZM2G429322    | 3.646574077   | lysine histidine transporter 2-like isoform X1                         |
| GRMZM2G118770    | 3.639035297   | Malic enzyme   |
| GRMZM2G003738    | 3.637147202   | Cell-linked locus protein  |
| GRMZM2G428554    | 3.635424492   | receptor-like protein kinase   |

| Zm gene       | SRZ-SRS<br>logFC | Annotation  |
|---------------|------------------|---|
| GRMZM2G025190 | 3.612950811      | Glutathione S-transferase GSTU6   |
| GRMZM2G098167 | 3.622186857      | class II heat shock protein   |
| GRMZM2G131055 | 3.606529021      | Glycosyltransferase   |
| GRMZM2G160279 | 3.602594224      | pumilio-like protein  |
| GRMZM2G083810 | 3.5738401        | 17.5 kDa class II heat shock protein  |
| GRMZM2G442763 | 3.573430252      | uncharacterized protein   |
| GRMZM2G169628 | 3.573279663      | UDP-glycosyltransferase 85A5-like   |
| GRMZM2G437100 | 3.573279663      | 16.9 kDa class I heat shock protein 1   |
| GRMZM5G849934 | 3.572989432      | hypothetical protein  |
| GRMZM2G302245 | 3.561305581      | putative regulator of chromosome condensation                                 |
| GRMZM2G119823 | 3.560551049      | Putative HLH DNA-binding domain superfamily protein                           |
| GRMZM2G528010 | 3.550474249      | probable nucleoporin  |
| GRMZM2G001375 | 3.512438246      | hypothetical protein  |
| GRMZM2G345330 | 3.509691         | hypothetical protein  |
| GRMZM2G163374 | 3.50645324       | hypothetical protein  |
| GRMZM2G046321 | 3.50645324       | hypothetical protein  |
| GRMZM2G053394 | 3.50645324       | putative calmodulin-binding family protein                                    |
| GRMZM2G400559 | 3.504529618      | probable WRKY transcription factor 63   |
| GRMZM2G076584 | 3.504279634      | putative O-glycosyl hydrolase family 17 protein                               |
| GRMZM2G391042 | 3.504170015      | calcium-transporting ATPase 8, plasma membrane-type-like                      |
| GRMZM2G169149 | 3.497872077      | WRKY62-superfamily of Transcription factors with WRKY and zinc finger domains |
| GRMZM2G343157 | 3.480719302      | ZIM motif family protein  |
| GRMZM2G373554 | 3.470676691      | hypothetical protein  |
| GRMZM2G418031 | 3.470676691      | BTB/POZ and MATH domain-containing protein 1-like                             |
| GRMZM2G154735 | 3.470578979      | HVA22-like protein  |
| GRMZM2G425603 | 3.469480386      | uncharacterized   |
| GRMZM2G124477 | 3.461989896      | nucleolar and coiled-body phosphoprotein 1-like                               |
| GRMZM2G421513 | 3.433039902      | enolase-phosphatase E1-like isoform X1  |
| GRMZM2G349839 | 3.424169364      | probable apyrase 3  |
| GRMZM2G463471 | 3.420294247      | Actin-depolymerizing factor   |
| GRMZM2G100360 | 3.416418449      | probable cytokinin riboside 5'-monophosphate phosphoribohydrolase             |
| GRMZM2G475380 | 3.412465467      | flavonol synthase/flavanone 3-hydroxylase-like                                |
| GRMZM2G021369 | 3.404059796      | putative AP2/EREBP transcription factor superfamily protein                   |
| GRMZM2G054949 | 3.395655078      | probable LRR receptor-like serine/threonine-protein kinase At1g14390          |
| GRMZM2G117603 | 3.388369336      | Actin-depolymerizing factor 1   |
| GRMZM2G052365 | 3.360344423      | subtilisin-like protease isoform X2   |
| GRMZM2G094304 | 3.357275663      | glutamine amidotransferase-like protein                                       |
| GRMZM2G167257 | 3.356471945      | DNA ligase-like, transposable element   |
| GRMZM2G145461 | 3.330334194      | chitinase 2   |
| GRMZM2G412885 | 3.329373128      | putative protein kinase superfamily protein                                   |
| GRMZM2G096591 | 3.322598386      | Glucan endo-1,3-beta-glucosidase  |
| GRMZM2G022740 | 3.314408642      | peroxidase 5-like   |
| GRMZM2G067402 | 3.307402938      | non-symbiotic hemoglobin, partial [Zea mays]                                  |
| GRMZM2G050234 | 3.306988953      | flavanone 3-dioxygenase-like  |
| GRMZM2G507763 | 3.302042598      | putative phytoalexin receptor (LRR repeat-containing protein kinase)          |
| GRMZM2G116087 | 3.292174879      | Chorismate mutase 5   |
| GRMZM2G103055 | 3.274610225      | alpha-amylase 2   |
| GRMZM2G011806 | 3.271169387      | putative leucine-rich repeat receptor-like protein kinase                     |
| GRMZM5G833207 | 3.252103563      | ABC transporter B family member 4-like  |
| GRMZM2G310431 | 3.24696385       | Heat shock 70 kDa protein   |
| GRMZM2G700200 | 3.232983242      | uncharacterized   |
| GRMZM2G008468 | 3.232710423      | golgi transport 1 protein B   |
| GRMZM2G055802 | 3.228450342      | Bowman-Birk type trypsin inhibitor-like                                       |
| GRMZM2G004528 | 3.212673753      | Zea mays catalyst inositol-3-phosphate synthase                               |
| GRMZM2G449133 | 3.210107615      | bifunctional epoxide hydrolase 2-like   |
| GRMZM2G104549 | 3.190647722      | chlorophyll a-b binding protein   |
| GRMZM2G014902 | 3.188208661      | LHY protein   |
| GRMZM5G899851 | 3.162256172      | indole-3-acetaldehyde oxidase   |
| GRMZM2G088613 | 3.161138968      | uncharacterized   |
| GRMZM2G064106 | 3.148384648      | L-ascorbate oxidase-like  |
| GRMZM2G013448 | 3.140162933      | 1-aminocyclopropane-1-carboxylate oxidase 1                                   |

| <b>Zm gene</b> | <b>SRZ-SRS<br/>logFC</b> | <b>Annotation</b>  |
|----------------|--------------------------|--|
| GRMZM2G104836  | 3.124704113              | glycine/proline-rich family protein                                |
| GRMZM2G018027  | 3.135313234              | uncharacterized  |
| GRMZM2G043878  | 3.087198693              | serine/threonine kinase-like protein                               |
| GRMZM2G324781  | 3.080795341              | putative SNF2-domain/RING finger domain/helicase domain protein    |
| GRMZM2G357873  | 3.132865748              | ATP binding protein  |
| GRMZM2G010044  | 3.076308621              | 3-isopropylmalate dehydratase large subunit 2                      |
| GRMZM2G077227  | 3.070400841              | calmodulin binding protein   |
| GRMZM2G093838  | 3.055530563              | zink finger protein  |
| GRMZM2G162158  | 3.052973273              | leucoanthocyanidin dioxygenase                                     |
| GRMZM2G112524  | 3.044157563              | Pathogenesis-related protein 10; Uncharacterized protein           |
| GRMZM2G332423  | 3.03951681               | 1-aminocyclopropane-1-carboxylate oxidase-like                     |
| GRMZM2G119975  | 3.028136544              | ATFP4  |
| GRMZM2G083350  | 3.02496701               | probable WRKY transcription factor 72                              |
| GRMZM2G041699  | 2.989269608              | cytokinin-O-glucosyltransferase 2                                  |
| GRMZM2G124229  | 2.985465409              | probable carboxylesterase  |
| GRMZM2G306258  | 2.985142497              | histone H2B.4  |
| GRMZM5G806108  | 2.979534042              | putative receptor-like kinase family protein                       |
| GRMZM2G002396  | 2.977083261              | CASP-like protein 3  |
| GRMZM2G381378  | 2.975897466              | probable WRKY transcription factor 70                              |
| GRMZM5G873446  | 2.972936574              | unknown [Zea mays]   |
| GRMZM2G088778  | 2.967665319              | ankyrin repeat-containing protein At5g02620                        |
| GRMZM2G118047  | 2.966763318              | HSF28 HSF type transcription factor                                |
| GRMZM2G114048  | 2.961587081              | SNF1-related protein kinase regulatory subunit gamma-1-like        |
| GRMZM2G087827  | 2.957044155              | esterase   |
| GRMZM2G127336  | 2.939881824              | (E)-beta-caryophyllene synthase                                    |
| GRMZM2G106622  | 2.930247619              | maize ABA responsive protein                                       |
| GRMZM2G145407  | 2.928277827              | putative tify domain/CCT motif transcription factor family protein |
| GRMZM2G039993  | 2.912811912              | anthranilic acid methyltransferase 1                               |
| GRMZM2G014089  | 2.907716688              | ABC transporter B family member 11-like isoform X1                 |
| GRMZM2G043191  | 2.899195942              | type I inositol 1,4,5-trisphosphate 5-phosphatase                  |
| GRMZM2G177878  | 2.895417058              | probable inactive poly [ADP-ribose] polymerase SRO3                |
| GRMZM2G032602  | 2.873088753              | disease resistance protein RPS2-like isoform X2                    |
| GRMZM2G091478  | 2.852645179              | ABC transporter A family member 7-like                             |

**Supplemental Table S3-** Sorghum and maize genes used for qRT-PCR

| Gene code     | Gene annotation    | logFC SRZ-SRS* | p-value* | RPKM        | RPKM        | RPKM               |
|---------------|--------------------|----------------|----------|-------------|-------------|--------------------|
|               |                    |                |          | SRZ-plant** | SRS-plant** | uninfected plant** |
| Sb03g030800   | Sb glucan synthase | 1.723643912    | 0.010594 | 13.864      | 4.361       | 1.142              |
| Sb03g030100   | Sb chitinase       | 3.814563512    | 1.76E-07 | 923.392     | 68.181      | 25.495             |
| Sb01g037970   | Sb PR10            | 3.082174413    | 1.3E-05  | 1276.72     | 156.621     | 18.55              |
| Sb02g000220   | Sb DFR3            | 3.681575658    | 4.83E-07 | 38.045      | 3.079       | 0.829              |
| Sb05g018800   | Sb LRR receptor    | 7.521456104    | 1.48E-16 | 28.05       | 0.157       | 0.029              |
| Sb08g022440   | Sb thaumatin-like  | 4.813878641    | 3.44E-10 | 421.574     | 15.568      | 4.825              |
| GRMZM2G430680 | Zm glucan synthase | 0.00981138     | 1        | 0,588       | 0,617       | 0,584              |
| GRMZM2G005633 | Zm chitinase       | 0.215584822    | 0.879844 | 0,802       | 0,695       | 0                  |
| GRMZM2G112538 | Zm PR10            | 2.39804901     | 0.092157 | 539,86      | 103,145     | 17,407             |
| GRMZM2G044481 | Zm AN2             | 1.586078348    | 0.253827 | 11,86       | 3,963       | 0,306              |
| GRMZM2G402631 | Zm PR5             | -0.138801929   | 0.918616 | 271,377     | 300,902     | 0,489              |
| GRMZM2G149809 | Zm thaumatin-like  | -1.795967899   | 0.232061 | 0,274       | 0,963       | 0,03               |

\* As determined by Edge R analysis

\*\* As determined by calculation of reads per kilobase per million mapped reads (RPKM) using CLC genomics

**Supplemental Table S4** - GO terms upregulated for SRZ in the comparison SRS-SRZ infected sorghum

| GO term    | Ont.* | Description   | Nr/<br>imput list | Nr/<br>BG/Ref | p-value | FDR      |
|------------|-------|---|-------------------|---------------|---------|----------|
| GO:0006468 | P     | protein amino acid phosphorylation                  | 215               | 1623          | 1.3e-19 | 7.8e-16  |
| GO:0016310 | P     | phosphorylation                                     | 219               | 1872          | 1.5e-14 | 4.4e-11  |
| GO:0006796 | P     | phosphate metabolic process                         | 225               | 2044          | 1.8e-12 | 2.6e-09  |
| GO:0006793 | P     | phosphorus metabolic process                        | 226               | 2050          | 1.4e-12 | 2.6e-09  |
| GO:0043687 | P     | post-translational protein modification             | 245               | 2301          | 3.8e-12 | 4.3e-09  |
| GO:0006952 | P     | defense response                                    | 128               | 977           | 1.1e-11 | 1.00E-08 |
| GO:0006464 | P     | protein modification process                        | 263               | 2593          | 5.8e-11 | 4.8e-08  |
| GO:0009607 | P     | response to biotic stimulus                         | 151               | 1355          | 5.5e-09 | 3.5e-06  |
| GO:0043412 | P     | macromolecule modification                          | 266               | 2765          | 5.2e-09 | 3.5e-06  |
| GO:0034050 | P     | host programmed cell death induced by symbiont      | 28                | 107           | 1.7e-08 | 9.1e-06  |
| GO:0009626 | P     | plant-type hypersensitive response                  | 28                | 107           | 1.7e-08 | 9.1e-06  |
| GO:0006805 | P     | xenobiotic metabolic process                        | 16                | 35            | 4.7e-08 | 2.2e-05  |
| GO:0009410 | P     | response to xenobiotic stimulus                     | 16                | 37            | 8.6e-08 | 3.8e-05  |
| GO:0009620 | P     | response to fungus                                  | 52                | 334           | 1.7e-07 | 6.9e-05  |
| GO:0050832 | P     | defense response to fungus                          | 39                | 215           | 07      | 7.8e-05  |
| GO:0045087 | P     | innate immune response                              | 59                | 411           | 07      | 0.00011  |
| GO:0006575 | P     | cellular amino acid derivative metabolic process    | 80                | 645           | 6.4e-07 | 0.00022  |
| GO:0051704 | P     | multi-organism process                              | 163               | 1629          | 8.3e-07 | 0.00027  |
| GO:0051707 | P     | response to other organism                          | 132               | 1255          | 9.6e-07 | 0.00028  |
| GO:0006955 | P     | immune response                                     | 68                | 522           | 9.5e-07 | 0.00028  |
| GO:0006950 | P     | response to stress                                  | 322               | 3705          | 1.2e-06 | 0.00034  |
| GO:0006725 | P     | cellular aromatic compound metabolic process        | 90                | 776           | 1.7e-06 | 0.00045  |
| GO:0048610 | P     | reproductive cellular process                       | 12                | 27            | 2.8e-06 | 0.00071  |
| GO:0044036 | P     | cell wall macromolecule metabolic process           | 25                | 123           | 5.4e-06 | 0.0013   |
| GO:0031347 | P     | regulation of defense response                      | 29                | 158           | 5.8e-06 | 0.0013   |
| GO:0042398 | P     | cellular amino acid derivative biosynthetic process | 59                | 460           | 7.5e-06 | 0.0017   |
| GO:0042221 | P     | response to chemical stimulus                       | 281               | 3244          | 8.8e-06 | 0.0019   |
| GO:0009698 | P     | phenylpropanoid metabolic process                   | 58                | 454           | 9.9e-06 | 0.002    |
| GO:0010033 | P     | response to organic substance                       | 195               | 2117          | 05      | 0.002    |
| GO:0042742 | P     | defense response to bacterium                       | 39                | 261           | 1.3e-05 | 0.0025   |
| GO:0006032 | P     | chitin catabolic process                            | 13                | 39            | 1.4e-05 | 0.0025   |
| GO:0006026 | P     | aminoglycan catabolic process                       | 13                | 39            | 1.4e-05 | 0.0025   |
| GO:0019748 | P     | secondary metabolic process                         | 90                | 826           | 1.6e-05 | 0.0027   |
| GO:0016998 | P     | cell wall macromolecule catabolic process           | 15                | 53            | 1.6e-05 | 0.0027   |
| GO:0009719 | P     | response to endogenous stimulus                     | 165               | 1755          | 1.9e-05 | 0.0031   |
| GO:0002376 | P     | immune system process                               | 71                | 613           | 2.2e-05 | 0.0035   |
| GO:0006030 | P     | chitin metabolic process                            | 13                | 42            | 2.7e-05 | 0.0042   |
| GO:0019438 | P     | aromatic compound biosynthetic process              | 56                | 452           | 05      | 0.0046   |
| GO:0070887 | P     | cellular response to chemical stimulus              | 98                | 941           | 3.5e-05 | 0.0051   |
| GO:0006629 | P     | lipid metabolic process                             | 131               | 1351          | 05      | 0.0058   |
| GO:0009737 | P     | response to abscisic acid stimulus                  | 74                | 664           | 4.6e-05 | 0.0065   |
| GO:0009699 | P     | phenylpropanoid biosynthetic process                | 47                | 363           | 4.9e-05 | 0.0068   |
| GO:0009813 | P     | flavonoid biosynthetic process                      | 31                | 200           | 5.3e-05 | 0.0071   |
| GO:0050896 | P     | response to stimulus                                | 489               | 6230          | 6.4e-05 | 0.0083   |
| GO:0080134 | P     | regulation of response to stress                    | 29                | 184           | 05      | 0.0089   |
| GO:0009415 | P     | response to water                                   | 49                | 393           | 05      | 0.01     |
| GO:0009812 | P     | flavonoid metabolic process                         | 33                | 227           | 9.3e-05 | 0.011    |
| GO:0048584 | P     | positive regulation of response to stimulus         | 23                | 133           | 0.00011 | 0.014    |
| GO:0031408 | P     | oxylipin biosynthetic process                       | 15                | 66            | 0.00014 | 0.016    |
| GO:0031407 | P     | oxylipin metabolic process                          | 15                | 66            | 0.00014 | 0.016    |

| GO term    | *Ont. | Description   | **Nr/<br>input list | **Nr/<br>BG/Ref | p-value | FDR      |
|------------|-------|---|---------------------|-----------------|---------|----------|
| GO:0009617 | P     | response to bacterium   | 49                  | 405             | 0.00015 | 0.017    |
| GO:0006022 | P     | aminoglycan metabolic process   | 14                  | 61              | 0.00021 | 0.023    |
| GO:0048583 | P     | regulation of response to stimulus  | 43                  | 351             | 0.0003  | 0.032    |
| GO:0009642 | P     | response to light intensity   | 25                  | 164             | 0.00033 | 0.036    |
| GO:0010876 | P     | lipid localization  | 7                   | 16              | 0.00038 | 0.04     |
| GO:0008219 | P     | cell death  | 82                  | 816             | 0.00041 | 0.042    |
| GO:0016265 | P     | death   | 82                  | 818             | 0.00044 | 0.045    |
| GO:0004713 | F     | protein tyrosine kinase activity  | 205                 | 1304            | 1.4e-26 | 2.4e-23  |
| GO:0004674 | F     | protein serine/threonine kinase activity                                    | 210                 | 1460            | 6.6e-23 | 5.7e-20  |
| GO:0004672 | F     | protein kinase activity   | 221                 | 1731            | 1.9e-18 | 1.1e-15  |
| GO:0016773 | F     | phosphotransferase activity, alcohol group as acceptor                      | 232                 | 1936            | 1.9e-16 | 8.4e-14  |
| GO:0032559 | F     | adenyl ribonucleotide binding   | 333                 | 3226            | 8.5e-15 | 3.00E-12 |
| GO:0005524 | F     | ATP binding   | 328                 | 3197            | 14      | 7.1e-12  |
| GO:0030554 | F     | adenyl nucleotide binding   | 348                 | 3444            | 2.7e-14 | 7.1e-12  |
| GO:0001883 | F     | purine nucleoside binding   | 348                 | 3449            | 3.3e-14 | 7.1e-12  |
| GO:0016301 | F     | kinase activity   | 241                 | 2152            | 4.7e-14 | 9.2e-12  |
| GO:0001882 | F     | nucleoside binding  | 348                 | 3471            | 7.3e-14 | 1.3e-11  |
| GO:0032555 | F     | purine ribonucleotide binding   | 341                 | 3495            | 3.7e-12 | 5.3e-10  |
| GO:0032553 | F     | ribonucleotide binding  | 341                 | 3495            | 3.7e-12 | 5.3e-10  |
| GO:0030246 | F     | carbohydrate binding  | 69                  | 384             | 12      | 9.4e-10  |
| GO:0017076 | F     | purine nucleotide binding   | 356                 | 3720            | 1.1e-11 | 1.3e-09  |
| GO:0003824 | F     | catalytic activity  | 1056                | 13636           | 1.2e-11 | 1.4e-09  |
| GO:0004497 | F     | monooxygenase activity  | 75                  | 474             | 1.7e-10 | 1.8e-08  |
| GO:0005529 | F     | sugar binding   | 53                  | 273             | 1.7e-10 | 1.8e-08  |
| GO:0016740 | F     | transferase activity  | 454                 | 5115            | 1.9e-10 | 1.9e-08  |
| GO:0004364 | F     | glutathione transferase activity  | 30                  | 98              | 2.4e-10 | 2.2e-08  |
| GO:0005506 | F     | iron ion binding  | 109                 | 890             | 1.1e-08 | 9.5e-07  |
| GO:0005509 | F     | calcium ion binding   | 72                  | 499             | 1.3e-08 | 1.1e-06  |
| GO:0009055 | F     | electron carrier activity   | 116                 | 984             | 2.4e-08 | 1.9e-06  |
| GO:0020037 | F     | heme binding  | 81                  | 626             | 1.1e-07 | 8.7e-06  |
| GO:0016298 | F     | lipase activity   | 36                  | 200             | 6.9e-07 | 5.00E-05 |
| GO:0008061 | F     | chitin binding  | 11                  | 19              | 06      | 6.9e-05  |
| GO:0016772 | F     | transferase activity, transferring phosphorus-containing groups             | 247                 | 2705            | 06      | 6.9e-05  |
| GO:0046906 | F     | tetrapyrrole binding  | 81                  | 669             | 1.3e-06 | 8.2e-05  |
| GO:0016765 | F     | transferase activity, transferring alkyl or aryl (other than methyl) groups | 36                  | 208             | 1.5e-06 | 9.6e-05  |
| GO:0016491 | F     | oxidoreductase activity   | 217                 | 2349            | 2.5e-06 | 0.00015  |
| GO:0000166 | F     | nucleotide binding  | 383                 | 4630            | 8.8e-06 | 0.00051  |
| GO:0004872 | F     | receptor activity   | 43                  | 301             | 1.3e-05 | 0.00073  |
| GO:0019825 | F     | oxygen binding  | 38                  | 255             | 1.8e-05 | 0.00096  |
| GO:0004867 | F     | serine-type endopeptidase inhibitor activity                                | 17                  | 70              | 2.4e-05 | 0.0013   |
| GO:0004568 | F     | chitinase activity  | 11                  | 32              | 5.1e-05 | 0.0024   |
| GO:0030247 | F     | polysaccharide binding  | 11                  | 32              | 5.1e-05 | 0.0024   |
| GO:0001871 | F     | pattern binding   | 11                  | 32              | 5.1e-05 | 0.0024   |
| GO:0004888 | F     | transmembrane receptor activity   | 27                  | 161             | 4.8e-05 | 0.0024   |
| GO:0005231 | F     | excitatory extracellular ligand-gated ion channel activity                  | 9                   | 25              | 0.00018 | 0.0077   |
| GO:0008066 | F     | glutamate receptor activity   | 9                   | 25              | 0.00018 | 0.0077   |
| GO:0035251 | F     | UDP-glucosyltransferase activity  | 25                  | 157             | 0.00019 | 0.0077   |
| GO:0005234 | F     | extracellular-glutamate-gated ion channel activity                          | 9                   | 25              | 0.00018 | 0.0077   |
| GO:0004970 | F     | ionotropic glutamate receptor activity                                      | 9                   | 25              | 0.00018 | 0.0077   |
| GO:0022834 | F     | ligand-gated channel activity   | 13                  | 53              | 0.0002  | 0.0078   |
| GO:0015276 | F     | ligand-gated ion channel activity   | 13                  | 53              | 0.0002  | 0.0078   |
| GO:0005230 | F     | extracellular ligand-gated ion channel activity                             | 9                   | 26              | 0.00023 | 0.009    |
| GO:0004807 | F     | triose-phosphate isomerase activity   | 6                   | 12              | 0.00058 | 0.022    |
| GO:0005516 | F     | calmodulin binding  | 31                  | 234             | 0.00063 | 0.023    |

| GO term    | Ont.* | Description                                       | Nr/<br>input list | Nr/<br>BG/Ref | p-value | FDR    |
|------------|-------|---|-------------------|---------------|---------|--------|
| GO:0060089 | F     | molecular transducer activity                     | 59                | 555           | 0.00076 | 0.027  |
| GO:0004871 | F     | signal transducer activity                        | 59                | 555           | 0.00076 | 0.027  |
| GO:0004806 | F     | triglyceride lipase activity                      | 13                | 63            | 0.00083 | 0.029  |
| GO:0016758 | F     | transferase activity, transferring hexosyl groups | 62                | 595           | 0.00089 | 0.03   |
| GO:0016165 | F     | lipoygenase activity                              | 6                 | 14            | 0.0011  | 0.036  |
| GO:0046527 | F     | glucosyltransferase activity                      | 25                | 183           | 0.0014  | 0.045  |
| GO:0005886 | C     | plasma membrane                                   | 152               | 1557          | 6.9e-06 | 0.0049 |

\* Ont.: Ontologie, P: Biological process, F: Molecular function, C: Cellular process

\*\* Nr/ input list: Number of genes in input list

\*\*\* Nr/in BG/Ref: Number of genes in the background reference

**Supplemental Table S5-** GO terms upregulated for SRS in the comparison SRS-SRZ infected sorghum

| GO term    | *Ont. | Description  | **Nr/<br>imput list | ***Nr/<br>in<br>BG/Ref | p-value  | FDR      |
|------------|-------|--|---------------------|------------------------|----------|----------|
| GO:0006414 | P     | translational elongation                             | 54                  | 189                    | 3.9e-34  | 1.3e-30  |
| GO:0006412 | P     | translation  | 100                 | 861                    | 2.6e-32  | 4.2e-29  |
| GO:0000022 | P     | mitotic spindle elongation                           | 20                  | 66                     | 7.5e-14  | 8.1e-11  |
| GO:0051231 | P     | spindle elongation                                   | 20                  | 69                     | 1.5e-13  | 9.8e-11  |
| GO:0010876 | P     | lipid localization                                   | 13                  | 16                     | 1.3e-13  | 9.8e-11  |
| GO:0022403 | P     | cell cycle phase                                     | 48                  | 588                    | 8.9e-11  | 4.8e-08  |
| GO:0042254 | P     | ribosome biogenesis                                  | 36                  | 379                    | 5.3e-10  | 2.1e-07  |
| GO:0034645 | P     | cellular macromolecule biosynthetic process          | 194                 | 4668                   | 5.2e-10  | 2.1e-07  |
| GO:0009059 | P     | macromolecule biosynthetic process                   | 194                 | 4721                   | 1.3e-09  | 4.6e-07  |
| GO:0044249 | P     | cellular biosynthetic process                        | 247                 | 6576                   | 1.00E-08 | 3.4e-06  |
| GO:0022402 | P     | cell cycle process                                   | 51                  | 765                    | 1.5e-08  | 4.4e-06  |
| GO:0065004 | P     | protein-DNA complex assembly                         | 18                  | 119                    | 2.4e-08  | 6.00E-06 |
| GO:0009791 | P     | post-embryonic development                           | 85                  | 1644                   | 2.4e-08  | 6.00E-06 |
| GO:0009058 | P     | biosynthetic process                                 | 254                 | 6890                   | 3.00E-08 | 7.00E-06 |
| GO:0007052 | P     | mitotic spindle organization                         | 21                  | 172                    | 4.8e-08  | 1.00E-05 |
| GO:0044085 | P     | cellular component biogenesis                        | 71                  | 1307                   | 6.4e-08  | 1.3e-05  |
| GO:0022613 | P     | ribonucleoprotein complex biogenesis                 | 36                  | 466                    | 7.6e-08  | 1.4e-05  |
| GO:0006334 | P     | nucleosome assembly                                  | 16                  | 102                    | 9.1e-08  | 1.6e-05  |
| GO:0060249 | P     | anatomical structure homeostasis                     | 7                   | 10                     | 1.3e-07  | 2.3e-05  |
| GO:0006323 | P     | DNA packaging  | 19                  | 159                    | 2.8e-07  | 4.6e-05  |
| GO:0000279 | P     | M phase  | 36                  | 496                    | 3.1e-07  | 4.8e-05  |
| GO:0034728 | P     | nucleosome organization                              | 16                  | 114                    | 3.5e-07  | 5.2e-05  |
| GO:0007051 | P     | spindle organization                                 | 21                  | 201                    | 5.2e-07  | 7.3e-05  |
| GO:0010467 | P     | gene expression                                      | 184                 | 4800                   | 5.6e-07  | 7.5e-05  |
| GO:0031497 | P     | chromatin assembly                                   | 16                  | 120                    | 6.6e-07  | 8.5e-05  |
| GO:0070925 | P     | organelle assembly                                   | 8                   | 25                     | 1.8e-06  | 0.00022  |
| GO:0007049 | P     | cell cycle   | 57                  | 1072                   | 2.5e-06  | 0.0003   |
| GO:0000278 | P     | mitotic cell cycle                                   | 36                  | 548                    | 2.8e-06  | 0.00032  |
| GO:0055046 | P     | microgametogenesis                                   | 5                   | 6                      | 5.1e-06  | 0.00057  |
| GO:0000084 | P     | S phase of mitotic cell cycle                        | 8                   | 34                     | 1.2e-05  | 0.0013   |
| GO:0051320 | P     | S phase  | 8                   | 34                     | 1.2e-05  | 0.0013   |
| GO:0006261 | P     | DNA-dependent DNA replication                        | 16                  | 157                    | 1.5e-05  | 0.0016   |
| GO:0000226 | P     | microtubule cytoskeleton organization                | 23                  | 305                    | 2.4e-05  | 0.0024   |
| GO:0048610 | P     | reproductive cellular process                        | 7                   | 27                     | 2.5e-05  | 0.0024   |
| GO:0034622 | P     | cellular macromolecular complex assembly             | 31                  | 499                    | 3.7e-05  | 0.0034   |
| GO:0010035 | P     | response to inorganic substance                      | 24                  | 338                    | 4.00E-05 | 0.0036   |
| GO:0006270 | P     | DNA replication initiation                           | 8                   | 43                     | 5.3e-05  | 0.0047   |
| GO:0030174 | P     | regulation of DNA replication initiation             | 6                   | 21                     | 6.1e-05  | 0.0051   |
| GO:0006268 | P     | DNA unwinding during replication                     | 6                   | 21                     | 6.1e-05  | 0.0051   |
| GO:0006333 | P     | chromatin assembly or disassembly                    | 16                  | 182                    | 7.9e-05  | 0.0064   |
| GO:0051325 | P     | interphase   | 12                  | 112                    | 0.00011  | 0.0087   |
| GO:0051329 | P     | interphase of mitotic cell cycle                     | 12                  | 112                    | 0.00011  | 0.0087   |
| GO:0009886 | P     | post-embryonic morphogenesis                         | 12                  | 122                    | 0.00024  | 0.018    |
| GO:0034621 | P     | cellular macromolecular complex subunit organization | 32                  | 586                    | 0.00026  | 0.019    |
| GO:0065003 | P     | macromolecular complex assembly                      | 33                  | 612                    | 0.00026  | 0.019    |
| GO:0006869 | P     | lipid transport                                      | 13                  | 143                    | 0.00027  | 0.019    |
| GO:0042255 | P     | ribosome assembly                                    | 8                   | 58                     | 0.00034  | 0.023    |
| GO:0007017 | P     | microtubule-based process                            | 25                  | 419                    | 0.00036  | 0.024    |
| GO:0010345 | P     | suberin biosynthetic process                         | 5                   | 20                     | 0.00043  | 0.029    |
| GO:0070301 | P     | cellular response to hydrogen peroxide               | 6                   | 36                     | 0.00078  | 0.048    |
| GO:0034614 | P     | cellular response to reactive oxygen species         | 6                   | 36                     | 0.00078  | 0.048    |
| GO:0042744 | P     | hydrogen peroxide catabolic process                  | 6                   | 36                     | 0.00078  | 0.048    |
| GO:0003735 | F     | structural constituent of ribosome                   | 95                  | 462                    | 6.1e-49  | 4.9e-46  |
| GO:0005198 | F     | structural molecule activity                         | 99                  | 677                    | 1.7e-39  | 6.7e-37  |
| GO:0019843 | F     | rRNA binding   | 18                  | 89                     | 4.1e-10  | 1.1e-07  |

| GO term    | Ont.* | Description                                  | Nr/<br>imput list | Nr/<br>in<br>BG/Ref | p-value  | FDR      |
|------------|-------|--|-------------------|---------------------|----------|----------|
| GO:0003723 | F     | RNA binding                                  | 72                | 1236                | 3.5e-09  | 7.00E-07 |
| GO:0022626 | C     | cytosolic ribosome                           | 87                | 264                 | 5.6e-59  | 3.1e-56  |
| GO:0033279 | C     | ribosomal subunit                            | 82                | 302                 | 4.3e-50  | 1.2e-47  |
| GO:0005840 | C     | ribosome                                     | 96                | 511                 | 1.8e-46  | 3.3e-44  |
| GO:0044445 | C     | cytosolic part                               | 77                | 331                 | 6.2e-43  | 8.6e-41  |
| GO:0022627 | C     | cytosolic small ribosomal subunit            | 42                | 113                 | 1.5e-30  | 1.6e-28  |
| GO:0030529 | C     | ribonucleoprotein complex                    | 98                | 901                 | 1.3e-29  | 1.2e-27  |
| GO:0015935 | C     | small ribosomal subunit                      | 42                | 129                 | 1.2e-28  | 9.2e-27  |
| GO:0043232 | C     | intracellular non-membrane-bounded organelle | 151               | 2124                | 1.00E-26 | 6.4e-25  |
| GO:0043228 | C     | non-membrane-bounded organelle               | 151               | 2124                | 1.00E-26 | 6.4e-25  |
| GO:0022625 | C     | cytosolic large ribosomal subunit            | 37                | 116                 | 3.9e-25  | 2.2e-23  |
| GO:0015934 | C     | large ribosomal subunit                      | 43                | 178                 | 6.5e-25  | 3.3e-23  |
| GO:0032993 | C     | protein-DNA complex                          | 25                | 125                 | 2.00E-13 | 9.4e-12  |
| GO:0005829 | C     | cytosol                                      | 103               | 1740                | 3.6e-13  | 1.5e-11  |
| GO:0005811 | C     | lipid particle                               | 23                | 154                 | 3.4e-10  | 1.4e-08  |
| GO:0032991 | C     | macromolecular complex                       | 150               | 3322                | 4.9e-10  | 1.8e-08  |
| GO:0035059 | C     | RCAF complex                                 | 9                 | 28                  | 3.8e-07  | 1.3e-05  |
| GO:0000786 | C     | nucleosome                                   | 14                | 90                  | 6.3e-07  | 2.1e-05  |
| GO:0000228 | C     | nuclear chromosome                           | 22                | 237                 | 1.7e-06  | 5.3e-05  |
| GO:0044454 | C     | nuclear chromosome part                      | 19                | 198                 | 5.6e-06  | 0.00016  |
| GO:0005618 | C     | cell wall                                    | 40                | 669                 | 6.7e-06  | 0.00019  |
| GO:0005694 | C     | chromosome                                   | 39                | 650                 | 8.1e-06  | 0.00021  |
| GO:0005656 | C     | pre-replicative complex                      | 5                 | 7                   | 8.6e-06  | 0.00022  |
| GO:0030312 | C     | external encapsulating structure             | 41                | 705                 | 9.6e-06  | 0.00023  |
| GO:0044422 | C     | organelle part                               | 178               | 4830                | 1.00E-05 | 0.00023  |
| GO:0044446 | C     | intracellular organelle part                 | 177               | 4811                | 1.2e-05  | 0.00027  |
| GO:0009505 | C     | plant-type cell wall                         | 35                | 565                 | 1.2e-05  | 0.00027  |
| GO:0000785 | C     | chromatin                                    | 23                | 296                 | 1.5e-05  | 0.00032  |
| GO:0044427 | C     | chromosomal part                             | 33                | 527                 | 1.8e-05  | 0.00036  |
| GO:0042555 | C     | MCM complex                                  | 5                 | 9                   | 2.1e-05  | 0.00037  |
| GO:0043601 | C     | nuclear replisome                            | 7                 | 26                  | 2.00E-05 | 0.00037  |
| GO:0030894 | C     | replisome                                    | 7                 | 26                  | 2.00E-05 | 0.00037  |
| GO:0043596 | C     | nuclear replication fork                     | 7                 | 33                  | 7.6e-05  | 0.0013   |
| GO:0044464 | C     | cell part                                    | 508               | 16988               | 0.00012  | 0.002    |
| GO:0005623 | C     | cell   | 508               | 16988               | 0.00012  | 0.002    |
| GO:0005657 | C     | replication fork                             | 9                 | 64                  | 0.00013  | 0.002    |
| GO:0001740 | C     | Barr body                                    | 5                 | 16                  | 0.00018  | 0.0028   |
| GO:0000805 | C     | X chromosome                                 | 5                 | 17                  | 0.00023  | 0.0035   |
| GO:0016585 | C     | chromatin remodeling complex                 | 10                | 93                  | 0.0004   | 0.0059   |
| GO:0001739 | C     | sex chromatin                                | 5                 | 25                  | 0.001    | 0.015    |
| GO:0000803 | C     | sex chromosome                               | 5                 | 30                  | 0.0021   | 0.03     |
| GO:0005700 | C     | polytene chromosome                          | 6                 | 50                  | 0.0035   | 0.048    |

\* Ont.: Ontologie, P: Biological process, F: Molecular function, C: Cellular process

\*\* Nr/ imput list: Number of genes in imput list

\*\*\* Nr/in BG/Ref: Number of genes in the background reference

### **6.3 Acknowledgments**

I am very grateful to my supervisor Prof. Jan Schirawski for his support, enthusiasm, patience, and for his untiring assistance, always taking the time to answer my questions and to give suggestions for my project.

I thank my dear Yulei (my Chinese sister) for her valuable company in the cozy-office and for making every lunch or fruit-time a great moment. A big thanks goes to Theresa, for being a wonderful colleague, but above all a great friend since I started in the lab, and also for having such a big heart. I also want to thank sweet Ute for her help and friendship, and Frank for being just awesome. In addition, I thank all the members of the Microbial Genetics lab for the support and for making my days very happy: Steven (Bro), Niko, Nilam, Kalle, Martin, Patrick, Erik, Maike, Melissa, Guido, Leo and all the past students. Many thanks also to the former members of the Department for Molecular Biology of Plant-Microbe-Interaction in Göttingen: Jenny, Hassan, Jan, and particularly Katja, for sharing her knowledge and for her precious help during the beginning of my studies.

I thank all the colleagues from the Institute of Applied Microbiology for the very nice and friendly atmosphere.

I would like to express my gratitude to the research group of Prof. Dominik Begerow at the University of Bochum, especially Sabine, Tanja and Sasha for all the efforts with scanning electron microscopy. I thank also Dr. Michael Hoppert from the University of Göttingen for the support with transmission electron microscopy. I am thankful to Prof. Franziska Krajinski and Dr. Nicole Gaude from Max Planck Institute of Plant Physiology in Golm for the introduction in laser microdissection.

I thank Prof. Alan Slusarenko for being my second examiner.

I am truly grateful to the German Academic Exchange Service (DAAD) for the scholarship that allowed me to pursue my studies.

I want to thank Sakya for encouraging and supporting me, for making me laugh, and for all the nice moments we shared.

Aos meus queridos amigos do Brasil, que mesmo estando longe sempre se fizeram presentes, especialmente Paula, Lia, Biduio, Flávia, Rodrigo, Mauro, Marcos, Moisés, Livia, Fernando, Karla e meu primo Nicolás.

Um muito obrigada a toda minha família, especialmente ao meu avô Patim que partiu antes que eu terminasse essa tese. Por fim, eu agradeço meus pais Marlene e Adriano, por entenderem minha ausência e por todo amor e carinho.

